

U.S. Department of the Interior  
U.S. Geological Survey



# Debris Flows from Failures of Neoglacial-Age Moraine Dams in the Three Sisters and Mount Jefferson Wilderness Areas, Oregon

Professional Paper 1606

**Cover photograph:** View northwest of Broken Top volcano and moraine-dammed lake. South, Middle, and North Sisters in background. Photograph by Austin Post, USGS, September 22, 1966.

# **Debris Flows from Failures of Neoglacial-Age Moraine Dams in the Three Sisters and Mount Jefferson Wilderness Areas, Oregon**

**By Jim E. O'Connor, Jasper H. Hardison III, and John E. Costa**

*A study of the recent debris flows from moraine-dammed lake releases at central Oregon Cascade Range volcanoes—Mt. Jefferson, Three Fingered Jack, and the Three Sisters/Broken Top*

---

**U.S. GEOLOGICAL SURVEY PROFESSIONAL PAPER 1606**

# U.S. DEPARTMENT OF THE INTERIOR

**GALE A. NORTON, Secretary**

## U.S. GEOLOGICAL SURVEY

**Charles G. Groat, Director**

Any use of trade, product, or firm names in this publication is for descriptive purposes only and does not imply endorsement by the U.S. Government.

Reston, Virginia, 2001

---

For sale by U.S. Geological Survey, Information Services  
Box 25286, Federal Center  
Denver, CO 80225

### **Library of Congress Cataloging-in-Publication Data**

O'Connor, Jim E., 1959–

Debris flows from failures of Neoglacial-age moraine dams in the Three Sisters and Mount Jefferson wilderness areas, Oregon / by J.E. O'Connor, J.H. Hardison III, and J.E. Costa.

p. cm.-- (U.S. Geological Survey professional paper; 1606)

Includes bibliographical references and index.

1. Debris avalanches--Oregon--Three Sisters Wilderness. 2. Debris avalanches--Oregon--Mount Jefferson Wilderness. 3. Moraines--Oregon--Three Sisters Wilderness. 4. Moraines--Oregon--Mount Jefferson Wilderness. I. Hardison, J.H. (Jasper H.), 1965– II. Costa, John E. III. Title. IV. Series

QE599.U5 O26 2001  
551.3'07--dc21

2001023270  
ISBN 0-607-96719-6

# CONTENTS

Abstract.....	1
Introduction .....	2
Background .....	2
Purpose and Scope .....	2
Acknowledgments.....	2
The Central Oregon Cascade Range.....	2
Physiography.....	2
Geologic and Topographic Setting .....	2
Climate and Vegetation .....	4
Glaciers.....	4
Previous Work.....	4
Neoglaciation in the Central Oregon Cascade Range .....	5
Neoglaciation and Little Ice Age Chronology and Deposits .....	5
Chronology .....	5
Neoglacial Deposits.....	6
19th- and 20th-Century Glacier Behavior.....	9
Glacier Activity .....	9
Climatic Forcing .....	13
Moraine-Dammed Lakes .....	15
Distribution .....	15
Chronology.....	24
Lake Basin Bathymetry and Topography .....	26
Formation and Preservation of Moraine-Dammed Lakes .....	26
Debris Flows from Lakes Dammed by Neoglacial Moraines .....	26
General Features .....	26
Indirect Discharge Estimation Methods.....	27
Velocity-Area Discharge Estimates.....	27
Critical-Flow Discharge Estimates .....	39
Case Studies in the Central Oregon Cascade Range.....	41
Mount Jefferson Wilderness Area .....	41
East Jefferson Park.....	42
West Jefferson Park .....	43
Waldo Glacier .....	44
Jack Glacier .....	45
Three Sisters Wilderness Area .....	46
Collier Glacier .....	46
Diller Glacier.....	53
Eugene Glacier .....	60
East Bend Glacier.....	65

Processes .....	69
Breaching of Moraine Dams .....	70
Downstream Flow Characteristics .....	73
Evaluation of Hazards from Moraine-Dammed Lake Breakouts .....	76
Assessing Potential Failure of Moraine Dams .....	76
Topographic Setting .....	76
Likelihood of Future Breaches in the Central Oregon Cascade Range .....	77
Assessing Downstream Flow Hazards .....	79
The Outflow Hydrograph at the Breach .....	79
Downstream Flow Behavior .....	81
Conclusions .....	85
References Cited .....	87

## PLATES

- I. Maps of the Neoglacial moraines and glacial positions since the culmination of the Little Ice Age for Mount Jefferson, Three Fingered Jack, and the Three Sisters Wilderness Area—**In pocket**
- II. Maps of debris flow paths for flows originating from moraine-dammed lakes in the Three Sisters Wilderness Area—**In pocket**

## FIGURES

1. Regional map of central Oregon Cascade Range and surrounding area .....	3
2. Graph of equilibrium line altitudes for present and reconstructed late Quaternary glaciers at Mount Jefferson and Three Sisters .....	5
3. Photograph of Neoglacial lateral moraines of Collier Glacier .....	7
4. Oblique aerial photograph of Carver Lake and terminus of northern lobe of Prouty Glacier .....	8
5. Matched photographs of ablation area of Diller Glacier .....	10
6. Matched photographs of the right lateral moraine and terminus of Hayden Glacier .....	11
7. Matched photographs of Collier Glacier .....	12
8. Graph of changes in the glacier areas of Three Sisters and Mount Jefferson since the culmination of the Little Ice Age .....	13
9. Oblique aerial photograph of Collier Glacier .....	13
10. Map showing extent of Collier Glacier at several times during the 20th century .....	14
11. Graph of equilibrium line altitude and glaciated area at Collier Glacier since the culmination of the Little Ice Age .....	15
12. Sequence of photographs by R.H. Keen from Collier Glacier viewpoint .....	16
13. Graphs of measured mean annual temperatures from northern hemisphere land data and Corvallis, Oregon .....	17
14. Graphs of annual climate data for Crater Lake, Oregon .....	18
15. Photographs of moraine-dammed lakes in the Three Sisters and Mount Jefferson Wilderness Areas, Oregon .....	23

16. Graphs of moraine-dammed lake chronologies for lakes in the Three Sisters and Mount Jefferson Wilderness Areas, Oregon .....	25
17. Maps of bathymetry and topography of lakes and lake basins dammed by Neoglacial moraines in the Three Sisters and Mount Jefferson Wilderness Areas .....	28
18. Graph of area-volume relations for moraine-dammed lakes and lake basins in the study area .....	30
19. Definition diagram for flow transforming from a state of subcritical to supercritical through a control section of critical flow .....	39
20. Schematic plan and profile illustrations of an ideal field situation for a critical flow discharge measurement.....	40
21. Critical depth and specific energy curves for a surveyed cross section .....	41
22. Aerial photograph of Mount Jefferson and the northern lobes of Whitewater Glacier .....	41
23. Composite of oblique aerial photographs of the debris flow at the terminus of a lobe of Whitewater Glacier, Mount Jefferson .....	42
24. Graphs of longitudinal profiles along the flow routes of debris flows from moraine-dammed lakes at terminal lobes of Whitewater Glacier, Mount Jefferson .....	43
25. Oblique aerial photograph of Waldo Glacier, Mount Jefferson .....	44
26. Photograph of moraine and outwash fan from Jack Glacier on Three Fingered Jack .....	46
27. Photograph of outlet from the basin that formerly contained the lake at the terminus of Collier Glacier, North Sister .....	47
28. Graph of surveyed cross section of outlets to the former lake at the terminus of Collier Glacier .....	48
29. Oblique aerial photograph of remnant lake, breached moraine, and downstream deposits left after the 1942 flow from the lake at Collier Glacier .....	48
30. Graph of stage-discharge relation for critical flow through the left breach at the outlet to the lake at Collier Glacier .....	49
31. Photograph of Sawyer Bar covered by bouldery deposits from the 1942 breach and debris flow from the lake at the terminus of Collier Glacier .....	49
32. Graph of longitudinal profile of White Branch, showing indirect discharge estimates and reaches of erosion and deposition during the 1942 debris flow from the breach of the lake at the terminus of Collier Glacier .....	50
33. Photograph of a single sinuous ridge of bouldery gravel along the 1942 flow path down White Branch.....	51
34. Photograph of deposits from the 1942 debris flow down White Branch .....	52
35. Graph of indirect estimates of peak discharge for the 1942 debris flow down White Branch .....	53
36. Graph of range of cumulative curves for 13 samples of matrix material from the 1942 White Branch debris-flow deposits .....	53
37. Graphs of downstream variation in particle-size distribution characteristics of matrix materials for the 1942 White Branch flow .....	54
38. Stereophotograph pairs of Diller Glacier before and after the September 7, 1970, breach of the moraine-dammed lake .....	55
39. Graph of longitudinal profile of North Fork Squaw Creek, showing indirect discharge estimates and reaches of erosion and deposition during the September 7, 1970, debris flow and flood from the breach of the lake at the terminus of Diller Glacier .....	56
40. Photograph of distal end of the large fan deposited below the September 7, 1970, breach in the Diller Glacier moraine .....	57

41. Photograph of a debris flow levee or boulder berm deposited by the 1970 North Fork Squaw Creek flow.....	58
42. Photograph of boulders trapped by trees in an overbank area during the 1970 North Fork Squaw Creek flow.....	58
43. Photograph of buried trees in depositional area of the 1970 North Fork Squaw Creek debris flow .....	59
44. Hydrograph for September 7, 1970 on Squaw Creek, 24 km from the breach .....	60
45. Graph of range of cumulative curves for 13 samples of matrix material from the 1970 North Fork Squaw Creek debris flow deposits .....	60
46. Graphs of downstream variation in particle-size distribution characteristics of matrix materials for the 1970 North Fork Squaw Creek debris flow .....	61
47. Graph of rock-type counts downstream from the breach of the moraine at Diller Glacier.....	61
48. Matched photographs of the north slope of South Sister from the summit of Middle Sister.....	62
49. Map of topographic setting of August 12, 1933, and 1946(?) moraine-dammed lake releases at Eugene Glacier, South Sister .....	63
50. Oblique aerial photograph of the August 12, 1933, lake breach and debris flow from Eugene Glacier .....	64
51. Graph of longitudinal profile of Separation Creek, showing indirect discharge estimates and reaches of erosion and deposition during the August 12, 1933, debris flow and flood from the breach of the lake at the terminus of Eugene Glacier .....	64
52. Graph of longitudinal profile of the drainage from East Bend Glacier, Broken Top, into Sparks Lake, showing indirect discharge estimates and reaches of erosion and deposition during the October 7, 1966 debris flow and flood from the breach of the lake at the terminus of the glacier .....	66
53. Photograph of the October 7, 1966, breach in the Neoglacial moraine impounding the lake at the terminus of East Bend Glacier, Broken Top.....	66
54. Photograph of valley-bottom bedrock erosion about 1.6 km downstream from breach of the East Bend glacial lake .....	67
55. Photograph downstream of deposits left by the October 7, 1966, debris flow from the lake at the terminus of East Bend Glacier .....	67
56. Photograph of a boulder and timber fan deposited by the October 7, 1966, debris flow from the lake at the terminus of East Bend Glacier, Broken Top .....	68
57. Graph of range of cumulative curves for four samples of matrix material and fine gravel from the 1966 debris flow from East Bend Glacier, Broken Top .....	69
58. Graphs of cumulative curves of particle sizes for three Neoglacial moraines in the Three Sisters Wilderness Area .....	70
59. Graphs of breach cross sections and previous lake levels at four sites of moraine-dammed lake releases in the Three Sisters and Mount Jefferson Wilderness Areas .....	72
60. Hydrographs and debris flow characteristics during the September 12, 1991, experiment at the Chemolgan Debris Flow Testing Ground, Kazakhstan .....	74
61. Graph of channel slopes associated with reaches of deposition, erosion, and conveyance for the debris flows on White Branch, Squaw Creek, Separation Creek, and Soda Creek.....	75
62. Topographic-setting criteria for qualitative assessment of the potential of a moraine-dam breach .....	78

63. Graphs of topographic profiles for the five largest moraine-dammed lakes in the Three Sisters and Mount Jefferson Wilderness Areas, and for Collier Glacier and adjacent basin .....	79
64. Graph of decadal incidence of formation and breaching of Neoglacial moraine-dammed lakes in the Three Sisters and Mount Jefferson Wilderness Areas .....	80
65. Hydrographs of effects of breach shape, erosion rate, and lake hypsometry on calculated erosion rates .....	81
66. Calculated hypothetical hydrographs for sis existing and potential moraine-dammed lakes in the Three Sisters and Mount Jefferson Wilderness Areas .....	82
67. Graph of downstream variation in peak discharges for debris flows from moraine-dammed lake releases in the Three Sisters Wilderness Area, Oregon, and other alpine areas. ....	84

**TABLES**

1. Lakes dammed by Neoglacial moraines in the Cascade Range, Oregon and Washington .....	19
2. Failed moraine dams in various mountainous areas worldwide .....	31
3. Hypothetical peak discharges from moraine-dammed lakes in the Three Sisters and Mount Jefferson Wilderness Areas for various breach erosion rates .....	79

**CONVERSION FACTORS AND VERTICAL DATUM**

Multiply	By	To obtain
<b>International system units to inch-pound units</b>		
millimeter (mm)	0.0397	inch (in)
meter (m)	3.281	feet (ft)
square kilometer (km <sup>2</sup> )	0.3861	square mile (mi <sup>2</sup> )
cubic meter (m <sup>3</sup> )	35.31	cubic foot (ft <sup>3</sup> )
cubic meters per second (m <sup>3</sup> /s)	35.31	cubic feet per second (ft <sup>3</sup> /s)

**Sea level:** In this report, “sea level” refers to the National Geodetic Vertical Datum of 1929 (NGVD of 1929) — a geodetic datum derived from a general adjustment of the first-order level nets of both the United States and Canada, formerly called “Sea Level Datum of 1929.”



# Debris Flows from Failures of Neoglacial-Age Moraine Dams in the Three Sisters and Mount Jefferson Wilderness Areas, Oregon

By Jim E. O'Connor, Jasper H. Hardison III, and John E. Costa

## Abstract

Cascade Range alpine glaciers have shrunk substantially as average annual temperature has risen 0.5 to 2 degrees Celsius since culmination of the Little Ice Age in the mid- to late 1800's. In recently deglaciated areas in the Cascade Range, hundreds of lakes have formed. Most of these newly formed lakes are partly or entirely bound by bedrock rims and are stable, but at least 30 are dammed by unconsolidated moraines that are susceptible to breaching.

The highest concentration of lakes dammed by Neoglacial moraines in the conterminous United States is in the Mount Jefferson and Three Sisters Wilderness Areas in central Oregon, where there are currently eight moraine-dammed lakes. The largest lake, Carver Lake on South Sister, has a volume of almost 1 million cubic meters. Most of these lakes formed between 1920 and 1940 during a period of substantial warming and glacier retreat. In the Mount Jefferson and Three Sisters Wilderness Areas, there have been 11 debris flows from 4 complete and 7 partial emptyings of moraine-dammed lakes. Most of these breaches occurred between 1930 and 1950, but some were as recent as the 1970's.

All moraine-dam breaches in the Three Sisters and Mount Jefferson Wilderness Areas occurred during the melt season (July-October), usually during periods of warm or rainy weather. Many breaches were probably a result of erosion of the steep outlet channels, triggered by unusually large discharges caused by (1) waves generated by rockfalls or ice avalanches into the lake or (2) increased lake outflow caused by precipitation and melting snow and ice. Water flows from breached moraine dams rapidly evolved into debris flows that traveled as far as 9

kilometers before stopping or evolving into sediment-laden water flows. Peak discharges of at least four of the flows exceeded 300 cubic meters per second. Flows from breached morainal dams transformed from clear water at the outlet into debris flows within 500 meters of the breaches by incorporating large volumes of loose Neoglacial till and outwash from the moraines and proglacial outwash. For the two largest lake releases, the volume of sediment eroded near the outlet exceeded 25 percent of the total volume of water released. Morphological evidence indicates that sediment was introduced into flows by bank collapse and channel incision. Indirect discharge estimates (primarily by a critical-depth procedure) show that peak discharges increased in erosional reaches; in one instance by more than a factor of four. Erosion and sediment entrainment was restricted to reaches with slopes that exceeded 8°, and deposition occurred in reaches with slopes less than 18°.

Several moraine-dammed lakes still exist, and some pose downstream hazards. Two of the lakes are remnants of previously larger lakes that have partially breached their moraine dams. Five lakes in the Three Sisters and Mount Jefferson Wilderness Areas are impounded by Neoglacial moraines that have not been breached. Qualitative assessments of downstream hazards from moraine-dammed lakes are possible on the basis of the topographic setting of the lake and downstream channel conditions. Quantitative assessment of the likelihood of breaching or the magnitude of downstream flows is difficult because of the variety of mechanisms that trigger breaches, the sensitivity of outflow hydrographs to breach shape and erosion rate, and the large uncertainty of downstream flow characteristics.

# INTRODUCTION

## Background

Recent floods and debris flows<sup>1</sup> resulting from moraine-dam failures are one of several geomorphic consequences of substantial 19th and 20th century alpine glacier retreat at the end of the Neoglacial period<sup>2</sup> (Clague and Evans, 1993; Evans and Clague, 1993; O'Connor and Costa, 1993). Worldwide retreat and thinning of glaciers from advanced late Neoglacial positions has resulted in the exposure of a large volume of unconsolidated, unvegetated, and locally ice-cored sediment. These deposits include moraines, outwash, and ice-stagnation drift and are commonly composed of a heterogeneous mixture of particle sizes emplaced on steep slopes. This sediment is readily mobilized, transported, and deposited by a variety of processes, including mass wasting, moraine-dammed lake failures, glacial outburst floods, rapid snow and ice melting, and precipitation-induced flooding. Although deglaciation has triggered these processes in all temperate glacierized environments, recent geomorphic activity on Cascade Range volcanoes has been notable because these volcanoes are steep, extensively glacierized, and composed of jointed and locally highly altered loose rock and fragmental material (Osterkamp and others, 1986; Walder and Driedger, 1994).

## Purpose and Scope

This report focuses on central Oregon Cascade Range stratovolcanoes of Mount Jefferson, Three

---

<sup>1</sup> Debris flows are slurries of rock debris, organic material, and water that have sufficient yield strength and viscosity to support gravel-sized particles in suspension (Pierson and Costa, 1992).

<sup>2</sup> The Neoglacial period was defined by Porter and Denton (1976) as encompassing the last 5,000 to 6,000 <sup>14</sup>C yr, when alpine glaciers reformed and advanced. The "Little Ice Age" (Matthes, 1939) is generally regarded as the culmination of the Neoglacial period, and is a term used by climatologists, geologists, and glaciologists to describe a period of worldwide lower temperatures and advanced glacier positions from the 16th century through the late 19th century (Grove, 1988, p. 3–5).

Fingered Jack, and the Three Sisters/Broken Top area because of the unique concentration of recent debris flows that have resulted from moraine-dammed lake releases. We evaluate the relevant late Holocene glacier and climate history of the Three Sisters and Mount Jefferson Wilderness Areas between Mount Jefferson and Crater Lake, Oregon (fig. 1) and describe conditions that led to formation and failure of Neoglacial moraine dams. We mapped, described, sampled deposits from, and calculated multiple indirect discharge measurements for four debris flows that resulted from breaching of moraine dams to determine and track aspects of flow characteristics as each debris flow moved downstream. The report concludes with a discussion of hazard assessment for existing moraine-dammed lakes in the Three Sisters and Mount Jefferson Wilderness Areas.

## Acknowledgments

Field assistance was provided by Janet Curran, Ross Hartlieb, Gerardo Benito, and Chris Surville (U.S. Geological Survey volunteers). David Wieprecht (U.S. Geological Survey) assisted with matching of historic photographs. William Scott, Kevin Scott, Joseph Walder, and Thomas Pierson, all of the U.S. Geological Survey, provided ideas, guidance, and unpublished data for use in this report. Previous versions of this report were reviewed by C. Waythomas, A. Laenen, W. Osterkamp, J. Major, J. Walder, R. Iverson, W. Scott, and K.M. Nolan, all of the U.S. Geological Survey. Editorial assistance, manuscript preparation, and graphics by Christine Janda.

## THE CENTRAL OREGON CASCADE RANGE

### Physiography

### Geologic and Topographic Setting

In the United States, the Cascade Range extends from northern California to northern Washington. In Oregon, south of Mount Hood, the Cascade Range is 50 to 120 km wide, and is composed primarily of upper Eocene to Quaternary volcanic, volcanoclastic, sedimentary, and igneous

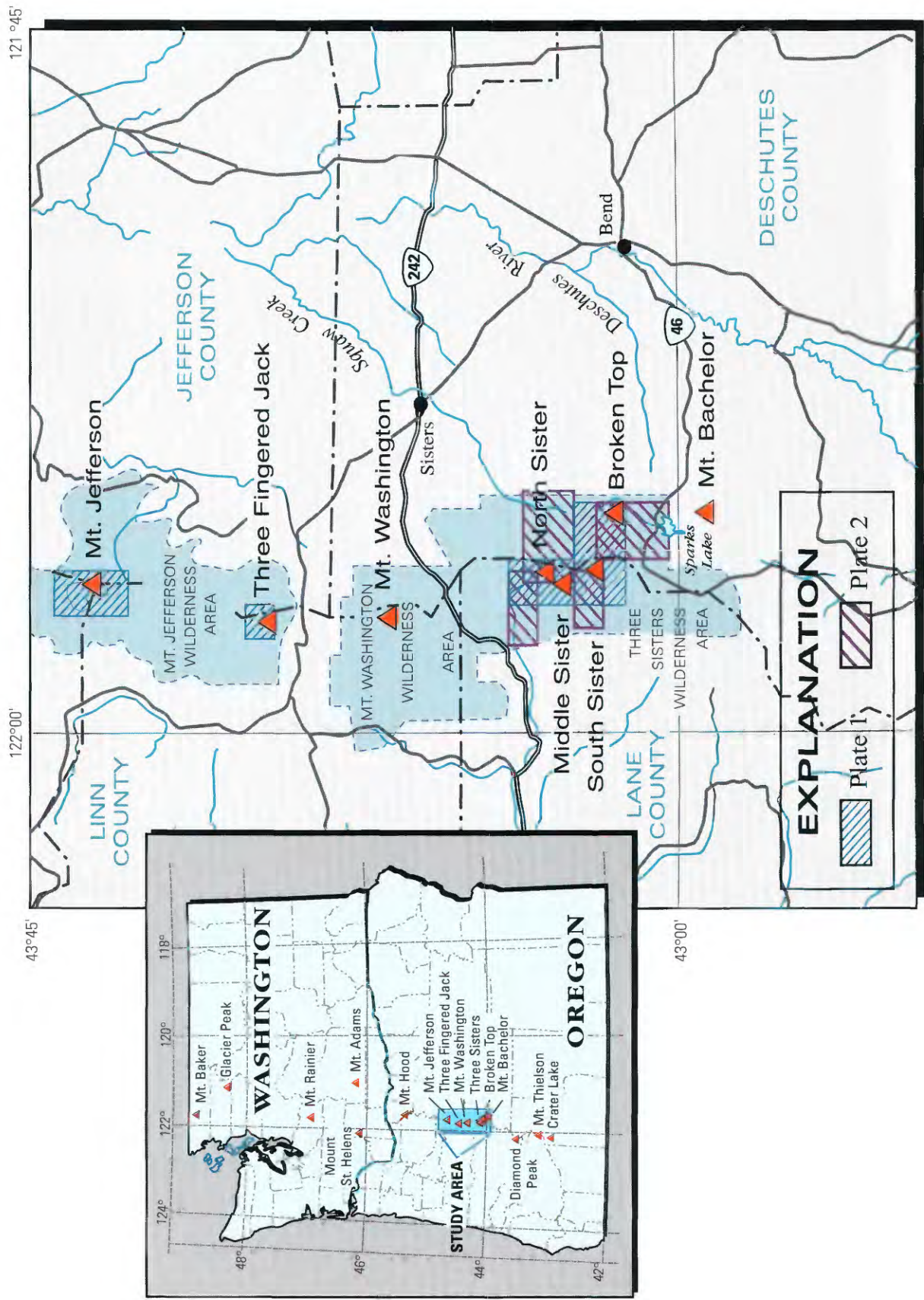


Figure 1. Central Oregon Cascade Range and surrounding area.

intrusive rocks. The crest of the Cascade Range is generally at an altitude of 1,500 to 2,000 m, with several of the high volcanoes exceeding 3,000 m (Callaghan and Buddington, 1938; Sherrod, 1986). The high stratovolcanoes and volcano remnants of the central Oregon Cascade Range include Mount Jefferson, Three Fingered Jack, Mount Washington, the three volcanoes of the Three Sisters, Broken Top, Mount Bachelor, Diamond Peak, Mount Thielsen, and Crater Lake Caldera (Mount Mazama)(fig. 1). These are all Pleistocene stratovolcanoes of rhyolitic to basaltic composition and are formed mostly of interlayered thin lava flows and pyroclastic deposits overlying cinder cone cores. Of the large stratovolcanoes, there has been Holocene volcanic activity on the summit and flanks of South Sister and at Mount Bachelor as well as the caldera-forming eruptions of Mount Mazama (Taylor, 1981; Taylor and others, 1987; Scott, 1989). The general conical morphology is best preserved on the volcanoes of Middle Sister, South Sister, and Mount Bachelor; the rest have been deeply eroded by Pleistocene glaciation.

## Climate and Vegetation

Western Oregon has a temperate maritime climate that is dominated by winter Pacific frontal systems moving eastward across the State. The Cascade Range is a major orographic barrier that intercepts much of the eastward-flowing moisture. Generally warm and dry summers result from northward expansion of the eastern Pacific high pressure system and diversion of the prevailing westerlies to the north. Consequently, precipitation generally occurs during the winter and is greatest at high altitudes. Annual precipitation is about 3,500 to 4,000 mm at the highest elevations within the Three Sisters and Mount Jefferson Wilderness Areas (Taylor, 1993) and falls mostly as snow. At Crater Lake (fig. 1), 90 percent of the 1,620 mm of annual precipitation falls between October 1 and May 31. Annual precipitation decreases eastward across the Oregon Cascade Range, diminishing from more than 2,500 mm on the western slopes to less than 400 mm within 30 km east of the range crest (Taylor, 1993).

The highest peaks of the central Oregon Cascade Range rise above treeline, which is about

2,200 m above sea level on the north side of Mount Jefferson, about 2,300 m on the north side of South Sister, and 2,500 m on the south side of Broken Top. The tallest trees of the subalpine forests and parks near timberline are mountain hemlock (*Tsuga mertensiana*) and whitebark pine (*Pinus albicaulis*).

## Glaciers

The central Oregon Cascade Range peaks that presently sustain glaciers or permanent ice masses are, from north to south, Mount Jefferson, Three Fingered Jack, North Sister, Middle Sister, South Sister, and Broken Top. In addition, Mount Bachelor, Diamond Peak, and Mount Thielsen all had small glaciers that persisted until the end of the Little Ice Age in the early 20th century. The Three Sisters Wilderness Area is the most extensively glacierized region of the central Oregon Cascade Range, with 17 named glaciers that presently cover about 7.5 km<sup>2</sup> (pl. 1). In the Three Sisters and Mount Jefferson Wilderness Areas, name assignments to some glaciers have varied over the years. In this report, we use the names on the current U.S. Geological Survey (USGS) topographic quadrangles (1988 provisional editions) and informally use the names “Jack Glacier” and “East Bend Glacier” for the unmapped glaciers or perennial ice masses in the northeast-facing cirques of Three Fingered Jack and Broken Top.

## Previous Work

Previous studies of debris flows and floods in other recently deglaciated alpine areas complement this analysis of debris flows that resulted from moraine-dammed lake releases in the Mount Jefferson and Three Sisters Wilderness Areas. Jackson (1979), Jackson and others (1989), and Leonard (1985) described the role of recent glacier retreat in promoting the incidence of debris flows and increased sediment flux in the Canadian Rockies. Walder and Driedger (1994) studied the formation of debris flows by incorporation of Neoglacial sediment at Tahoma Creek, Mount Rainier. Lundstrom (1992) analyzed the alpine geomorphology of Eliot Glacier and surrounding moraines on Mount Hood. Osterkamp and others

(1986) and Hupp and others (1987) evaluated the frequency and magnitude of debris flows from glacierized basins on Mount Shasta.

Floods and debris flows originating specifically from moraine-dammed lakes have been reported in Peru (Lliboutry and others, 1977; Reynolds, 1990), Canada (Blown and Church, 1985; Evans, 1987; Clague, 1987; Clague and Evans, 1994), Great Britain (Carling and Glaister, 1987), the Himalayas (Ives, 1986; Vuichard and Zimmermann, 1987; Ding and Liu, 1992), the European Alps (Haeberli, 1983; Eisbacher and Clague, 1984), and the former Soviet Union (Yesenov and Degovets, 1979). For the central Oregon Cascade Range, Laenen and others (1987, 1992) provided a summary of known debris flows from moraine-dammed lakes in the Three Sisters Wilderness Area in their analysis of the hazard posed by failure of the moraine dam impounding Carver Lake. A 1966 debris flow from a moraine-dammed lake on Broken Top was described by Nolf (1966).

## NEOGLACIATION IN THE CENTRAL OREGON CASCADE RANGE

Except for areas subject to recent volcanism, glacial processes and deposits of the last few millennia are the dominant influences on the landforms and deposits of glaciated alpine areas in the Cascade Range. Recent reviews of Holocene glacier fluctuations in the North American Cordillera are provided by Osborn and Luckman (1988), Davis (1988), Grove (1988), Ryder (1989), and Luckman and others (1993).

### Neoglaciation and Little Ice Age Chronology and Deposits

In the central Oregon Cascade Range, sharp-crested, largely unvegetated Neoglacial moraines stand within 2 km of the present glacier termini, contrasting with older, more densely vegetated moraines that are blanketed by Mazama tephra ( $6,845 \pm 50$   $^{14}\text{C}$  yr BP; Bacon, 1983) and on the south flank of Broken Top, scoria from Cayuse Crater ( $>9,520 \pm 100$   $^{14}\text{C}$  yr BP; Scott and

Gardner, 1992). Altitudes of Neoglacial terminal moraines indicate that equilibrium line altitudes (ELA) varied widely but were as much as 200 m below present (fig. 2) (Scott, 1977; Dethier, 1980). The wide variation in their ELA's probably reflects topographic controls on accumulation, insolation, and debris cover of these small glaciers.

### Chronology

In the absence of historical records, periods of glacier retreat and advance are difficult to date accurately. According to the summary of Davis

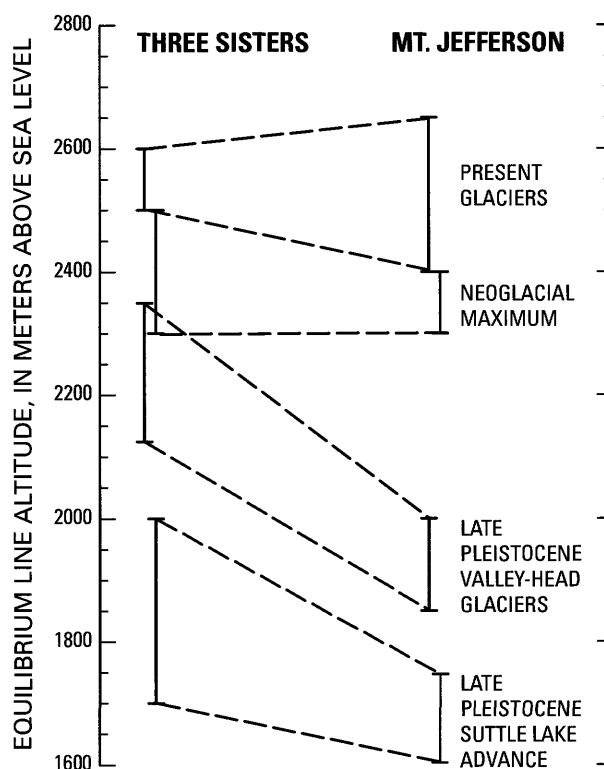


**Figure 2.** Equilibrium line altitudes (ELA) for present and reconstructed late Quaternary glaciers at Mount Jefferson and Three Sisters, Oregon. ELA calculations were based on an accumulation area ration of 0.6. Data for the later Pleistocene Suttle Lake advance and the valley-head (Canyon Creek) glaciers are from Scott (1989, p. 14) and are for glaciers east of the Cascade Range crest. Data for present and Neoglacial ELA's are from this study, (Scott, 1974, p. 68; 1977, fig. 11; 1989, p. 14), and Dethier (1980).

(1988), however, there were at least three periods of advanced ice positions during late Holocene time in the North American Cordillera: (1) a poorly dated early Neoglacial phase believed to date between 5 and 2.5 ka<sup>3</sup>; (2) a middle Neoglacial phase, which is recognized only in the Rocky Mountains of Colorado and Wyoming, where moraines date between 2 and 1 ka; and (3) a late Neoglacial, or Little Ice Age readvance (Davis, 1988). Ages of early Neoglacial and Little Ice Age moraines in the Cascade Range have been determined by tephrochronology, radiometric dating, dendrochronology, and lichenometry. Early Neoglacial advances, all dated by radiocarbon dating of stratigraphically linked deposits, occurred between 5.5 and 3.0 ka at Glacier Peak (Beget, 1984); between 4.0 and 2.0 ka at Mount Rainier (Crandell and Miller, 1964); younger than 4 ka at Mount Adams (Hopkins, 1976); older than 1.5 to 1.8 ka at Mount Hood (Lundstrom, 1992, p. 143); and between 6.8 and 2.1 ka at Broken Top and Mount Bachelor (Scott, 1989). These dates are consistent with results of recent studies in the Canadian Rockies that indicate a period of glacier advance between 3.1 to 2.5 ka (Luckman and others, 1993).

In the Three Sisters and Mount Jefferson Wilderness Areas, most early Neoglacial deposits were removed or buried by Little Ice Age glacier advances during the last few centuries. This is consistent with many observations throughout the world that the Little Ice Age was, in general, the period of most advanced glacier positions of the Holocene (Grove, 1988). Evidence from lichenometric and dendrochronologic studies in Oregon and Washington indicates that glaciers reached maximum downvalley positions during the 17th, 18th, and 19th centuries. At Mount Rainier, which has had the most thoroughly developed Little Ice Age chronology, the outermost terminal moraines of most major glaciers stabilized between 1750 and 1850 AD, and there was general and substantial retreat between 1830 AD and 1950 AD (Crandell and Miller, 1964; Sigafos and

Hendricks, 1972; Burbank, 1981, 1982). The maximum advance of Eliot Glacier on Mount Hood culminated about 1740 AD (Lawrence, 1948; Lundstrom, 1992, p. 118–126).

Late Neoglacial moraines formed by the glaciers of the central Oregon Cascade Range may have stabilized somewhat later than those constructed by the larger glaciers at Mount Rainier and Mount Hood. On Three Fingered Jack, the oldest tree cored on the Neoglacial moraine crest germinated about 1884 (Scott, 1974, p. 81). Similarly, the oldest trees growing on the left lateral moraine of Skinner Glacier, on the north flank of South Sister, germinated about 1865. This evidence indicates that the maximum late Neoglacial advance in the Central Oregon Cascade Range probably culminated in the 1850's and 1860's. A substantially older moraine, however, was formed by a post- 2.3-ka advance of Lewis Glacier. The moraine was not covered by a tephra erupted 2.3 to 2.0 ka (Scott and Gardner, 1992) but does have large mountain hemlocks and whitebark pines growing on it, including one that germinated more than 500 years ago. Although they had thinned substantially, most glaciers in the Three Sisters area remained in contact with Neoglacial-age moraines through the first two decades of the 20th century.

## Neoglacial Deposits

Late Holocene glaciers have effectively eroded and transported a large volume of sediment to proglacial positions. Massive lateral and end moraines, and downstream outwash fans were left as glaciers retreated from early 20th century positions. The lateral and end moraines are large constructional forms with crests rising to at least 120 m above the adjacent terrain (fig. 3). The volume of Neoglacial lateral and end moraines on North, South, and Middle Sisters, determined by using the methods outlined by Lundstrom (1992, p. 137–139), is about 40 million m<sup>3</sup>, equivalent to about 30 percent of the present ice volume (Driedger and Kennard, 1986).

Neoglacial moraines in the study area are composed of poorly sorted bouldery, gravelly, silty sand. The large lateral and end moraines appear to be abandoned “dump moraines” (Small, 1983)

<sup>3</sup> “ka” is an abbreviation for “kilo-annum,” referring to 10<sup>3</sup> years. In this report, dates reported in this format are on the basis of radiocarbon dates that have not been calibrated to a calendar year reference.

formed by supraglacial debris sliding onto the moraine surface from glacier margins that sloped above the moraine crest. Moraine stratigraphy is consistent with this interpretation. Fresh exposures reveal crude layering, defined by strata of varying boulder concentration, dipping orthogonally from the moraine crest at angles of 30° to 40°.

Some of these moraines are possibly ice-cored. Excavations into the moraine impounding Carver Lake exposed glacier ice at depths less than a meter (Rector, 1988). Dense ice was observed in a landslide scar on the proximal face of the end moraine of Thayer Glacier (L.D. Sorensen and M.A. Groesch, Oregon State University, unpub. data, 1982). Scott (1977) inferred that the moraine impounding the proglacial lake on Three Fingered Jack may be ice-cored because of its steepness and wet landslide scars on its proximal face. We observed stagnant glacier ice in the ground

moraine left by Collier Glacier near Collier Cone and near the termini of Skinner and Diller Glaciers.

Many of the proglacial areas are covered with morainal material, stagnant ice, and outwash sediment deposited during the maximum advance of the Little Ice Age and during subsequent retreat, masking most deposits of earlier Neoglacial advances (pl. 1). Little Ice Age moraines are sharp-crested and steep, with side slopes commonly 40° to 45°. Only a few plants are found growing in windblown accumulations of sand and silt on the moraine slopes, and protected boulder surfaces have less than 20 percent lichen cover.

Distinct Neoglacial moraines that predate the Little Ice Age are scarce. Older lateral moraines locally flank Little Ice Age moraines, and, in a few locations, older Neoglacial terminal moraines protrude up to a few hundred meters downvalley



**Figure 3.** View northeast of Neoglacial lateral moraines of Collier Glacier, Oregon, September 8, 1993. Note people on left lateral moraine.

from Little Ice Age moraines (pl. 1, fig. 4). Such pre-Little Ice Age moraines are not mantled with Mazama tephra, readily distinguishing them from late Pleistocene moraines that are found immediately downvalley (Scott, 1989). Pre-Little Ice Age moraines have slightly more rounded crests than do Little Ice Age moraines, and are commonly vegetated with krummholz-form whitebark pines on lee surfaces. Protected boulder surfaces are 50 to 100 percent lichen-covered, and within boulder interstices, there are accumulations of locally oxidized sand and silt several centimeters thick.

For most of these pre-Little Ice Age moraines, it is unclear if they represent advances during the

early Neoglacial (5 to 2 ka), or perhaps later Neoglacial advances. In the southern part of the Three Sisters Wilderness Area, early Neoglacial moraines are distinguished from Little Ice Age and Pleistocene moraines by a 2.3 to 2.0 ka tephra that is found only on these deposits (Dethier, 1980; Scott, 1987). On the basis of tephra relations, moraines that are clearly early Neoglacial (5 to 2 ka) have been mapped beyond the southern portion of Prouty Glacier on South Sister, Bend Glacier on Broken Top (Dethier, 1980), and on Mount Bachelor (Scott, 1987; Scott and Gardner, 1992). Outside the southern part of the Three Sisters Wilderness Area, the 2.3 to 2.0 ka tephra is thin or absent and cannot be used to date pre-Little

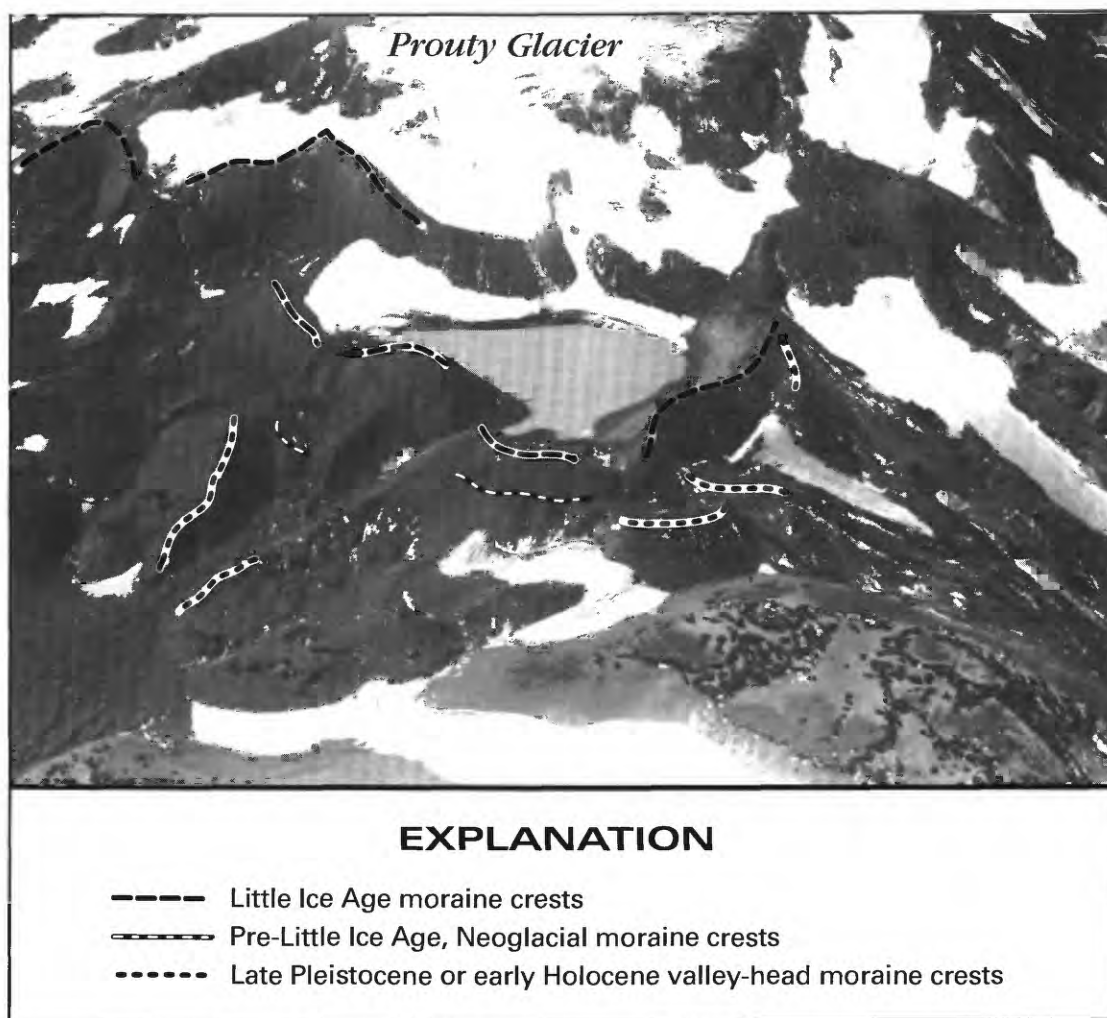


**Figure 4.** View southwest of Carver Lake and terminus of northern lobe of Prouty Glacier, October 1956. Moraine crests of Little Ice Age, pre-Little Ice Age, and late Pleistocene valley-head glaciers are indicated. Photo reproduced with permission of Ackroyd Photography (neg. 7145-65).

Ice Age moraines. Older Neoglacial moraines are possibly correlative with the early Neoglacial moraines described above, or perhaps resulted from a later advance, similar to the 0.5 to 2 ka moraines of Lewis Glacier.

## 19th– and 20th–Century Glacier Behavior

### Glacier Activity

The remarkable shrinkage of Cascade Range glaciers since the late 1800's has set the stage for current geomorphic activity in glacierized basins of the Cascade Range (figs. 5, 6, and 7). Dendrochronologic evidence described above indicates that late Neoglacial moraines in the central Oregon Cascade Range did not stabilize until the mid-1800's. Historical 19th-century records of glacier positions in the central Oregon Cascade Range are restricted to anecdotal accounts by early mountaineers and explorers. J.S. Newberry, geologist for the Pacific Railroad Survey of 1855, viewed glaciers on the volcanoes of the Cascade Range in Oregon, but made no detailed observations. J.S. Diller, of the USGS, reconnoitered the central Oregon Cascade Range in 1883, ascending Mount Thielsen and Diamond Peak. Russell (1885) stated that Diller observed “glaciers of considerable magnitude on Mount Jefferson, Diamond Peak, and the Three Sisters,” and that “the group of peaks known as the Three Sisters is considered by Mr. Diller as probably affording the most interesting field for glacial studies in the United States, with the exception of Alaska.”

Twentieth-century records of central Oregon glaciers begin with the 1903 observations of USGS geologist I.C. Russell (1905). His photographs of several glaciers on the east side of Middle and South Sister (figs. 5A and 6A) show that glaciers abutted against their Neoglacial moraines but had thinned somewhat. Russell (1905, p. 126) recognized this “recent shrinkage,” noting that the margin of Hayden Glacier was 12 to 20 m lower than the moraine crests. Photographs of the north side of Mount Jefferson (Oregon Historical Society neg. 73427) and of Collier Glacier (fig. 7A), taken in the first decade of the 20th century, also reveal

similar relations: by 1910, all glaciers had thinned considerably, but remained in contact with Neoglacial lateral and terminal moraines.

Glacier activity in central Oregon during the first half of the 20th century has been recorded by the Mazamas, an alpine club based in Portland, Oregon. Articles, photographs, and aerial surveys sponsored and published by the Mazamas (Williams, 1916; Hatch, 1917; Research Committee of the Mazamas, 1938; Phillips, 1938; unpub. aerial photographs taken in October, 1956 [available for inspection at the Mazama library, Portland, Oregon]; and Hopson, 1960) document substantial and rapid glacier retreat. These records, combined with photographs from the archives of the Oregon Historical Society and U.S. Forest Service vertical aerial photographs taken in 1949, 1967, 1974, and 1990, provided sufficient information for us to map glacier termini and compute glacier area at various times this century (pl. 1; fig. 8).

The most complete record of historic glacier retreat is for Collier Glacier, which has its source on the northwest flank of Middle Sister (figs. 7 and 9). Collier Glacier is the largest glacier in the central Oregon Cascade Range, presently covering about 0.85 km<sup>2</sup>. At its maximum advance during the Little Ice Age, Collier Glacier covered nearly 2.4 km<sup>2</sup> and had an ELA about 195 m lower than present. The pattern of shrinkage of Collier Glacier, illustrated in figures 10 and 11, was apparently common to most central Oregon Cascade Range glaciers. Substantial reduction in glacier mass during the period between the late Neoglacial maximum (assumed to be about 1850 locally) and about 1910 was accommodated by glacier thinning, whereas termini positions did not retreat substantially from Little Ice Age moraines until early in the 20th century. The response lag probably was due to the large volume of ice stored behind the tall terminal and lateral moraines. Between 1910 and 1950 there was rapid retreat of the Collier Glacier terminus and reduction of glacierized area and ice volume (Hopson, 1960; McDonald, 1995) (fig. 12).

Beginning about 1950, glacier retreat slowed or reversed worldwide (Haerberli and others, 1989). This reversal was also observed in the Cascade Range and Olympic Mountains of Washington,

where, by 1955, most glaciers were advancing (Hubley, 1956; Meier and Post, 1962). Glaciers in the Cascade Range of northern Washington and on Mount Baker and Mount Rainier continued to advance until the late 1970's and early 1980's (Heikkinen, 1984; Driedger, 1986, 1993). Ground and aerial photographs show that most glaciers in the Three Sisters Wilderness Area stabilized at or near positions shown on 1949 photographs (pl. 1; fig. 8), and small lateral and terminal moraines a few meters high formed during the 1960's and 1970's at the margins of many glaciers.

Since the early 1980's, and through the mid-1990's, there has been renewed retreat of glaciers

in the Cascade Range. This recent retreat has been noted in the more extensively glacierized northern Cascades (Pelto, 1993) and on the glacierized volcanoes in Washington State. About 75 percent of northern Cascades glaciers were retreating in 1988 and all glaciers on Mount Baker retreated between 7 and 75 m from 1979 through 1990 (Pelto, 1993). Most termini of glaciers on Mount Rainier have been retreating since the mid 1980's (Driedger, 1993). Termini of many glaciers in the Three Sisters Wilderness Area have retreated several meters from the small terminal moraines formed in the 1960's and 1970's. Glacier retreat between 1967 and 1990 has been more substantial



**Figure 5.** Approximately matched views southeast toward the ablation area of Diller Glacier from near the left lateral moraine at altitude 2,620 m. *A*, Composite of August 16, 1903 (USGS Photographs by I.C. Russell; negs. 815 and 816). These photographs probably were taken from the glacier surface. *B*, Composite of September 12, 1993, photographs taken several meters east (left) of the original photograph. The icefalls and bergschrund are at approximately the same locations, although the glacier has thinned and shrunk substantially. The breached moraine (from September 7, 1970, lake release) is visible near the glacier terminus. (Photographs by David E. Wieprecht, USGS).



**Figure 6.** Approximately matched views northeast toward the terminus of Hayden Glacier from near the right lateral moraine at altitude 2,560 m. *A*, Photograph by I.C. Russell, USGS (neg. 812) taken August 16, 1903; *B*, Photograph by David E. Wieprecht, USGS, taken from the same location on September 12, 1993, shows substantial thinning and shrinkage of Hayden Glacier. There also has been several meters of erosion and lowering of the crest and inner slope of the right lateral moraine between photograph dates, eliminating the double crest noted by Russell (1905, p. 126) and probably contributing to the rubble at the base of the slope.

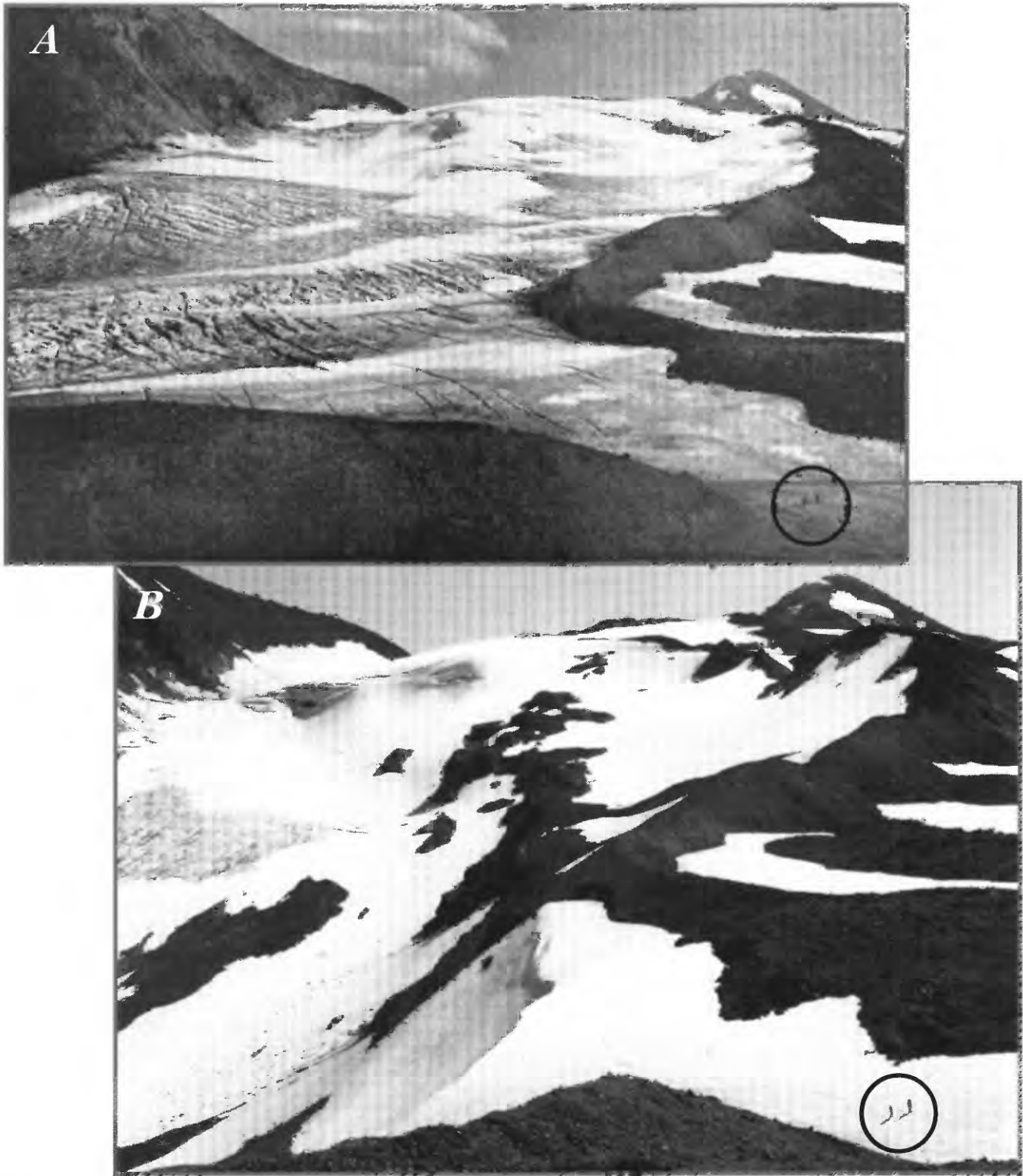


**Figure 7.** Approximately matched views southeast toward Collier Glacier from near the right lateral moraine at elevation 7,600 m. *A*, Photograph by Kiser Photo Co. appears in the 1912 Mazama Annual and is reproduced with permission of the Oregon Historical Society (Photograph 4799, album 663). Based on Mazama Club records, the photograph was probably taken during the 1910 annual summer outing. The glacier surface was several meters below the moraine crest, but still occupied the entire area bound by the moraines. *B*, September 8, 1993 photograph showing present terminus of Collier Glacier and illustrating the remarkable shrinkage during the last 80 years. A large mass movement removed much of the moraine crest visible in the foreground of the 1910 view. (Photograph by David E. Weiprecht, USGS.)

in the Mount Jefferson Wilderness Area where termini of several glaciers have retreated several tens of meters (pl. 1).

## Climatic Forcing

The observed 19th- and 20th-century glacier activity in the central Oregon Cascade Range is likely the result of regional and worldwide warming since the late 19th century. Alpine glaciers respond sensitively to climate, adjusting to periods of positive or negative mass balance by thickening and advancing or thinning and retreating. For Cascade Range glaciers, the changes in temperature or precipitation required to cause a terminus response are quite small. Tangborn (1980) demonstrated that a decrease in mean summer temperature of  $0.5^{\circ}\text{C}$  or an increase in winter snow accumulation by 10 percent is sufficient to overcome the mass balance deficit that accompanied the extreme retreat of northern Cascade glaciers during the first half of this century. Furthermore, the time between climatic perturbation and the consequent terminus response

for Cascade Range glaciers is short—on the order of 1 to 5 years (Hubley, 1956; Burbank, 1982).

Historical temperature changes clearly had a large effect on glacier behavior in the Cascade Range. The profound retreat of glaciers worldwide from late Neoglacial positions accompanies a  $0.45 \pm 0.15^{\circ}\text{C}$  increase in global (combined land and ocean) air temperature since the late 19th century (Folland and others, 1990). On the decadal scale, temperature change has not been monotonic, but irregular, with periods of rapid temperature increase separated by periods of steady or declining temperature. Surface air temperatures measured over land increased in the northern hemisphere by about  $0.4^{\circ}\text{C}$  between 1920 and 1940 (fig. 13). This corresponds to the period of greatest glacier retreat in the central Oregon Cascade Range. Temperatures then decreased by about  $0.2^{\circ}\text{C}$  between 1940 and 1970, resulting in renewed advance of many Cascade Range glaciers, especially in the northern Cascades and at Mount Rainier, and stabilization of the central Oregon Cascade Range glaciers. Temperatures have increased again by about  $0.3^{\circ}\text{C}$  since 1970

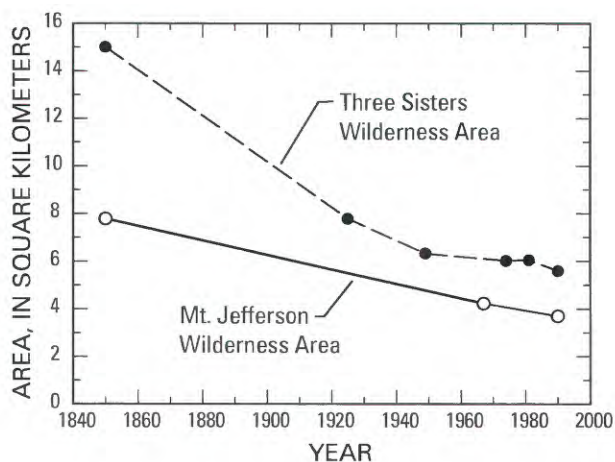


**Figure 8.** Glacier areas of the Three Sisters and Mount Jefferson Wilderness Areas since the culmination of the Little Ice Age (assumed locally to be about 1850). Neoglacial glacier areas measured from planimetry of moraine crests. Glacier areas in the Three Sisters Wilderness Area in 1925 and 1981 are measurements reported in Hodge (1925) and Driedger and Kennard (1986). All other glacier areas were measured from dated vertical aerial photographs.



**Figure 9.** Oblique aerial photograph of Collier Glacier flowing northwest from the saddle between Middle and North Sisters. Photograph by Austin Post, USGS (September 1, 1965, photograph F655-119).

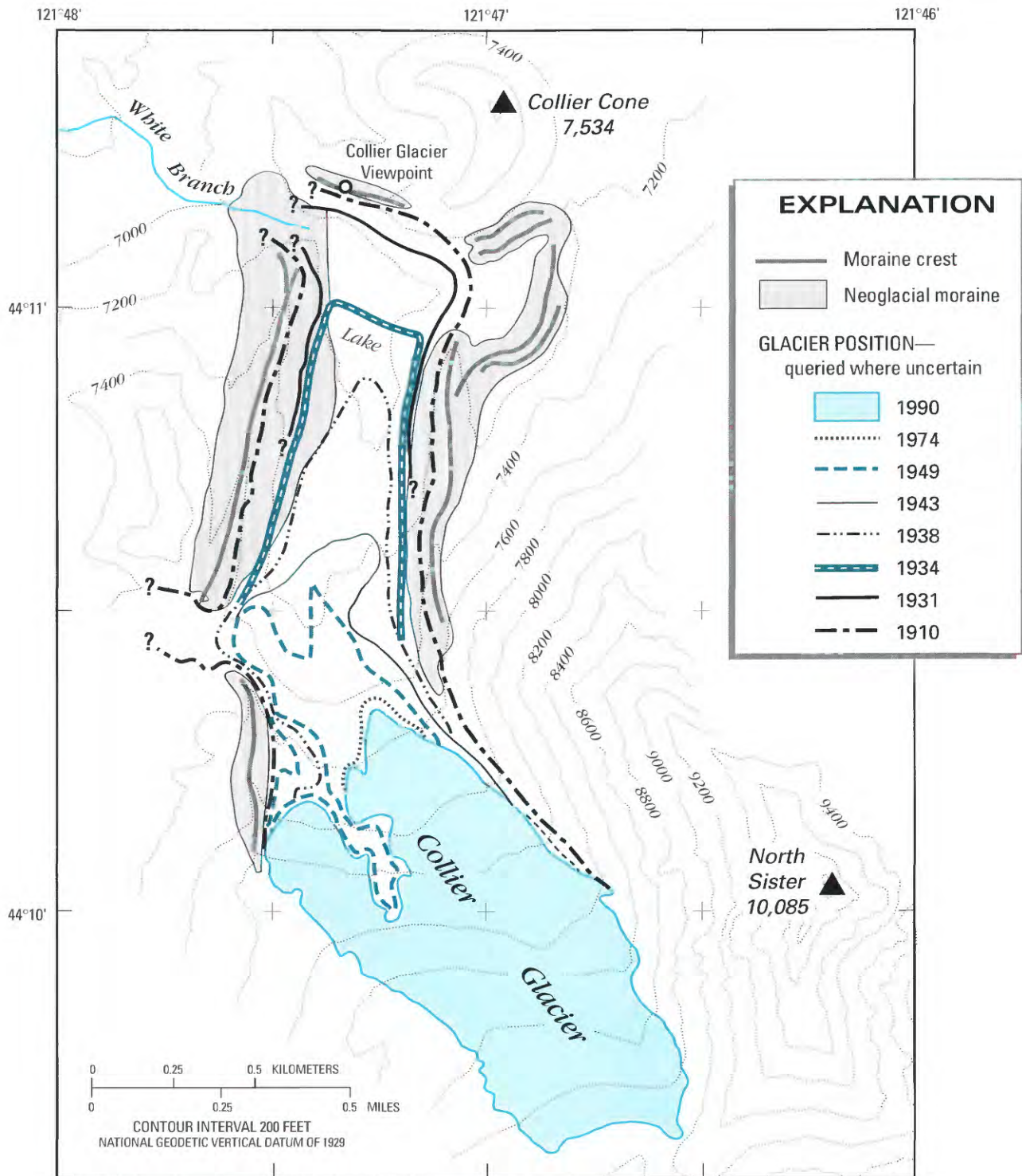


**Figure 10.** The extent of Collier Glacier at several times during the 20th century. The moraine crest approximates the maximum Neoglacial extent in the late 19th century. Limits shown for years 1910 and 1931 are very approximate because they are based on single photographs (fig. 7 and Oregon Historical Society [neg. DB1568]) and inferences from descriptions. Limits for 1934, 1938, and 1943 are from vertical aerial photographs. McDonald (1995) presents a similar, but more detailed analysis of Collier Glacier mass balance and geometry changes since the Little Ice Age.

(Folland and others, 1990). During the 1980's, globally averaged land temperatures have been higher than during any other decade since the middle of the 19th century (Jones, 1988; Hansen and Lebedeff, 1988) (fig. 13).

The latter part of this northern-hemisphere temperature record accords with records from weather stations in Oregon, although regional temperature fluctuations have been greater than those for the entire northern hemisphere (fig. 13). At Corvallis, 115 km west of Mount Jefferson, the average annual temperature rose about 2°C between 1890 and 1940, the period of most rapid historical glacier retreat. The most complete higher-elevation data set that we have found is for Crater Lake National Park (altitude 1,975 m), about 100 km south of the Three Sisters Wilderness Area (fig. 14). Records starting in 1932 indicate an approximate 1°C decline in average daily temperature between 1940 and 1970. Over the same time period, the average daily June, July, and August temperature dropped almost 2°C. In the central Oregon Cascade Range, this temperature decline corresponds to cessation of terminus retreat and formation of small moraines. From 1980 through 1992, average annual temperatures at Crater Lake rose, recouping most of the 1940–1970 drop (fig. 14).

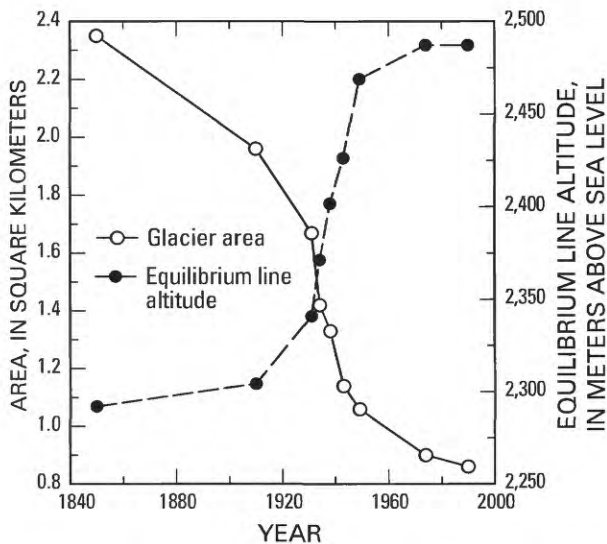


**Figure 11.** Equilibrium line altitude (ELA) (based on an accumulation area ratio of 0.6) and glaciated area at Collier Glacier since the culmination of Neoglacial time.

Cascade Range glaciers respond to the combined influence of winter snowfall accumulation and summer ablation (Tangborn, 1980). At Crater Lake, there has been no apparent relation between precipitation and temperature patterns over the last 60 years (fig. 14). There were two periods, however, when precipitation and temperature anomalies apparently combined to change regional glacier behavior substantially. The halt of rapid glacier retreat and readvance of many glaciers in the 1940's and 1950's corresponds with the temperature decline noted above and a period of higher than average precipitation and winter snowpack (fig. 14). Between 1982 and 1992, there was a substantial decline in precipitation in conjunction with higher average temperatures, which corresponds to the substantial glacier retreat of the late 1980's and early 1990's. During water year 1992, when the warmest average daily temperatures since 1934 combined with one of the driest years of record, the result was substantial glacial mass-balance deficit.

The terminus positions of most central Oregon Cascade Range glaciers have fluctuated in tandem with temperature and precipitation patterns. Some glaciers, however, have responded to nonclimatic influences. For example, the terminus of the southern lobe of Prouty Glacier advanced 450 m between 1949 and 1974 (pl. 1), probably because the glacier was partially insulated by a debris avalanche from Hodge Crest that occurred during that time period. Similar debris avalanches appear to have affected the mass balances and termini behavior of Lost Creek Glacier and the northern lobe of Diller Glacier. The termini of Thayer Glacier on the east flank of North Sister and East Bend Glacier on Broken Top calve into moraine-dammed lakes. Consequently, their positions have not changed substantially since the formation of the lakes in the 1920's.

## MORaine-DAMMED LAKES

### Distribution

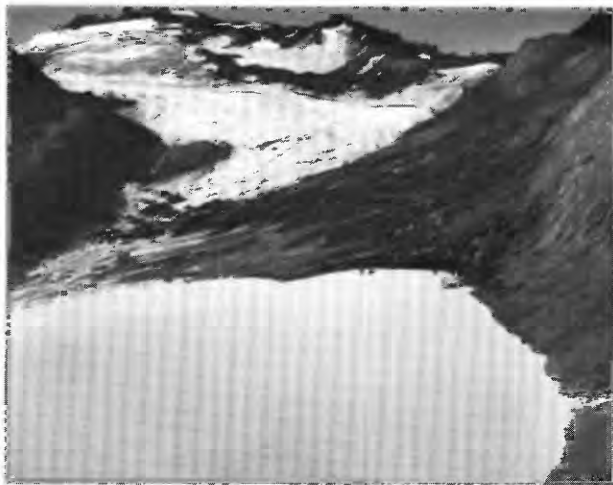
In the wake of rapid glacier retreat during the first part of the 20th century, lakes dammed by Neoglacial moraines have formed in most glacierized regions of the world. Thirty-five



1934



1938



1940



1942



1949



1960

**Figure 12.** Sequence of photographs from Collier Glacier viewpoint (fig. 10), reproduced with permission of R.H. Keen. Photographs show the retreat and thinning of Collier Glacier and the growth and demise of the proglacial moraine-dammed lake. The lake breached the moraine dam and partially emptied in July 1942 at the site of the former outlet through the left lateral moraine (on the right edge of the photographs).

moraine-dammed lakes have been documented in the Cordillera Blanca of the Peruvian Andes (Lliboutry and others, 1977). At least 29 of these lakes formed prior to 1950, and at least 9 more formed between 1932 and 1950. About 130 lakes dammed by Neoglacial moraines have been identified in the Himalaya of Nepal and Tibet (Fushimi and others, 1985; Vuichard and Zimmermann, 1987; Liu and Sharma, 1988; Ding and Liu, 1992). Moraine-dammed lakes also exist in mountain ranges in Kazakhstan, Asia (Yesenov and Degovets, 1979; Popov, 1990), the European Alps (Eisbacher and Clague, 1984; Haeberli, 1983; Dutto and Mortara, 1992), and the Canadian Cordillera (Clague and others, 1985; Blown and Church, 1985; Evans, 1987; Clague and Evans, 1992, 1994).

Several dozen proglacial lakes formed this century in the Cascade Range in areas abandoned by Neoglacial-age glaciers. Basins of most of these lakes are partly rimmed by resistant bedrock barriers, but several are completely bounded by Neoglacial lateral and terminal moraines (table 1). The highest concentration of past and present Neoglacial moraine-dammed lakes in the conterminous United States is in the central Oregon Cascade Range. There are seven moraine-dammed lakes in the Three Sisters Wilderness Area and one in the Mount Jefferson Wilderness Area that have surface areas larger than 5,000 m<sup>2</sup> (table 1; figs. 15, 16, and 17). In addition, there were five other moraine-dammed lakes with surface areas as great as 10<sup>5</sup> m<sup>2</sup> that existed as long as 40 years before breaching their morainal dams. This high

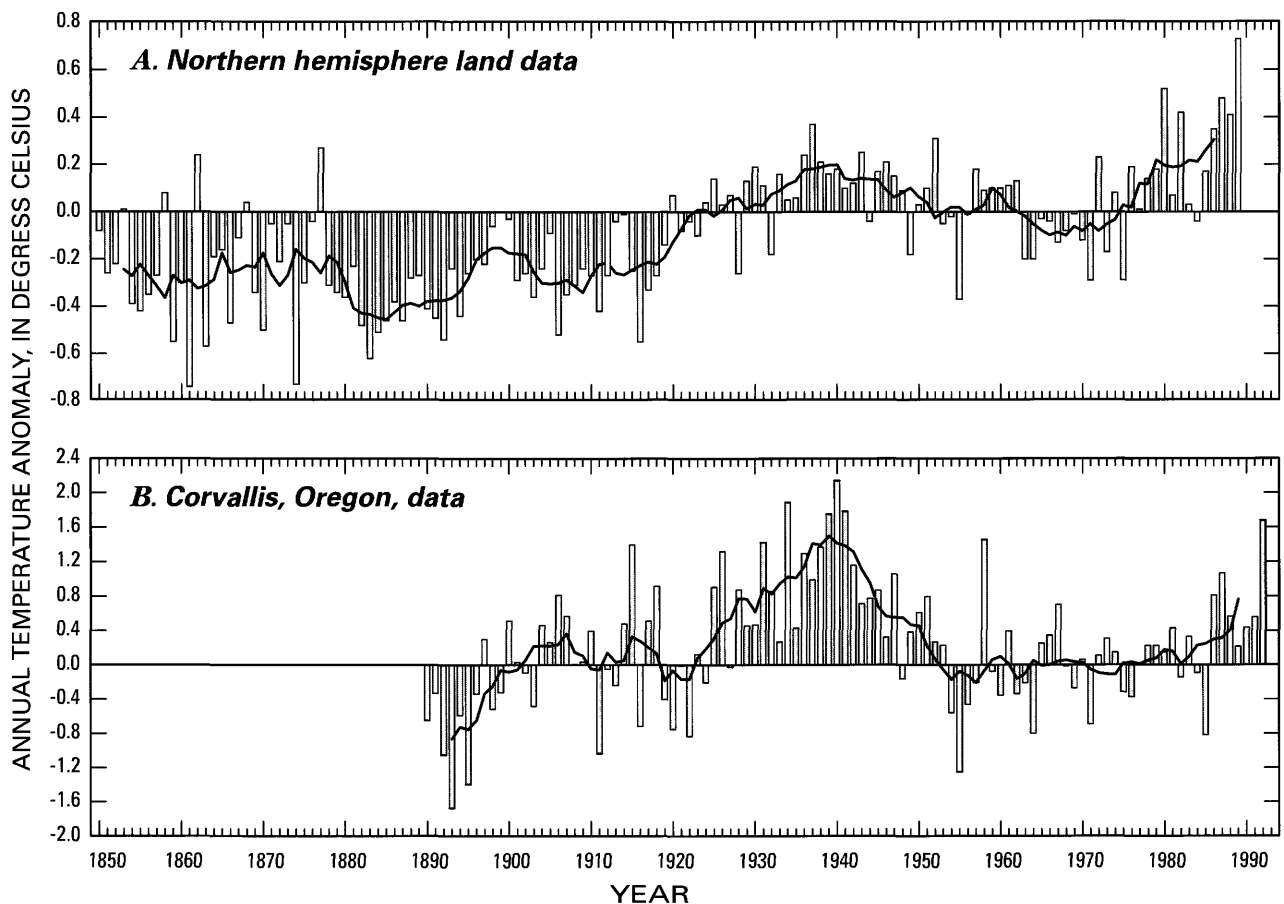


**Figure 13.** Measured mean annual temperature, portrayed as anomalies from 1951–1970 averages. Curves are 7-year moving averages. *A*, Average northern hemisphere land data from Jones and Bradley (1992); *B*, Average annual temperature at Corvallis, Oregon (data from Western Regional Climate Center, Reno, Nevada).

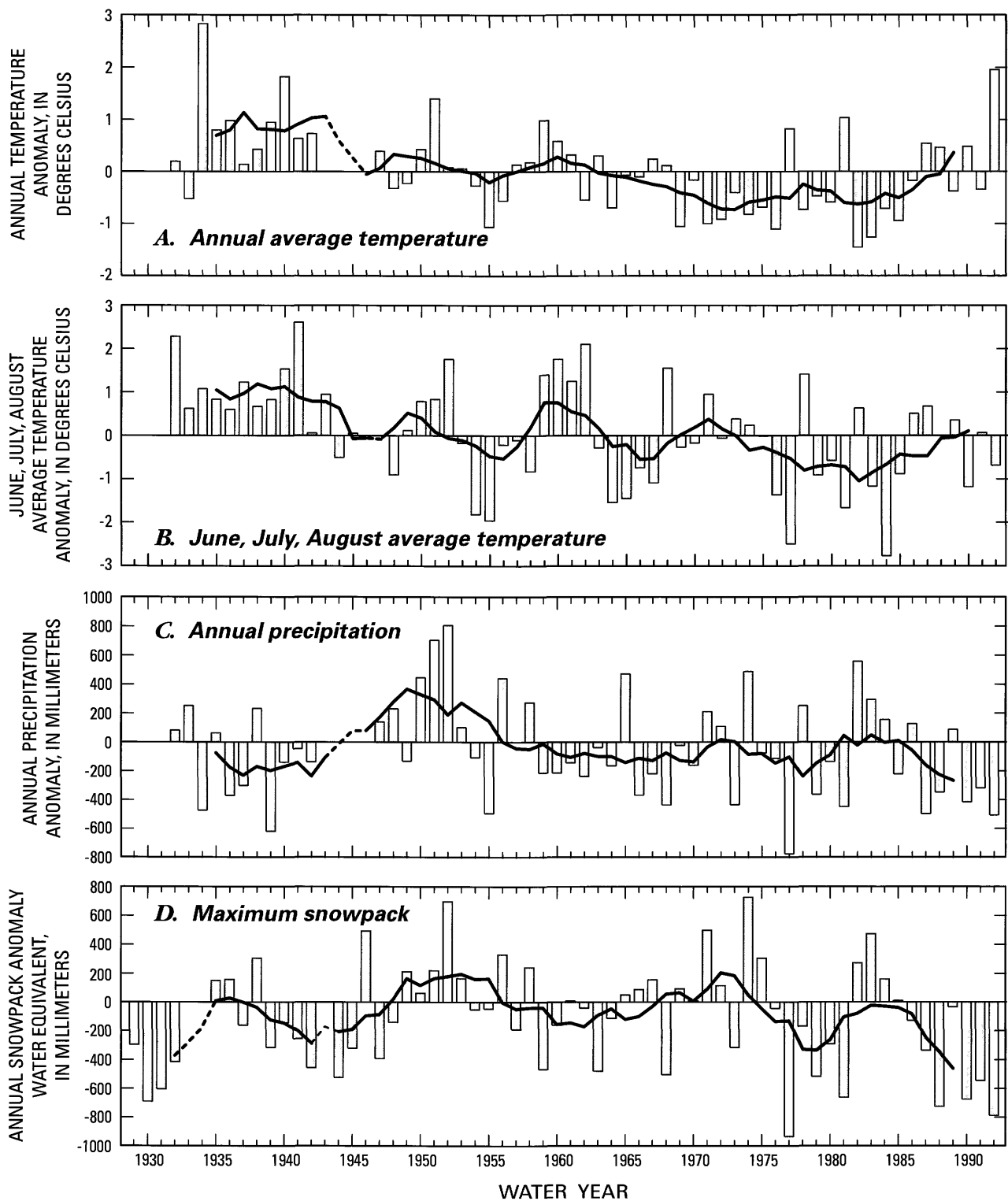


**Figure 14.** Annual climate data for Crater Lake, Oregon (elevation 1,975 m). Data are plotted as anomalies from 1951–1970 average. Curves are 7-year moving averages. All data are plotted for water years (October 1 to September 30). *A*, Annual average temperature; *B*, June, July, and August average temperature; *C*, Annual precipitation. Dashed line indicates incomplete or missing records. Data from Western Regional Climatic Center, Reno, Nevada. *D*, Maximum annual snowpack at Annie Springs, Crater Lake, Oregon (1,835 m). Data from Natural Resources Conservation Service, Portland, Oregon.

**Table 1. Lakes dammed by Neoglacial Moraines in the Cascade Range, Oregon and Washington**

[This list of lakes is based on inspections of aerial photographs maintained in U.S. Forest Service, National Park Service, and U.S. Geological Survey office collections. Dates of photographs range from 1970 to 1992. Areas of present glaciers and lakes measured from aerial photographs and current U.S. Geological Survey topographic maps. Maximum Neoglacial glacier areas based on photointerpretation. The indicated release potential ranges from 1 (highest) to 3 (lowest) and is based on qualitative assessment of the topography of the lake setting (fig. 62). For areas outside the Mount Jefferson and Three Sister Wilderness Areas, this assessment is based solely on photograph inspection. km<sup>2</sup>, square kilometers; m<sup>2</sup>, square meters; m, meters; —, unnamed; Mtn., mountain]

USGS 7.5 min. quadrangle	Glacier	Maximum Neoglacial glacier area (km <sup>2</sup> )	Present glacier area (km <sup>2</sup> )	Lake area (m <sup>2</sup> )	Lake altitude (m)	Latitude (decimal degrees north)	Longitude (decimal degrees west)	Release potential	Comments
Forbidden Peak, Washington	—	0.4	0.1	40,000	1,570	48.587	121.125	1	Lake drains over steep, sharp-crested moraine.
Mount Shuksan, Washington	Price Glacier	2.9	1.5	180,000	1,190	48.863	121.600	3	Large lake drains over multiple broad-crested end moraines.
Mount Baker, Washington	Sholes Glacier	2.5	1.1	20,000	1,600	48.803	121.759	1	Steep subaerial outlet. Glacier calves into lake.
Mount Challenger, Washington	—	2.6	1.2	27,000	1,110	47.540	121.425	1	Deep lake drains over steep, 100-m high moraine.
Mount Challenger, Washington	(2 km west-south- west of Luna Peak)	.7	.3	51,000	1,490	48.823	121.295	1	Large, deep lake drains over sharp crest of tall, steep moraine. Lake lies below steep, 600-m high ridge of rock and ice.
Mount Triumph, Washington	(1 km north of Triumph Pass)	.3	.1	34,000	1,460	48.715	121.367	1	Lake drains over steep, partially breached moraine. Campground about 13 km downstream.

**Table 1. Lakes dammed by Neoglacial Moraines in the Cascade Range, Oregon and Washington—Continued**

USGS 7.5 min. quadrangle	Glacier	Maximum Neoglacial glacier area (km <sup>2</sup> )		Present glacier area (km <sup>2</sup> )	Lake area (m <sup>2</sup> )	Lake altitude (m)	Latitude (decimal degrees north)	Longitude (decimal degrees west)	Release potential	Comments
Damnation Peak, WA	(5 km southwest of Mount Despair)	0.2	0.1	0.1	19,000	1,335	48.709	121.438	1	Small lake drains over steep, sharp-crested moraine.  Lake lies below 600 m high ridge of rock and ice.
Downey Mtn., Washington	(5 km north of Bench Lake)	.8	.4	.4	15,000	1,690	48.368	121.133	1	Lake drains through small incision in terminal moraine.  Lake area has increased by a factor of five between 1958 and 1985.
Snowking Mtn., Washington	(2 km south of Snowking Mtn.)	.8	.4	.4	60,000	1,770	48.395	121.283	3	Lake is growing as glacier retreats.  Outlet presently on bedrock, but large release prior to 1955.
Snowking Mtn., Washington	(2 km southeast of Snowking Mtn.)	1.0	.3	.3	45,000	1,540	48.400	121.257	2	Lake drains over moraine, but bedrock appears to be close to outlet level.  Outlet gradient is low.
Big Snow Mtn., Washington	(1 km northwest of Overcoat Peak)	.4	0	0	45,000	1,755	47.517	121.302	2	Lake presently does not drain subaerially.

**Table 1. Lakes dammed by Neoglacial Moraines in the Cascade Range, Oregon and Washington—Continued**

USGS 7.5 min. quadrangle	Glacier	Maximum Neoglacial glacier area (km <sup>2</sup> )	Present glacier area (km <sup>2</sup> )	Lake name	Lake area (m <sup>2</sup> )	Lake altitude (m)	Latitude (decimal degrees north)	Longitude (decimal degrees west)	Release potential	Comments
Blanca Lake, Washington	(2 km east-south- east of Monte Cristo Peak)	0.4	0.1	Goblin Lake	11,000	1,265	47.965	121.313	1	Lake drains over partially breached moraine.
Glacier Peak West, Washington	White Chuck Glacier	4.8	2.8	—	36,000	1,960	48.058	121.132	2	Drains over moraine.
Lime Mountain, Washington	Milk Lake	.9	.5	Milk Lake	100,000	1,835	48.153	121.150	1	Growing lake in front of calving glacier.
Walupt Lake, Washington	Conrad Glacier	1.2	.6	—	35,000	1,955	46.498	121.402	2	Lake drains over moraine.
Mount Adams East, Washington	Gorchen	.6	.3	—	10,000	2,180	46.160	122.575	2	No subaerial drainage and several meters of freeboard.
Mount Adams West, Washington	Adams Glacier (north lobe)	.8	.6	—	18,000	2,290	46.235	121.511	2	Shallow Lake, low gradient outlet.
<b>Mount Jefferson and Three Sisters Wilderness Areas</b>										
Three Fingered Jack, Oregon	Jack Glacier	.1	.01	—	6,000	2,180	44.483	121.838	1	Lake drains over steep outlet.
North Sister, Oregon	Thayer Glacier	.29	.1	—	40,000	2,330	44.163	121.758	2	Lake has 7.5 m of freeboard.

**Table 1. Lakes dammed by Neoglacial Moraines in the Cascade Range, Oregon and Washington—Continued**

USGS 7.5 min. quadrangle	Glacier	Maximum		Present glacier area (km <sup>2</sup> )	Lake area (m <sup>2</sup> )	Lake altitude (m)	Latitude (decimal degrees north)	Longitude (decimal degrees west)	Release potential	Comments
		Neoglacial glacier area (km <sup>2</sup> )	Glacier							
South Sister, Oregon	Carver Glacier	1.4	0.2	26,000	2,190	44.125	121.85	3	Lake has 26 m of freeboard.	
South Sister, Oregon	Carver Glacier	1.4	.2	9,000	2,200	44.125	121.833	3	Lake has 0.2 m of freeboard. Low-gradient outlet.	
South Sister, Oregon	Carver Glacier	1.4	.02	13,000	2,210	44.123	121.85	3	Low-gradient outlet.	
South Sister, Oregon	Prouty Glacier	1.9	1.1	70,000	2,385	44.115	121.755	1	Large lake with steep outlet over moraine.	
South Sister, Oregon	Lewis Glacier	1.3	.3	5,000	2,695	44.092	121.768	2	Small lake with several meters of freeboard.	
Broken Top, Oregon	East Bend Glacier	.2	.05	30,000	2,440	44.082	121.687	1	Lake drains over partially breached moraine.	



**A**, Jack Glacier is mostly shaded by the serrated ridge of Three Fingered Jack in this westward view. The 26,500 m<sup>3</sup> lake with its steep outlet probably formed after 1930 as the glacier retreated from the sharp-crested moraine that now dams the lake. Photograph by Austin Post (R21-51), September 21, 1960.

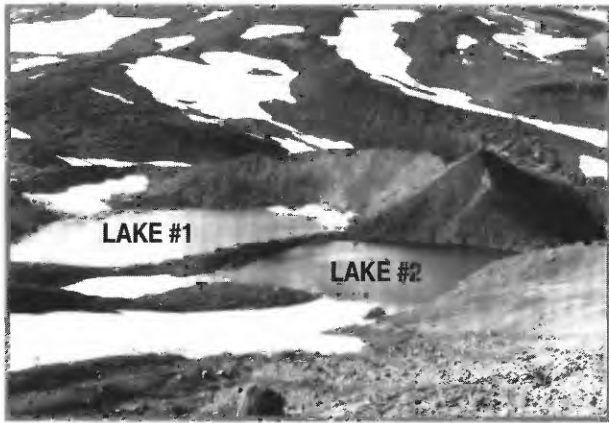


**B**, View north-northeast of the lake at terminus of Thayer Glacier, North Sister. At the time of this photograph, September 14, 1991, the lake surface was 7.5 m below the level of the surface outlet through the notch in the moraine. The lake presently drains through the moraine, with water exiting from several springs 100–110 m below the lake surface on the outer moraine slope. At the present lake level, the impounded volume is 360,000 m<sup>3</sup>, but the lake would contain twice this volume if it filled to the level of the surface outlet.



**C**, Aerial view of Diller Glacier, Middle Sister, showing the glacier calving into the moraine-dammed lake that breached September 7, 1970. Photograph by Austin Post (R21-74), September 21, 1960.

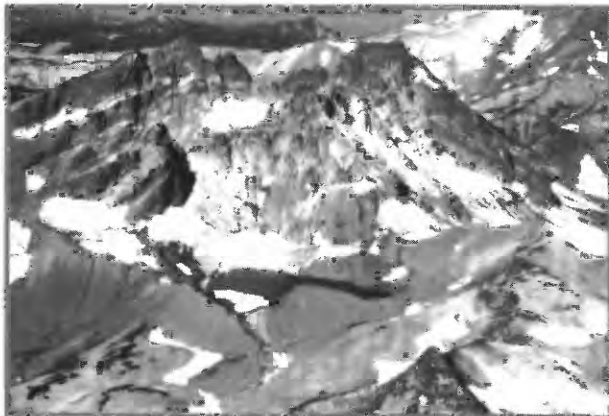
**Figure 15.** Moraine-dammed lakes in the Three Sisters and Mount Jefferson Wilderness Areas, Oregon.



*D*, View north of Chambers Lakes No. 1 and No. 2. At the time of September 10, 1991, surveys of the basins, Chambers Lake No. 1 had a volume of 260,000 m<sup>3</sup> and 26 m of freeboard; Chambers Lake No. 2 had a volume of 70,000 m<sup>3</sup> and 0.2 m of freeboard. Photograph by Robert L. Schuster, USGS.



*E*, Oblique aerial view of Carver Lake impounded by Neoglacial moraines at the terminus of Prouty Glacier on South Sister. Carver Lake is the largest of the moraine-dammed lakes in the Oregon Cascade Range, with a surface area of 700,000 m<sup>2</sup> and a volume of 900,000 m<sup>3</sup>. Photograph courtesy of U.S. Department of Agriculture, Forest Service, September 3, 1986.



*F*, Oblique aerial view of lake at the terminus of East Bend Glacier on Broken Top. Prominent notch at outlet was cut October 7, 1966, when 140,000 m<sup>3</sup> of water escaped in conjunction with 4.4 m of lake-level lowering.

**Figure 15**—Continued. Moraine-dammed lakes in the Three Sisters and Mount Jefferson Wilderness Areas, Oregon.

concentration of moraine-dammed lakes is unique in respect to the rest of the Cascade Range. On other Cascade Range volcanoes, we have identified only nine other lakes that are partly impounded by Neoglacial moraines; two are on Mount Adams, one is in the Goat Rocks Wilderness Area (between Mount Adams and Mount Rainier), two are near Glacier Peak, and one is on Mount Baker. There

are, however, at least 10 other moraine-dammed lakes on nonvolcanic peaks in the Cascade Range (table 1).

## Chronology

Historical maps, climbers' accounts, newspaper reports, and photographs document that

most lakes dammed by Neoglacial moraines in the central Oregon Cascade Range formed in the 1920's and 1930's during rapid glacier retreat (fig. 16). The best documented is the lake bounded by moraines of Collier Glacier. Hopson (1960) documented the growth and demise of this lake in a series of photographs taken between 1934 and 1960 (fig. 12), noting that the lake formed in 1934; photographs show that the lake had not yet formed in 1931 when the terminus of Collier Glacier still impinged on Collier Cone (Oregon Historical Society photograph, neg. DB-1568). Some moraine-dammed lakes existed for very short times before rupturing their bounding moraines. For example, two small lakes at the termini of lobes of

Whitewater Glacier on Mount Jefferson, and a small water body at the terminus of the central lobe of Eugene Glacier on South Sister, possibly formed the same summer as their release. Since about 1940, all long-lived lakes, except Carver Lake and Chambers Lakes No. 1, No. 2, and No. 3 have become smaller (fig. 16). Carver Lake and Chambers Lakes No. 1 and No. 2 have remained the same size; Chambers Lake No. 3 grew between 1931 and 1949 as Carver Glacier retreated. The remainder of the lakes have shrunk, either by eroding outlets into their morainal dams, or by establishing subsurface drainage that has caused lake levels to drop below outlet elevations.

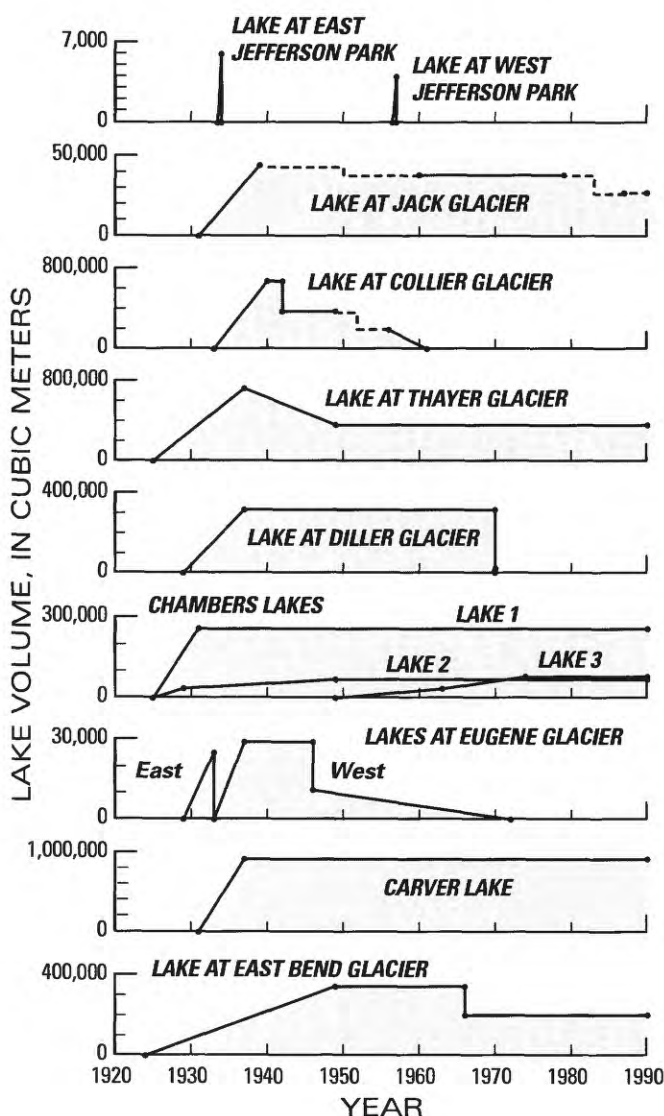


**Figure 16.** Moraine-dammed lake chronologies for lakes in the Three Sisters and Mount Jefferson Wilderness Areas, Oregon. Lake volumes are from surveys of the lake basins at Jack Glacier, Collier Glacier, Thayer Glacier, Diller Glacier, East Bend Glacier, Chambers Lakes No. 1 and No. 2, and Carver Lake. Volumes of the lakes at the termini of Eugene and Whitewater Glaciers and Chambers Lake No. 3 were determined on the basis of estimates of lake area (from aerial photographs and field measurements) and a generalized area-volume relation for moraine-dammed lakes (see fig. 18). Data points are dates of information regarding lake presence and size. This information is primarily from historic photographs, climbers' accounts, newspaper reports, dated topographic maps, and aerial photographs. Dashed lines show magnitudes of lake releases where the date of the breach is only known to the constraints indicated by the adjacent solid circles. Vertical lines between solid circles indicate lake releases at known or inferred dates by partial or complete breach of the moraine dam. Because of insufficient information, this diagram does not include the small lake at the terminus of Waldo Glacier on Mount Jefferson.

## Lake Basin Bathymetry and Topography

We surveyed bathymetry and topography of five of the moraine-dammed lakes and lake basins in the Three Sisters Wilderness Area. Laenen and others (1992 and unpub. data) surveyed two additional lakes. The results of these surveys are shown in figure 17 and lake-basin hypsometric relations are shown in figure 18. Measured areas of existing lakes range from 6,000 to 30,000 m<sup>2</sup>. At its maximum extent, however, the lake at the terminus of Collier Glacier covered 100,000 m<sup>2</sup>. Past and present volumes range from 30,000 m<sup>3</sup> to Carver Lake's 900,000 m<sup>3</sup>. The lakes at the termini of Thayer and Collier Glaciers had, at their maximum extent, volumes of approximately 700,000 m<sup>3</sup>.

Because all the lakes, except for the lake at the terminus of Collier Glacier, were dammed by tall Neoglacial moraines emplaced on steep slopes, they have relatively large depths for their areas. The maximum depth of Carver Lake is about 33 m. Likewise, the lakes bounded by the termini of Thayer, Diller, and East Bend Glaciers had maximum depths of at least 20 m. The basin in front of Collier Glacier is broader and more shallow than the other proglacial lake basins at their maximum extent (fig. 18). Consequently, the lake at the terminus of Collier Glacier had a maximum depth of only 10 m, but a volume of 700,000 m<sup>3</sup>.

## Formation and Preservation of Moraine-Dammed Lakes

Moraine-dammed lakes form where glaciers have retreated from moraines sufficiently high and impervious to impound drainage from the glacial basin. This process requires conditions similar to those of the last few centuries, including (1) a prolonged period of relatively stable glacier terminus positions resulting in large lateral and terminal moraines and (2) a subsequent period of substantial and rapid glacier retreat. In the Cascade Range, moraine-dammed lakes are associated with small cirque and valley glaciers that had maximum Neoglacial areas of 0.13 to 2.9 km<sup>2</sup> (table 1). Larger glaciers in the Cascade Range probably

generated meltwater discharges great enough to maintain a graded profile through the morainal sediment. The largest glaciers to have moraine-dammed lakes form, such as Collier Glacier in the Three Sisters Wilderness Area and Price Glacier in the North Cascades, Washington, terminate on low-gradient valley floors where competence of meltwater streams was low. Here, terminal and lateral moraines impounded large, shallow lakes. Glaciers with Neoglacial areas less than about 0.15 km<sup>2</sup> apparently did not deposit terminal and lateral moraines large enough to impound proglacial lakes.

## DEBRIS FLOWS FROM LAKES DAMMED BY NEOGLACIAL MORAINES

### General Features

Lakes that formed behind Neoglacial moraines have been known to pose significant hazards for several decades. Most of the attention to these hazards has been outside the United States, where there have been accounts of about 60 floods and debris flows from rapid lake releases (table 2). Most reported incidents have been in glacierized areas of the European Alps (Eisbacher and Clague, 1984), the Andes and Cordillera Blanca of Peru (Lliboutry and others, 1977; Reynolds, 1992), and the Himalayas of Nepal and Tibet (Ives, 1986; Vuichard and Zimmerman, 1987; Xu, 1988; Ding and Liu, 1992). These alpine areas are more intensely developed than those in North America; consequently, alpine floods and debris flows triggered by various processes, including moraine-dam failures, have caused substantial property damage (Eisbacher and Clague, 1984; Evans, 1987). Because of the generally higher population densities in these areas, several outburst floods from moraine-dammed lakes have been lethal. For example, 6,000 people perished after rapid breaching of the moraine impounding Laguna Cohup in the Cordillera Blanca of Peru (Ericksen and others, 1970; Lliboutry and others, 1977). After the Laguna Cohup disaster, a program was established in Peru to lower levels of several moraine-dammed lakes that were perceived to be dangerous (Lliboutry and others, 1977). Likewise,

inventories of potentially hazardous glacial lakes have been completed in the Himalayas (Ives, 1986; Liu and Sharma, 1988) where debris flows and floods from moraine-dammed lake releases and glacial outburst floods pose risks to potential and developed sites of hydroelectric facilities.

The absence of intense development in alpine areas of North America generally restricts the hazards of moraine-dammed lakes to recreationists and their associated facilities. In this regard, the U.S. Department of Agriculture, Forest Service, has issued a "hazard alert" for moraine-dammed Carver Lake in the Three Sisters Wilderness Area. In British Columbia, the potential of floods and debris flows from moraine-dammed lakes has received interest because of potential hazards to hydroelectric facilities (Blown and Church, 1985).

## Indirect Discharge Estimation Methods

A key aspect of analysis of debris flows in the central Oregon Cascade Range was the use of indirect discharge estimation methods to determine peak discharges resulting from moraine-dammed lake releases. Two primary discharge-estimation methods were used and they are described in this report as the "velocity-area" and "critical-flow" methods. These methods are modified for the purposes of this study from those described by Barnes and Davidian (1978). These methods of calculating debris-flow discharges are approximate and are not intended to yield discharge estimates that are as accurate as those normally published for water flows by the USGS.

## Velocity-Area Discharge Estimates

Velocity-area discharge estimates were obtained simply by computing the product of the channel cross-sectional area at peak stage and an estimate of flow velocity. For this study, cross sectional areas were surveyed in the field, either by electronic distance meter or by tape and Abney level. Maximum flow stage was determined by surveying the highest evidence of inundation at the cross section. Such evidence included flow deposits, tops of boulder levees or berms, organic debris accumulations, and tree scars. Debris-flow

velocity was assumed to be between 3 and 6 m/s and results were presented as a discharge range on the basis of this range of velocity values.

The assumed velocity range of 3 to 6 m/s is based on observed velocities of rubbly debris flows in other alpine environments. Examples from moraine-dammed lakes and glacial outburst floods include measurements and estimates of 5.5 to 7 m/s in the Swiss Alps (Haeberli, 1983), 5 to 6 m/s for the flow from the moraine-dammed lake release of Midui Lake, Tibet (Li and You, 1992), 4 to 5 m/s velocity for the flood wave from the release of moraine-dammed Dig Tsho, Nepal (Vuichard and Zimmerman, 1987), 3.8 m/s velocity for the flood wave resulting from the 1977 moraine breach on the Dudh Kosi River, Nepal (Buchroithner and others, 1982), and 4 to 8 m/s at the Chemolgan Debris Flow Testing Ground, Kazakhstan (Khegai and others, 1992). Higher velocities have also been measured for the largest flows from moraine-dammed lakes. Notable examples include (1) the *alluvions* in the Cordillera Blanca that resulted from releases of Lago Ayhuinyarahu and Laguna Jancarurish and apparently had velocities of about 9 m/s judging from Liboutry and others (1977) account of flood wave arrival times, and (2) the debris flow resulting from the breach of Moraine Lake number 13 in Kazakhstan for which Yesenov and Degovets (1979) reported velocities of 12 to 15 m/s.

Velocities measured for rubbly alpine debris flows triggered by mechanisms other than natural dam failures include 2.5 m/s at Mayflower Gulch, Colorado (Curry, 1966), 5.5 m/s in the Cathedral Mountains, Canada (Jackson and others, 1989), 5 m/s at Bullock Creek, New Zealand (Pierson, 1980), 1.2 to 4.4 m/s at Wrightwood Canyon, California (Sharp and Nobles, 1953), 7 m/s at Charles Creek, Canada (VanDine, 1985), and 3.4 to 4 m/s at Monument Creek, Arizona (Webb and others, 1988).

The 3 to 6 m/s velocity range assumed for the debris flows in the Three Sisters and Mount Jefferson Wilderness Areas encompasses most of the reported velocities of rubbly debris flows in a variety of environments. It is possible, however, that at some cross sections debris-flow velocities were outside of the 3 to 6 m/s velocity range, and in these locations the reported discharge range

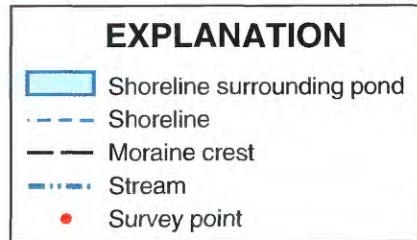
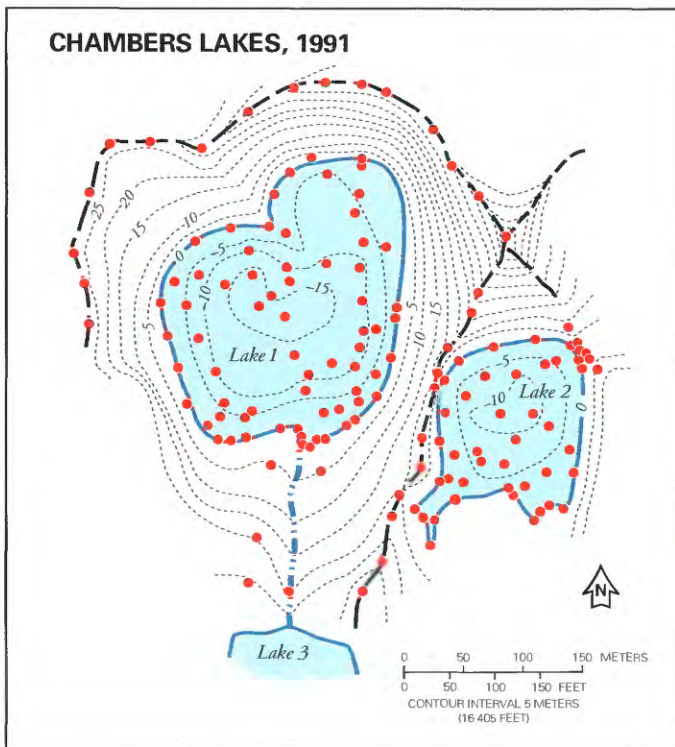
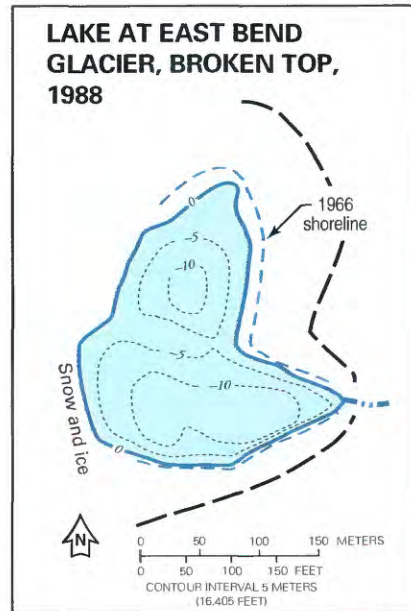
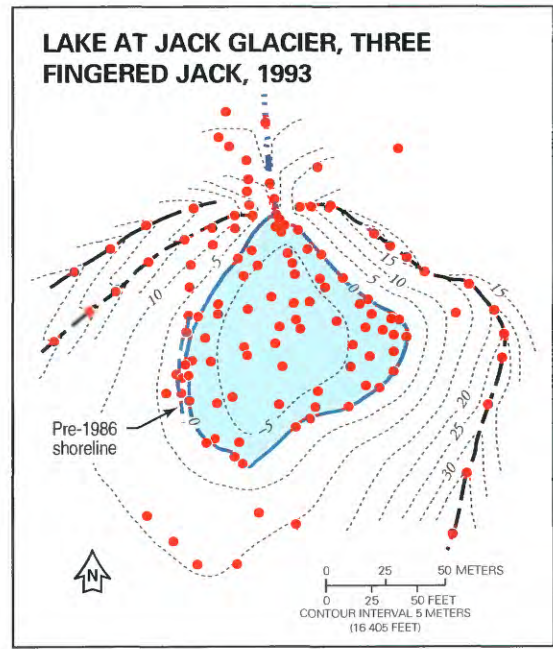
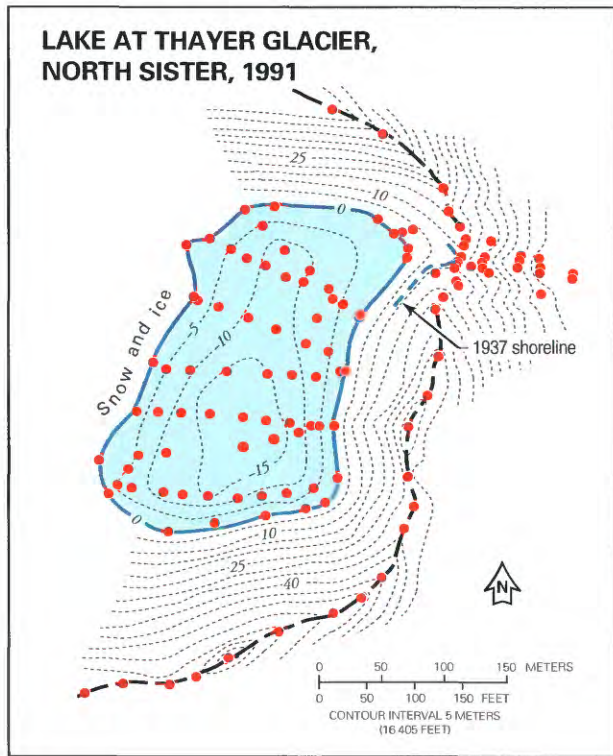


**Figure 17.** Bathymetry and topography of seven lakes and lake basins dammed by Neoglacial moraines in the Three Sisters and Mount Jefferson Wilderness Areas. Datum is present lake surface except for the basin at the terminus of Diller Glacier, Middle Sister, where the datum is arbitrary, but near the bottom of the former lake. Bathymetry for Carver Lake and the lake at the terminus of East Bend Glacier is from Laenen and others (1992 and unpub. data).

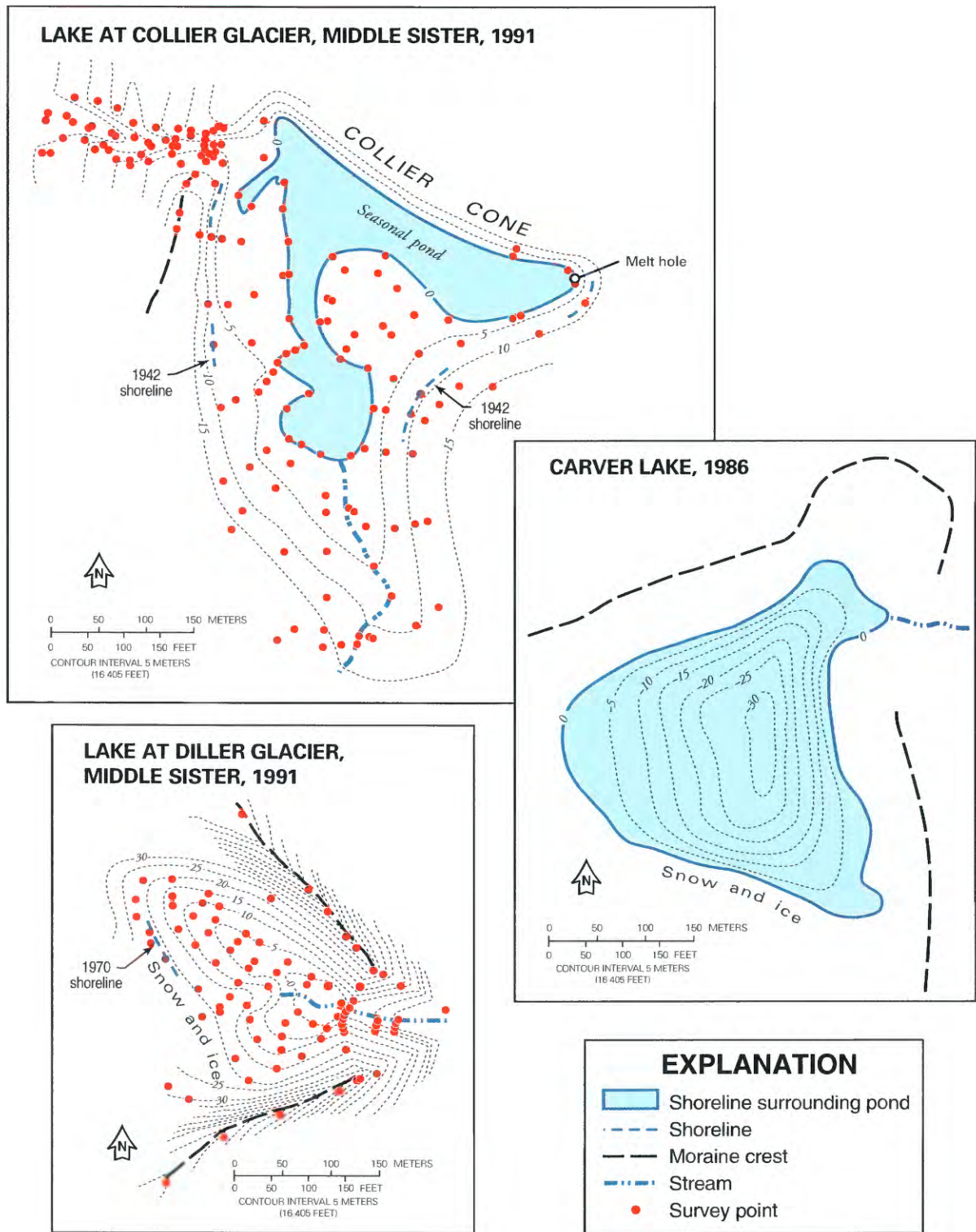


**Figure 17**—continued. Bathymetry and topography of seven lakes and lake basins dammed by Neoglacial moraines in the Three Sisters and Mount Jefferson Wilderness Areas. Datum is present lake surface except for the basin at the terminus of Diller Glacier, Middle Sister, where the datum is arbitrary, but near the bottom of the former lake. Bathymetry for Carver Lake and the lake at the terminus of East Bend Glacier is from Laenen and others (1992 and unpub. data).

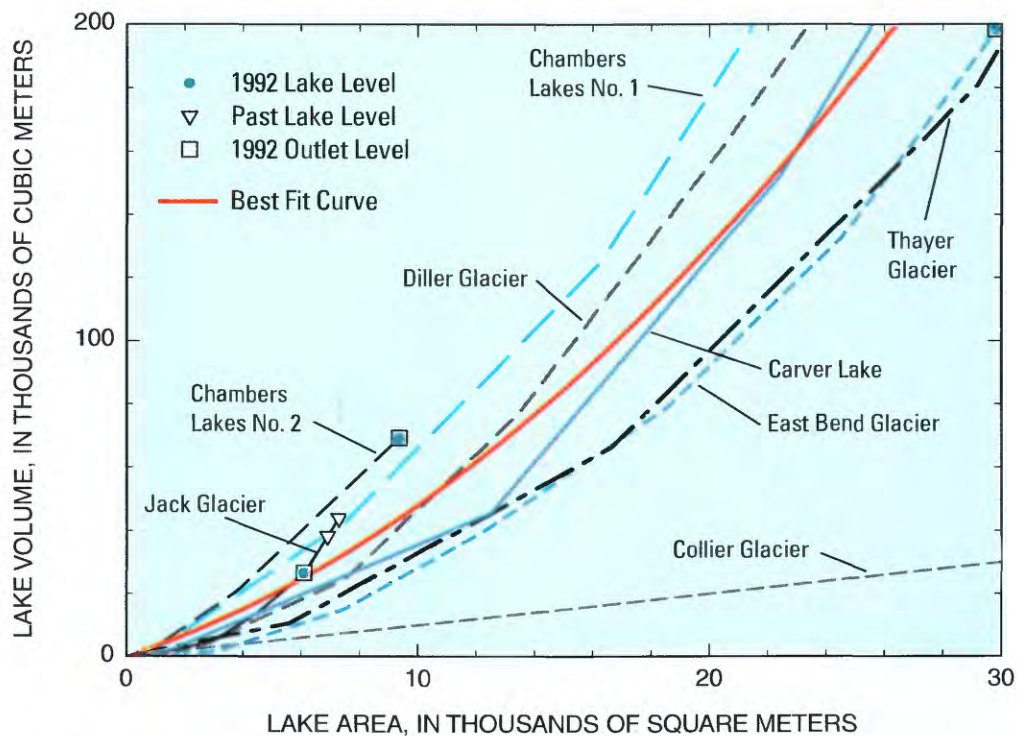
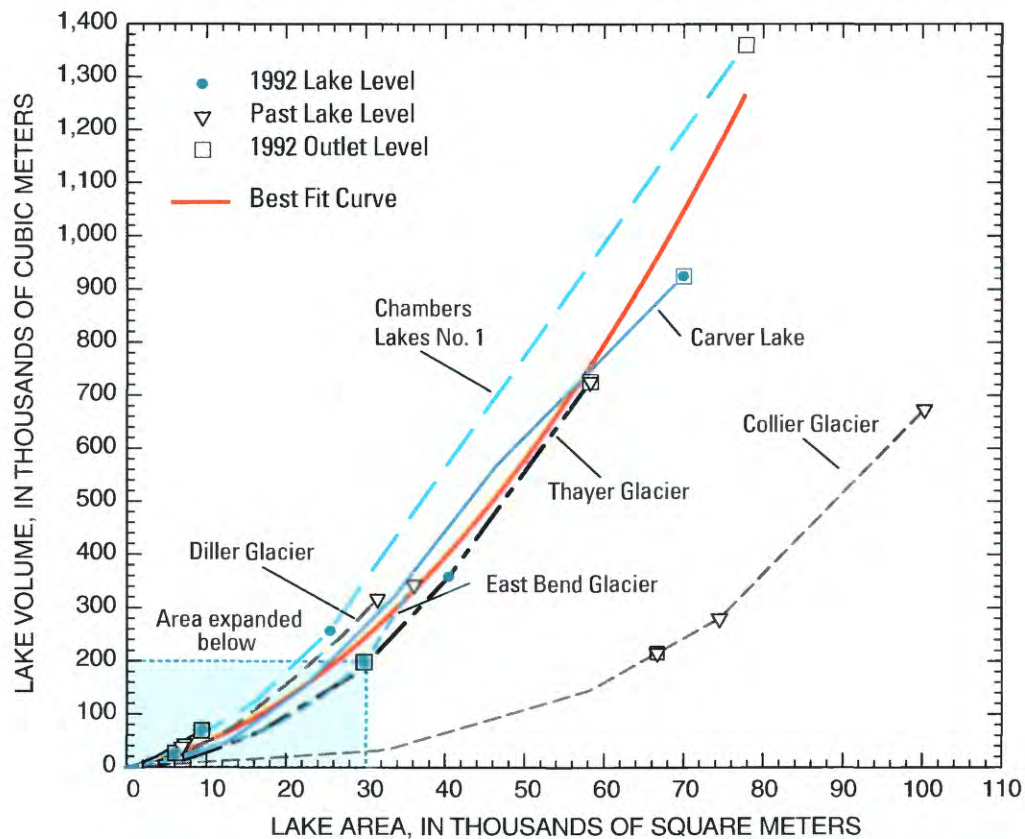


**Figure 18.** Area-volume relations for moraine-dammed lakes and lake basins in the study area, calculated on the basis of the surveys shown in figure 17. A second-order polynomial ( $V=3.114 A + 0.0001685 A^2$ , where  $V$  is lake volume in cubic meters, and  $A$  is lake area in square meters) was fit to the data in figure 18, excluding Collier Glacier Lake, to predict volumes for the unsurveyed lakes at the termini of Eugene and Whitewater Glaciers, and Chambers Lake No. 3.

**Table 2. Failed moraine dams in various mountainous areas worldwide**

[This list is based on published accounts of moraine dams that have failed and our unpublished observations. Queries indicate author-expressed uncertainty in a value or failure mechanism. Discharge values are peak discharges as reported by authors. Many of the discharge estimates are indirect estimates and are of uncertain accuracy. Discharge values calculated at the breach are, in most cases, maximum values based on breach geometry and should not be used in developing relations between breach geometry and peak discharge. Reported discharge values known to us to be based on empirical relations between peak discharge and dam or lake geometry have not been included. m, meters; m<sup>3</sup>/s, cubic meters per second; km, kilometers; —, no data.]

Lake or site name	Location	Date	Change in lake level (m)	Volume discharged (thousands of m <sup>3</sup> )	Maximum discharge (m <sup>3</sup> /s)	Failure mechanism	Reference
<b>North American Cordillera</b>							
Tats Creek	St. Elias Mountains, British Columbia, Canada	June 28, 1990	0.4	4.0	—	—	Clague and Evans, 1992.
Tide Lake	Coast Mountains, British Columbia, Canada	1927-1930	—	—	—	—	Clague and Mathews, 1992; Clague and Evans, 1994.
Nostetuko Lake	Coast Mountains, British Columbia, Canada	July 19, 1983	38.4	6,500	570 at 67 km <sup>1</sup> 340 at 112 km <sup>1</sup>	Ice fall?	Blown and Church, 1985.
South Macoun Lake	Columbia Mountains, British Columbia, Canada	Before 1949	7	400	—	Ice fall?	Evans, 1987.
North Macoun Lake	Columbia Mountains, British Columbia, Canada	July 1983	—	—	—	Piping?	Evans, 1987.
Patience Mountain	Columbia Mountains, British Columbia, Canada	1951-1966	8	300	—	—	Evans, 1987.
Klittasine Lake	Coast Mountains, British Columbia, Canada	1971-1973	13	1,700	—	Piping? Ice fall?	Clague and others, 1985; Blown and Church, 1985.
Bridge Glacier	Coast Mountains, British Columbia, Canada	1964-1970	11	1,200	—	—	Ryder, 1991.
Snowking Mountain	Cascade Range, Washington, USA	Before 1955	5-8	200	—	—	O'Connor and Hardison, unpub.data.

**Table 2. Failed moraine dams in various mountainous areas worldwide—Continued**

Lake or site name	Location	Date	Change in lake level (m)	Volume discharged (thousands of m <sup>3</sup> )	Maximum discharge (m <sup>3</sup> /s)	Failure mechanism	Reference
Jefferson Park (east)	Cascade Range, Oregon, USA	Aug. 21, 1934	—	10	300-600 at 1.2 km	Rapid melting?	This report.
Jefferson Park (west)	Cascade Range, Oregon, USA	1957?	<5	2.5	150-300 at 0.5 km	—	This report.
Waldo Glacier	Cascade Range, Oregon, USA	Before 1937	—	—	—	—	This report.
Waldo Glacier	Cascade Range, Oregon, USA	July 1951	—	—	—	—	This report.
Three Fingered Jack	Cascade Range, Oregon, USA	Before, 1960	0.8?	5.7?	—	—	This report.
Three Fingered Jack	Cascade Range, Oregon, USA	1979-1988	1.8	11.7	—	—	This report.
Eugene Glacier (east)	Cascade Range, Oregon, USA	Aug 12, 1933	—	—	175-350 at 1 km 185 at 2.5 km 20 at 4.5 km	—	This report.
Eugene Glacier (west)	Cascade Range, Oregon, USA	1933-1949	—	—	—	—	This report.
Collier Glacier	Cascade Range, Oregon, USA	July 1942	5.4	460	≤140 at breach 245-490 at 0.5 km 530 at 1.4 km 545 at 1.8 km 215 at 3.0 km 260 at 3.7 km 160 at 4.2 km 150 at 4.6 km 120 at 5.4 km 100 at 5.7 km	Rapid melting?	This report; Hopson, 1960.

**Table 2. Failed moraine dams in various mountainous areas worldwide—Continued**

Lake or site name	Location	Date	Change in lake level (m)	Volume discharged (thousands of m <sup>3</sup> )	Maximum discharge (m <sup>3</sup> /s)	Failure mechanism	Reference
					225-450 at 5.8 km 130 at 6.3 km 43 at 6.8 km 0 at 8 km		
Diller Glacier	Cascade Range, Oregon, USA	Sept. 7, 1970	22.4	320	280 at 0.8 km 450 at 2.8 km 490 at 4.6 km 65 at 6.7 km 50-100 at 8 km 50-100 at 9 km 36 at 11.5 km 35 at 24 km	Precipitation?	This report.
Broken Top	Cascade Range, Oregon, USA	Oct. 7, 1966	4.4	320	≤80 at breach 190-380 at 0.5 km 150 at 1.7 km 180 at 2.4 km 50 at 4.0 km 20-40 at 6.0 km 170 at 7.0 km	Ice fall?	This report; Nolf, 1966.
Conness Glacier	Sierra Nevada, California, USA	Summer, 1939	—	—	—	—	Hopson, 1960.

**South American Cordillera**

Laguna Jancamurish	Cordillera Blanca, Peru	Oct. 20, 1950	21	600-1,000	7,000-8,000 <sup>2</sup>	Ice fall	Liboutry and others, 1977.
Safuna Alta	Cordillera Blanca, Peru	June 1970	38	—	—	Piping	Liboutry and others, 1977.
Laguna Artesa	Cordillera Blanca, Peru	Jan. 20, 1938	10-15	250-500	—	Ice fall	Kinzl (1940); Liboutry and others, 1977.

**Table 2. Failed moraine dams in various mountainous areas worldwide—Continued**

Lake or site name	Location	Date	Change in lake level (m)	Volume discharged (thousands of m <sup>3</sup> )	Maximum discharge (m <sup>3</sup> /s)	Failure mechanism	Reference
Palcacocha	Cordillera Blanca, Peru	Dec. 13, 1941	—	1,850	—	Ice fall	Openheim, 1946; Bodenlos and Ericksen, 1955; Lliboutry and others, 1977.
Artesoncocha	Cordillera Blanca, Peru	July 16, 1951	7	1,130	—	Ice fall	Lliboutry and others, 1977; Reynolds, 1992.
Laguna Ayhuñiarju	Cordillera Blanca, Peru	Jan. 17, 1945	—	—	14,000 at 17 km	Rock fall	Indacochea and Iberico, 1947 Lliboutry and others, 1977.
Quebrada Huachasca	Cordillera Blanca, Peru	—	—	—	—	—	Bodenlos and Ericksen, 1955.
Alicocha	Cordillera Blanca, Peru	Before 1950	—	—	—	—	Lliboutry and others, 1977.
Huascarán	Cordillera Blanca, Peru	—	—	—	—	—	Lliboutry and others, 1977.
Quebrada Shantoc	Cordillera Blanca, Peru	—	—	—	—	—	Lliboutry and others, 1977.
Chacucocha	Cordillera Blanca, Peru	Before 1950	—	—	—	—	Lliboutry and others, 1977.
Laguna Soltera	Cordillera Huayhuash, Peru	March 14, 1932	—	—	—	—	Lliboutry and others, 1977.
Uta Quebrada	Cordillera Blanca, Peru	April 1939	—	—	—	—	Kinzi, 1940.
Quebrada Santa Cruz	Cordillera Blanca, Peru	1932-1951	—	—	—	—	Lliboutry and others, 1977.
Alicocha	Cordillera Blanca, Peru	Before 1970	—	—	—	—	Lliboutry and others, 1977.
Témpanos	Patagonian Andes, Argentina	1942-1953	<10	—	—	Rapid melting?	Rabassa and others, 1979.

**Table 2. Failed moraine dams in various mountainous areas worldwide—Continued**

Lake or site name	Location	Date	Change in lake level (m)	Volume discharged (thousands of m <sup>3</sup> )	Maximum discharge (m <sup>3</sup> /s)	Failure mechanism	Reference
<b>European Alps</b>							
Rosegletcher, Vadr et da Roseg	Switzerland	Aug. 21-22, 1954	0.85	120	—	Precipitation	Haeberti, 1983; Töndury, 1954.
Steingletscher	Switzerland	1956	—	—	—	—	Haeberti, 1983.
Galtrutfemer	Austria	1890	—	—	—	Ice fall	Eisbacher and Clague, 1984.
Madarcherner Glacier	Austria	Aug. 5, 1874	—	—	—	—	Eisbacher and Clague, 1984.
Miage	Italy	Aug. 9, 1990	—	—	—	—	Durto and others, 1992.
Miage	Italy	July 8, 1986	—	—	—	—	Durto and others, 1992.
Miage	Italy	1964	—	—	—	—	Durto and others, 1992.
Miage	Italy	August 1963	—	—	—	—	Durto and others, 1992.
Miage	Italy	1962	—	—	—	—	Durto and others, 1992.
Miage	Italy	1961	—	—	—	—	Durto and others, 1992.
Miage	Italy	June 1956	—	—	—	—	Durto and others, 1992.
Miage	Italy	July 20, 1955	—	—	—	—	Durto and others, 1992.
Miage	Italy	Aug. 10, 1950	—	180	—	—	Durto and others, 1992.
Miage	Italy	Aug. 1930	—	—	—	—	Durto and others, 1992.
Settentrionale delle Locce	Italy	July 17, 1979	—	300	—	Rapid melting	Durto and others, 1992.
Settentrionale delle Locce	Italy	August 2, 1978	—	—	—	—	Durto and others, 1992.
Settentrionale delle Locce	Italy	July 7, 1970	—	—	—	—	Durto and others, 1992.

**Table 2. Failed moraine dams in various mountainous areas worldwide—Continued**

Lake or site name	Location	Date	Change in lake level (m)	Volume discharged (thousands of m <sup>3</sup> )	Maximum discharge (m <sup>3</sup> /s)	Failure mechanism	Reference
Gemelli di Ban	Italy	Oct. 1971	—	—	—	—	Dutto and others, 1992.
Scersen	Italy	Aug. 10, 1927	—	500	—	—	Dutto and others, 1992.
Scerscen	Italy	Aug. 6-7, 1924	—	—	—	—	Dutto and others, 1992.
<b>Himalayas</b>							
Midui	Tibet	July 15, 1988	17	5,400	1,250 at 1.8 km <sup>1</sup>	Rapid melting?	Li and You, 1992.
Boqu River	Tibet	July 11, 1981	32	19,000	9,165 at 6 km 6,430 at 20 km 4,099 at 26 km 2,865 at 31 km 2,619 at 40 km 2,316 at 52 km 1,296 at 56 km <sup>1</sup>	Overtopping after closure (freezing?) of subsurface drainage	Xu, 1988.
Boqu River	Tibet	July 1964	—	—	—	—	Ding and Liu, 1992.
Jinco	Tibet	Aug. 27, 1982	—	—	—	Rapid melting?	Liu and Sharma, 1988.
Taraco	Tibet	Aug. 28, 1935	—	—	—	Piping?	Liu and Sharma, 1988.
Qubixiama	Tibet	June 10, 1940	—	—	—	Ice fall	Liu and Sharma, 1988.
Gelhapuco	Tibet	Sept. 21, 1964	41	23,400	—	Ice fall	Liu and Sharma, 1988.
Damenlahai Glacier, Tangbulang Gully	Tibet	Sept. 26, 1964	17	3,700	≤2,010 at breach 2,812 at 14 km	Rock fall	Liu and Li, 1986.
Zhanlonba	Tibet	1902	—	—	—	—	Ding and Liu, 1992.
Hailuogou	Tibet	July 1955	—	—	—	—	Ding and Liu, 1992.

**Table 2. Failed moraine dams in various mountainous areas worldwide—Continued**

Lake or site name	Location	Date	Change in lake level (m)	Volume discharged (thousands of m <sup>3</sup> )	Maximum discharge (m <sup>3</sup> /s)	Failure mechanism	Reference
Hailuogou	Tibet	July 1966	—	—	—	—	Ding and Liu, 1992.
Hailuogou	Tibet	Aug. 30, 1976	—	—	—	—	Ding and Liu, 1992.
Longda	Tibet	Aug. 25, 1964	—	—	—	Ice fall	Ding and Liu, 1992.
Ayaco	Tibet	August 15, 1965	—	—	—	Ice fall	Ding and Liu, 1992.
Ayaco	Tibet	August 17, 1969	—	—	—	Ice fall	Ding and Liu, 1992.
Ayaco	Tibet	August 18, 1970	—	—	—	Ice fall	Ding and Liu, 1992.
Bugyai	Tibet	July 23, 1972	—	—	—	—	Ding and Liu, 1992.
Zari	Tibet	June 24, 1981	—	—	—	Ice fall	Ding and Liu, 1992.
JZirema	Tibet	July 11, 1981	—	—	—	Ice fall	Ding and Liu, 1992.
Gule	Tibet	July 15, 1988	—	—	—	Ice fall	Ding and Liu, 1992.
Sangwang	Nepal	July 16, 1954	—	—	—	—	Liu and Sharma, 1988.
Dig Tsho	Nepal	Aug. 4, 1985	18	5,100-6,750	1,600 at 3 km	Ice fall	Galay, 1985; Vuichard and Zimmerman, 1987.
Dudh Kosi River others,	Nepal	Sept. 2, 1977	30	4,900	1,100 at 9 km 830 at 80 km <sup>1</sup>	Melting of ice core?	Buchroithner and 1982; Fushimi and others, 1985.

**Table 2. Failed moraine dams in various mountainous areas worldwide—Continued**

Lake or site name	Location	Date	Change in lake level (m)	Volume discharged (thousands of m <sup>3</sup> )	Maximum discharge (m <sup>3</sup> /s)	Failure mechanism	Reference
Moraine Lake No. 13	Kazakhstan	Aug. 3, 1977	5.2	0.86	210 at breach 1,000 at 3 km 3,400-3,900 at 7 km 7,000-11,000 at 15 km 76 at 27 km <sup>1</sup> 46 at 30 km <sup>1</sup>	Piping?	Yesenov and Degovets, 1979.
Akkul	Kazakhstan	July 8, 1963	—	—	—	—	Gerasimov, 1965.
Austre Okstindbreen Glacier	Norway	Aug. 5, 1977	—	—	—	—	Reynolds, 1992.
Keppel Cove Tarn	Great Britain	Oct. 29, 1927	8-12	124	108 at 0.1 km 90 at 4.35 km	Precipitation	Carling and Glaister, 1987.

**Other Locations**

<sup>1</sup>Gaged discharge measurement.

<sup>2</sup>Average discharge.

would be inaccurate. Because most velocity-area measurements were in or immediately downstream from confined reaches on steep slopes, it is most likely that if velocities were outside the 3 to 6 m/s range, they were higher, and the reported discharge values may err by being too low. Nevertheless, where velocity-area discharge estimates are near locations of critical-depth estimates, there is general agreement, lending support to the supposition that debris-flow velocities in the study area were generally between 3 and 6 m/s.

### Critical-Flow Discharge Estimates

Critical-flow discharge estimates were calculated where there were suspected transformations from subcritical flow to supercritical flow (fig. 19). This type of transformation can take place at free outflows from lakes, at severe width constrictions, and at increases in channel slope (Henderson, 1966). The procedure used in this study is a simplified version of the critical-flow method described by Barnes and Davidian (1978, p. 189-190). The method is premised on the occurrence of critical flow at control sections along

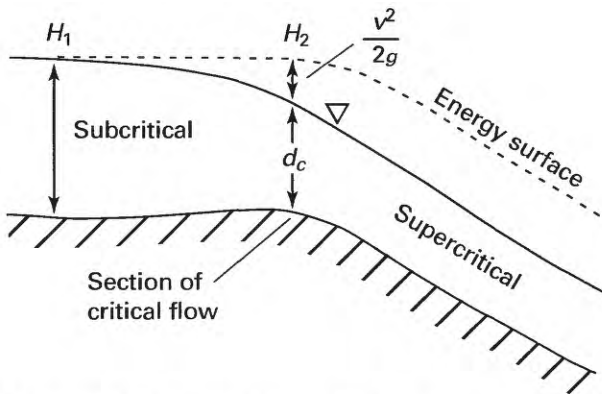


**Figure 19.** Definition diagram for flow transforming from subcritical flow to supercritical flow through a control section of critical flow. In calculating critical-depth discharge measurements, (1) flow velocity at  $H_1$  is assumed to be negligible ( $\frac{v^2}{2g} = 0$ ), and (2) energy loss between the subcritical and critical sections is negligible ( $H_1 = H_2$ ).  $H$  is the specific energy of the flow,  $v$  is the mean flow velocity,  $g$  is the acceleration of gravity, and  $d_c$  is the flow depth at the section of critical flow.

the flow path so that there is a fixed relation between the specific energy of flow and discharge. Flow is critical when the Froude number ( $F$ ), which is the dimensionless ratio of inertial forces (expressed as velocity) to gravitational forces (expressed as flow depth and gravitational acceleration), is unity:

$$F = \alpha \frac{v^2}{\sqrt{gd}} = 1, \quad (1)$$

where  $\alpha$  is the energy coefficient accounting for nonuniform velocity distribution (typically varies between 1.0 [uniform velocity distribution] and 2.0),  $v$  is the mean cross-section velocity,  $g$  is the acceleration of gravity, and  $d$  is the mean flow depth for any consistent set of units.

Because the Froude number is a dimensionless ratio based only on conservation of energy, the critical-flow concept is valid for all types of gravitationally driven free-surface flows, regardless of density and rheology. For debris flows in steep channels, which travel at velocities and depths comparable to water flows (Costa, 1984; Pierson and Costa, 1987), flow is likely to pass through states of subcritical, critical, and supercritical flow. Critical flow is the basis for discharge estimates at weirs and sluice gates, although these devices are generally calibrated. The chief advantages of critical-flow estimates are that (1) estimates of friction slopes and energy-loss coefficients are not required, and (2) critical flow is the maximum possible flow for a given specific energy ( $H = d + v^2/2g$ ), thus allowing confident statements about the maximum possible discharge at a site if field conditions are appropriate.

To obtain the debris-flow discharge estimates for this study, we chose reaches of resistant channel boundaries where there were severe channel constrictions or where there were abrupt increases in channel slope, such as near brinks of waterfalls. A single cross section was surveyed at these locations, and evidence of maximum flow stage was related to the elevation datum of the surveyed cross section (fig. 19). Highwater marks were surveyed to estimate the specific energy of the flow entering the control section. Consequently, the best field situation was where flow ponded upstream of the cross section and left deposits in backwater

areas. Deposits in areas of flow runup immediately upstream of the control cross section (fig. 20) also provided a minimum indication of the energy surface. Because the channels in the Three Sisters Wilderness Area are irregular, with abundant channel steps, changes in gradient, and changes in width, several suitable sites for critical-flow estimates were found on each debris flow path. The search for highwater marks was generally confined to within 20 m upstream of the control cross section.

For the general case considered one-dimensionally at critical flow,

$$Q = A(gd)^{1/2}, \quad (2)$$

where  $A$  is the channel cross-sectional area. Continuity also requires that

$$Q = Av. \quad (3)$$

For a measured cross section at a suspected site of critical flow, we calculated curves of specific energy ( $H = d + v^2/2g$ ) vs. discharge using equations 1, 2, and 3. The field evidence for the local specific energy (maximum flow stage a few channel widths upstream of the cross section) was

compared to this curve to obtain a discharge estimate for the cross section (fig. 21).

Hydraulic assumptions fundamental to the critical-flow discharge estimates are (1) fluid density is constant, (2) flow is steady, (3) flow is hydrostatic, and (4) flow is critical at or near the measured cross section. These assumptions are not required to be valid for the entire flow hydrograph, but simply for the brief span of time during which the evidence for the maximum energy surface is emplaced and the flow peak passes through the control section within a few meters downstream. The steadiness assumption is most susceptible to violation. If there are dynamic (energy) waves pulsing down the channel, the elevation of the deposits left by the dynamic waves may be higher than the energy surface actually associated with the maximum discharge; hence, leading to discharge overestimation (Iverson and others, 1994). Although, theoretically, dynamic waves should not pass through reaches of critical flow. Short wavelength kinematic waves will not result in erroneous estimates of peak instantaneous discharge, but the resulting discharge estimate will be that of the wave itself and may not be representative of the entire debris flow. Notably,

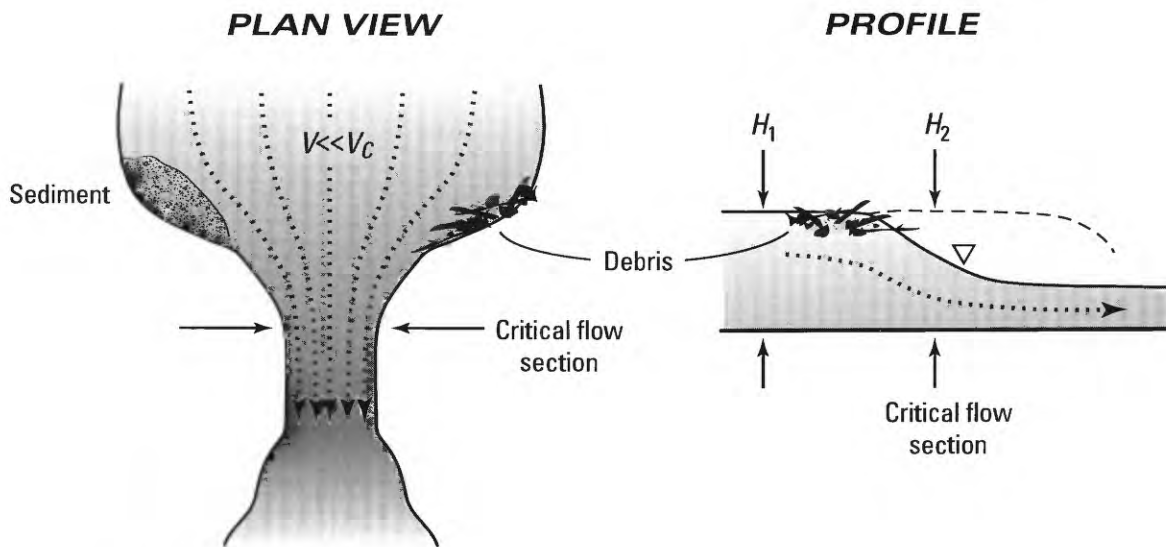


**Figure 20.** Schematic plan and profile illustrations of an ideal field situation for a critical-flow discharge estimate at a flow constriction where debris or sediment give an accurate indication of the specific energy of the flow entering the constriction ( $H_2$  of figure 19).

violations of these assumptions, except for flow steadiness, result in discharge overestimation. In hydraulically complex areas, the maximum error may be as large as a factor of 0.5, but more likely is within a factor of 0.25 considering a reasonable range in hydraulic uncertainties at suitable field sites.

Field conditions in which the observed evidence of maximum flow stages fail to accurately represent the specific energy of the incoming flow can lead to discharge underestimation. The two most plausible scenarios of error introduction are situations where (1) observable evidence of maximum upstream ponding stages was not preserved to highest ponding levels, and (2) flow through the ponded reach had substantial velocity. For most plausible situations where field settings are appropriate for critical-flow discharge estimates, these errors will lead to discharge underestimation by a factor less than 0.5. Consequently, the critical-flow procedure used in this study is assumed to have an accuracy of  $\pm 50$  percent.

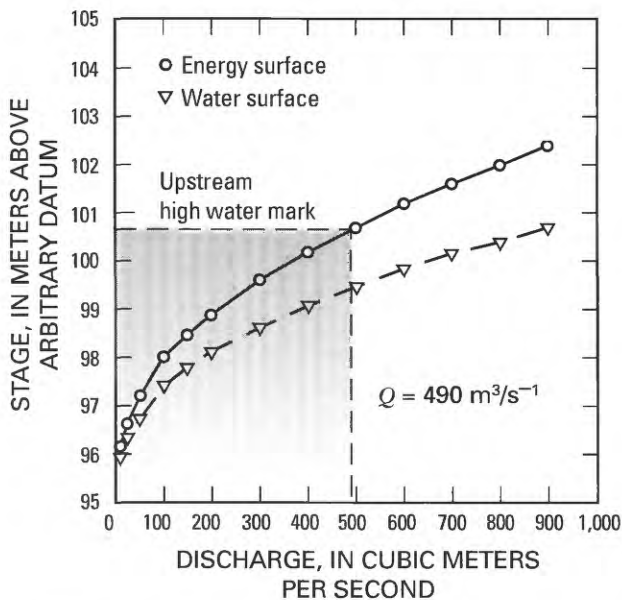


**Figure 21.** Example of critical depth ( $\nabla$ ;  $d$  of figure 19) and specific energy ( $\bullet$ ;  $H_2$  of figure 19) plotted for a hypothetical surveyed cross section of critical flow. A peak discharge is estimated for the critical-flow section by relating the elevation of the upstream high-water evidence to the calculated specific energy curve for the critical-flow section.

## Case Studies in the Central Oregon Cascade Range

In the Mount Jefferson and Three Sisters Wilderness Areas, deposits and source areas were studied at nine sites where debris flows resulted from rapid emptying or partial release of moraine-dammed lakes (pl. 2). Two small flows from a small lake at the terminus of Waldo Glacier, Mount Jefferson, also have been reported in newspaper accounts and are evident on aerial photographs. Although all debris flows affected popular recreational areas, and many occurred during the recreation season, the only adverse effects were damage to trails and campsites and the temporary burial of a county highway. The largest debris flows, nevertheless, substantially affected downstream valleys, locally eroding and depositing sediment on surfaces covered with Mazama tephra, indicating that these flows affected surfaces that had been previously unmodified for at least the last 7,000 years.

The sections that follow describe debris flows at the individual locations. Although information was collected on flows in both the Mount Jefferson and Three Sisters Wilderness Areas, the most complete observations were compiled for the four largest flows that resulted from releases of moraine-dammed lakes at the termini of Collier, Diller, Eugene, and East Bend Glaciers in the Three Sisters Wilderness Area. Deposits left by the flows in the Mount Jefferson Wilderness Area are indicated on plate 1; deposits left by flows in the Three Sisters Wilderness Area are shown on plate 2.

### Mount Jefferson Wilderness Area

Two debris flows originated on the north flank of Mount Jefferson from rapid emptying of short-lived proglacial lakes that formed at the margins of northern lobes of Whitewater Glacier (fig. 22). Another large debris flow in 1955 apparently was triggered by mass movement of Neoglacial till downvalley from Russell Glacier (Scott, 1974, p. 57). A small lake in front of Waldo Glacier, on the southeast side of Mount Jefferson, apparently partially breached its morainal dam at least twice. Three Fingered Jack, a separate volcanic center

within the Mount Jefferson Wilderness Area, has had at least two small flows from the lake at the terminus of Jack Glacier.

### East Jefferson Park

Whitewater Glacier is the largest glacier on Mount Jefferson, covering most of the eastern and northern flanks of the volcano (pl. 2; fig. 22). There have been two debrisflows from small and short-lived moraine-dammed lakes that formed at northern lobes of the glacier (fig. 22). The largest flow, on August 21, 1934, deposited silt, sand, gravel, and boulders over much of the broad, lake-dotted alpine meadows of Jefferson Park before entering the drainage of Whitewater River (pl. 2, fig. 23). Downstream from Jefferson Park, the flow continued as sediment-laden streamflow.

The east Jefferson Park debris flow was described in newspaper articles reporting aerial surveys and ground expeditions that examined the debris-flow deposit in the weeks after the event (*The Oregonian*, Aug. 27, 1934; *The Oregon Daily Journal*, Oct. 19, 1934). According to these reports, the debris flow resulted from the emptying of a small, 4,000 m<sup>2</sup> moraine-dammed lake at 2,660 m that had formed that same summer. The lake breached the moraine, eroding an outlet about 15 m deep through the moraine. The resulting flow eroded a new channel up to 10 m deep as it continued down the steep distal slope of the Neoglacial moraine and over older till, outwash, and colluvium composing the steep slopes below (fig. 23). Deposition began at 1,860 m on a steep forested outwash fan at the base of the Mount Jefferson edifice and covered 320,000 m<sup>2</sup> of

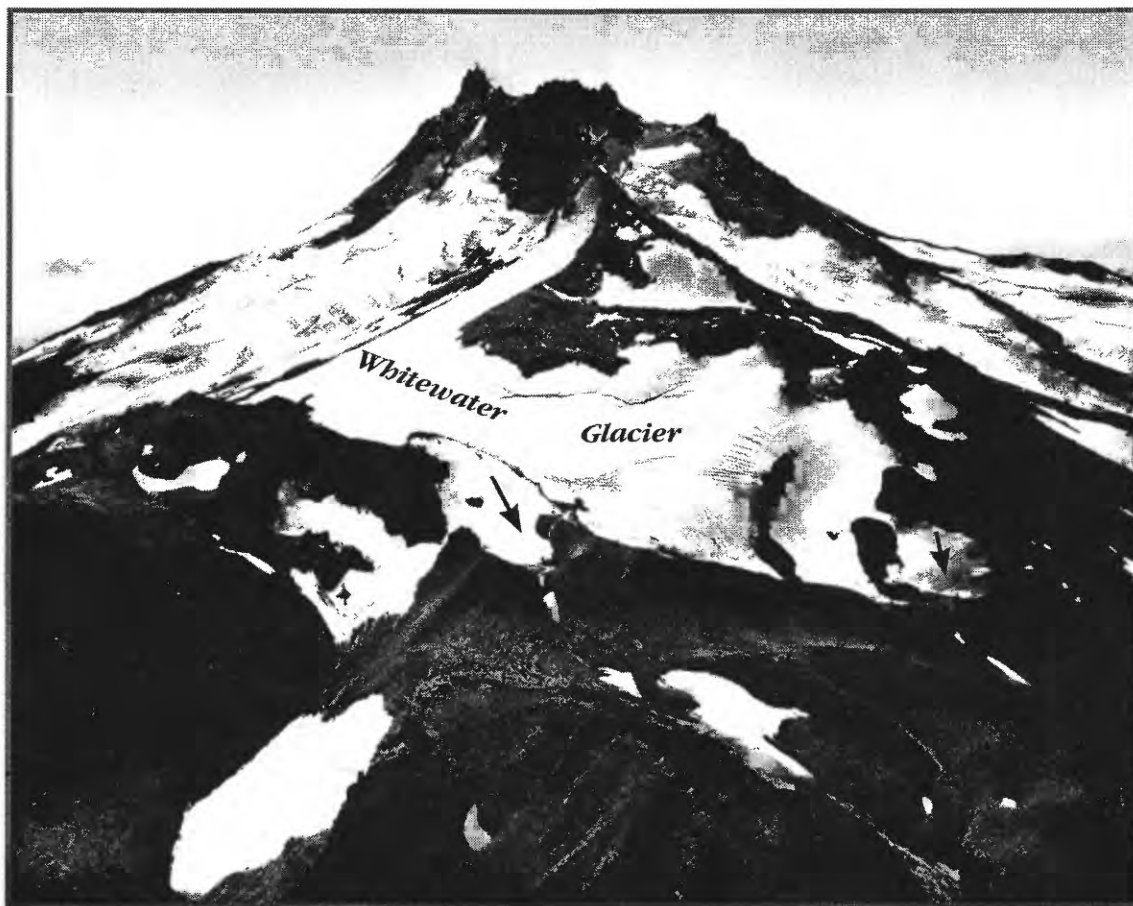


**Figure 22.** Aerial view south of Mount Jefferson and the northern lobes of Whitewater Glacier. Moraine-dammed lake releases came from the indicated locations. Photograph by Austin Post (R21-32), September 21, 1960.

eastern Jefferson Park, where two established forest camps were buried by flow deposits (pl. 2; figs. 22 and 23). U.S. Department of Agriculture, Forest Service personnel, at the site within weeks, reported that the park was covered with “boulders, sand, and tree trunks to a depth of from 1 to 6 or 8 feet” (The Oregon Daily Journal, Oct. 19, 1934). At the fan apex, debris flow levees on the margins of an incised channel define a cross-section area of 100 m<sup>2</sup>. An assumed flow velocity of 3 to 6 m/s yields a peak discharge estimate of 300 to 600 m<sup>3</sup>/s.

### West Jefferson Park

In west Jefferson Park, one debris flow from a Neoglacial-dammed lake is documented at a site 0.5 km west of the 1934 breach. No historical

records of this lake, or resulting debris flows, are known except for Scott’s description (1974, p. 57) of a “very recent flood deposit, perhaps no more than 5 years old.” This lake formed at an elevation of 2,150 m behind a low Neoglacial moraine at the terminus of the northernmost lobe of Whitewater Glacier (pl. 2, fig. 22) sometime following the east Jefferson Park debris flow. The absence of records of this lake indicates that it was short-lived, perhaps forming the same year as the debris flow. The size of the lake is not known. However, the topography of the outlet area indicates that the maximum possible lake area was about 15,000 m<sup>2</sup>, with a maximum depth of 5 m. The flow resulting from the lake breakout travelled down the 27° slope of the moraine, incorporated Neoglacial and older till, and deposited sediment over 170,000 m<sup>2</sup> of Jefferson Park (pl. 2; fig. 24). At the fan apex,

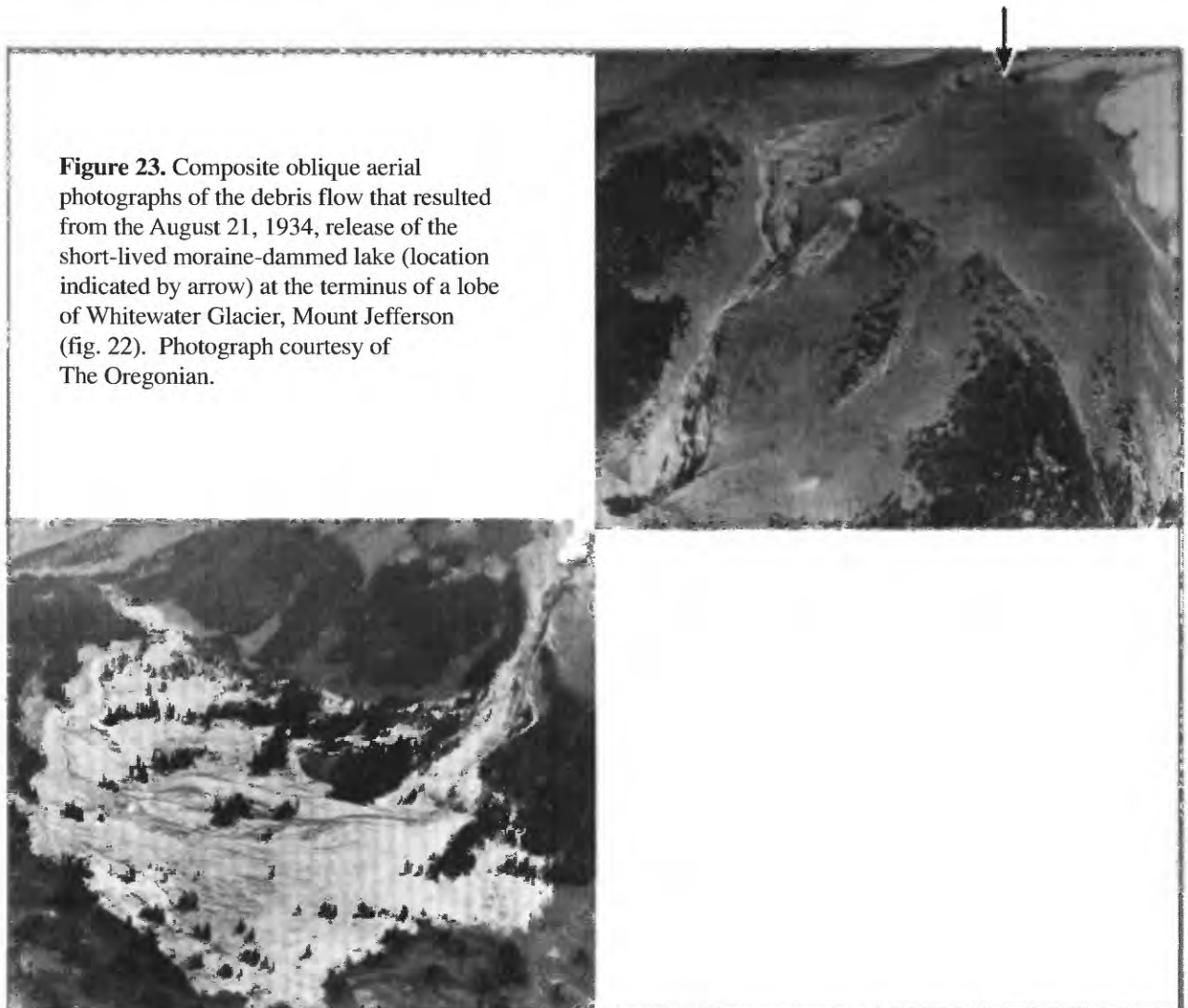


**Figure 23.** Composite oblique aerial photographs of the debris flow that resulted from the August 21, 1934, release of the short-lived moraine-dammed lake (location indicated by arrow) at the terminus of a lobe of Whitewater Glacier, Mount Jefferson (fig. 22). Photograph courtesy of The Oregonian.

0.5 km from the breach, bouldery levee crests 5 m above the 17° channel thalweg define a cross section area of 50 m<sup>2</sup>. An assumed average flow velocity of 3 to 6 m/s yields a peak discharge estimate of 150 to 300 m<sup>3</sup>/s.

Aerial photographs (fig. 22) show that this flow occurred prior to 1960. A mountain hemlock in the path of the debris flow had its 15-cm-thick parent stem sheared off at a height of 1.5 m; this resulted in eccentric growth of a former branch that became the tree's main stem. A core through this stem shows a change in growth pattern that was detected by ring counting to 1957, providing a tentative date for the damage-causing event. A

false ring produced during the same year further indicates that the damage occurred during the spring and summer growing season.

### Waldo Glacier

Waldo Glacier is a small, 0.3-km<sup>2</sup> glacier that flows down the south flank of Mount Jefferson within the Warm Springs Indian Reservation (fig. 25). During maximum Neoglacial advances, the glacier was about twice its present areal extent and built large lateral and terminal moraines that later impounded a lake with a maximum surface area of about 26,000 m<sup>2</sup> at an elevation of 2,180 m. Fresh-appearing scars in the terminal moraine are visible

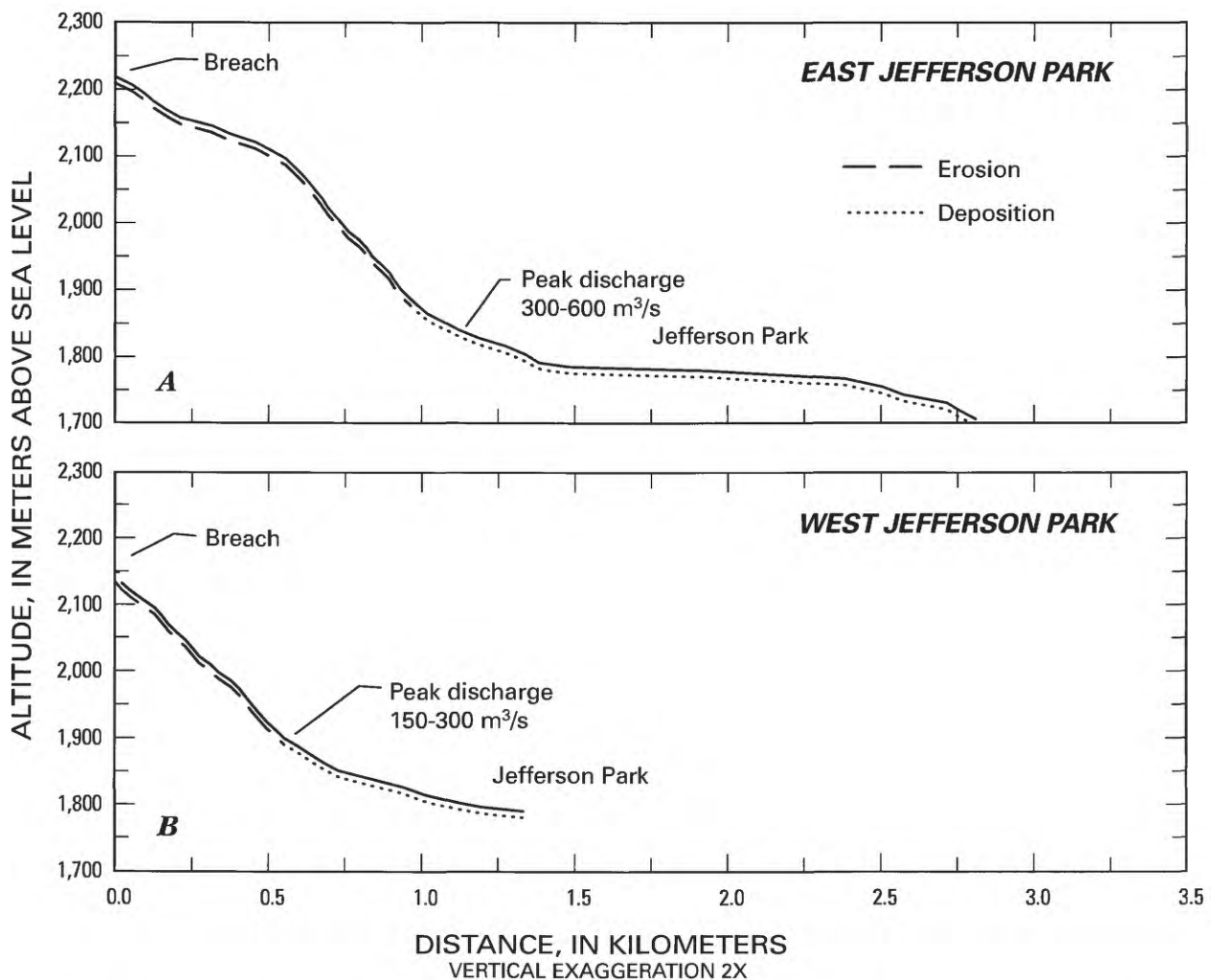


**Figure 24.** Longitudinal profiles along the flow routes of debris flows from moraine-dammed lakes at terminal lobes of Whitewater Glacier, Mount Jefferson. *A*, 1934 debris flow into east Jefferson Park; *B*, (1957(?)) debris flow into west Jefferson Park.

on 1937 aerial photographs (Research Committee of the Mazamas, 1938), indicating that a previously larger lake had partially breached the moraine. A subsequent breach was noted by The Oregon Daily Journal (August 9, 1951, p. 5), which reported that a Mazamas climbing party had traced recent (late July, 1951) “mud-dying” (presumably meaning the mud-coloration) of the Metolius and Deschutes Rivers to an emptying of the lake behind the terminal moraine of Waldo Glacier. Aerial photographs taken in 1990 show there to be little water impounded behind the moraine.

Waldo Glacier was not visited; however, on the basis of inspection of aerial photographs taken before and after the 1951 lake breakout, the 1951 debris flow followed the same outlet channel as the

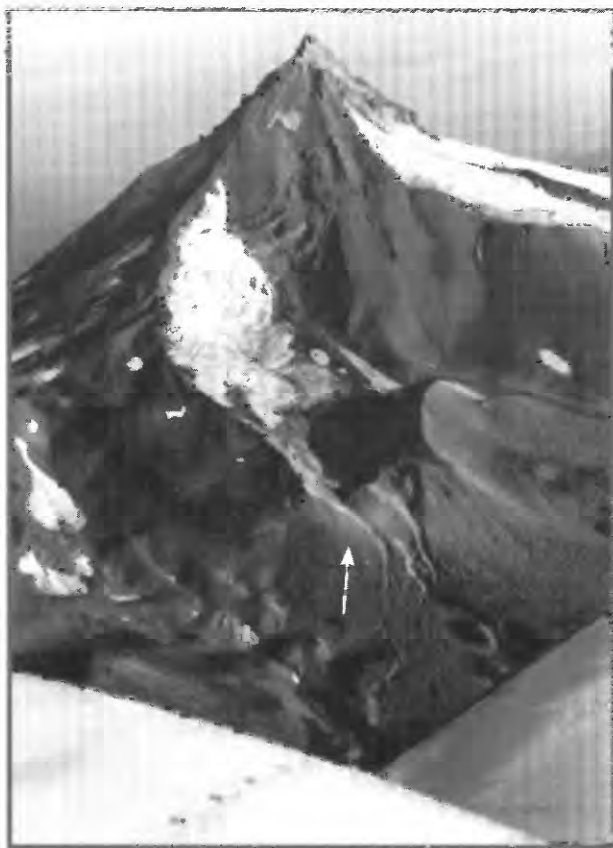


**Figure 25.** Oblique aerial view northwest toward Mount Jefferson. A small moraine-dammed lake at the terminus of Waldo Glacier has breached its morainal dam at least twice, generating small debris flows. Photograph September 1987.

pre-1937 one. The 1951 flow slightly enlarged the breach and deposited bouldery debris over 100,000 m<sup>2</sup> on an outwash fan at an elevation between 2,070 m and 1,890 m. The debris flow apparently continued down an unnamed tributary of Jefferson Creek for at least another kilometer (pl. 1).

### Jack Glacier

Jack Glacier (an informal name proposed by Phillips [1938]) is a small, probably stagnant, ice body not shown on USGS topographic maps. The ice is in a deep and shaded cirque on the northeast side of the serrated ridge that forms Three Fingered Jack (pl. 1). The present extent of ice covers about 0.01 km<sup>2</sup>. During maximum Neoglacial advances, however, Jack glacier covered 0.13 km<sup>2</sup> and formed 50-m-high moraines on its periphery. Jack Glacier is protected from insolation by high ridges to the south and west and is one of the lowest Oregon Cascade Range glaciers, lying between 2,000 and 1,860 m elevation.

The Neoglacial moraine dams a lake with a 1993 surface area of 6,120 m<sup>2</sup>, a maximum depth of 8.0 m, and a volume of 26,500 m<sup>3</sup> (figs. 15A and 17). This lake was present in 1937 (Phillips, 1938), but is not shown on USGS topographic maps that were surveyed in 1928 and 1929, nor is it noted in a 1929 description of the scenery from the top of Three Fingered Jack (Lynch, 1929, p. 114). The lake overflows through a narrow, boulder-paved outlet and down a steep channel incised in the 30° distal moraine slope. This lake has one of the steepest outlets of the remaining moraine-dammed lakes and its seemingly precarious stability is apparently due to a few boulders, less than 1 m in diameter, that pave the channel thalweg at the outlet.

Debris-flow deposits on the fan below the lake were left by at least two partial breaches of the moraine dam (pl. 2). The first breach was prior to September 1960 and left anastomosing splays of bouldery debris-flow deposits over 12,000 m<sup>2</sup> of the outwash fan at the base of the moraine. The second release further incised the upper part of the moraine and left a fan-shaped deposit on the outwash fan (fig. 26). Comparison of dated aerial photographs indicates that the second flow

occurred between August 1979 and September 1987. Neither debris-flow deposit extended past the outwash fan at the base of the Neoglacial moraine, 0.4 km from the outlet.

Two shorelines  $2.6 \pm 0.1$  m and  $1.8 \pm 0.1$  m above the present lake level are preserved on the west margin of the lake. Abandonment of these two shorelines possibly corresponds to the two sets of deposits on the outwash fan. If true, the first lake level lowering resulted in release of  $5,700 \text{ m}^3$ , and the second release was about  $11,700 \text{ m}^3$ . Considering the present topography of the outlet, the maximum possible water discharge at the breach during the second event was about  $25 \text{ m}^3/\text{s}$ .

### Three Sisters Wilderness Area

At least five debris flows caused by breaches of moraine-dammed lakes have occurred within the Three Sisters Wilderness Area since 1933. The largest were the debris flows from lakes at the termini of Collier, Diller, and East Bend Glaciers

on North and Middle Sisters and Broken Top, respectively. These debris flows traveled for 7.5 to 9 km, and had peak discharges between 200 and  $500 \text{ m}^3/\text{s}$  in their upper reaches. Two smaller flows were caused by releases from two small, short-lived lakes at the terminus of Eugene Glacier on the north flank of South Sister.

### Collier Glacier

A large Neoglacial moraine-dammed lake formed behind the Neoglacial moraine of Collier Glacier (fig. 9). Ruth Hopson Keen observed, photographed (fig. 12), and described conditions near the glacier terminus between 1933 and 1973 (Hopson, 1960, 1961, 1962, 1963, 1965; Keen 1969, 1978, 1981). According to her observations, the lake first formed between August 1933 and September 1934, and grew until 1940 as Collier Glacier retreated. At its maximum extent, the lake covered  $100,000 \text{ m}^2$  and had a volume of  $670,000 \text{ m}^3$  (figs. 16, 17, and 18). The lake spilled over the low point in the lateral moraine, forming



**Figure 26.** Moraine and outwash fan from Jack Glacier on Three Fingered Jack. The outer slope of the moraine has been eroded and debris deposited on the fan by two partial releases from the lake impounded by the moraine. Photograph taken September 1987.

the primary source of White Branch. According to Hopson (1960, p. 4):

“At the northwest, White Branch has always breached the terminal moraine. This stream formerly flowed from under the ice where it now flows from the lake. Before 1940, the lake merely spilled over at this point, and spread out among the rocks leaving a few stepping stones above water. By 1941, the overflowing water had eroded to a depth of 1 or 2 feet. Pressure from increased meltwater, following a hot spell in July 1942, caused a sudden outbreak [prior to July 23, 1942]. This cut a gorge several feet deep at the outlet, and as much as 30 feet deep a few hundred yards down stream. Farther along, White Branch changed its course in a few places. As much as a mile and a half below the glacier, it spread boulders over outwash plains. It covered the lowest outwash plain with fine

sediment, and generally changed the picture of upper White Branch Valley.”

Our survey of the lake basin indicated that during the July 1942 flow there was  $5.4 \pm 0.5$  m of incision at the outlet (fig. 27), resulting in release of about  $460,000 \text{ m}^3$  of water. The lake remained at this level until sometime between September 1954 and October 1956, when a second breach in the lateral moraine formed 15 m to the north of the first breach (figs. 27 and 28). The 1942 flow resulted from the south breach and caused most of the visible incision in the moraine and the downstream deposition at Sawyer Bar. The sequence of events that led to development of the second breach is not clear. Its net effect, however, was 0.8 m of lake-level lowering and release of as much as  $50,000 \text{ m}^3$  of water. A 1956 aerial photograph shows the lake draining through the second breach (fig. 29). According to Hopson (1961), between July 1960 and August 1961 the lake almost completely drained, and meltwater from Collier Glacier no longer flowed into White

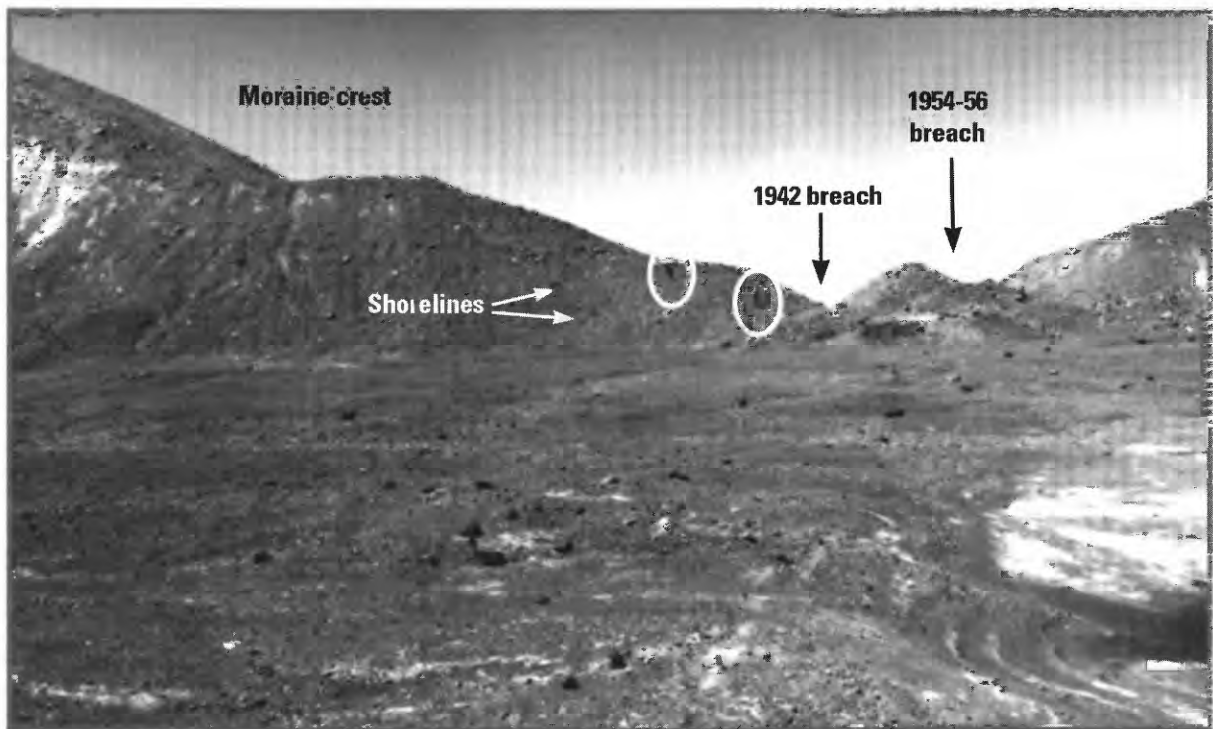


**Figure 27.** View west toward outlet from the basin that formerly contained the lake at the terminus of Collier Glacier, North Sister. The marked shorelines (note people for scale) indicate two former lake levels before and after the 1942 breach in the lateral moraine. A second breach formed about 15 m to the north (right) between 1954 and 1956 and resulted in a further 0.8 m of lake-level lowering. Photograph taken August 12, 1987.

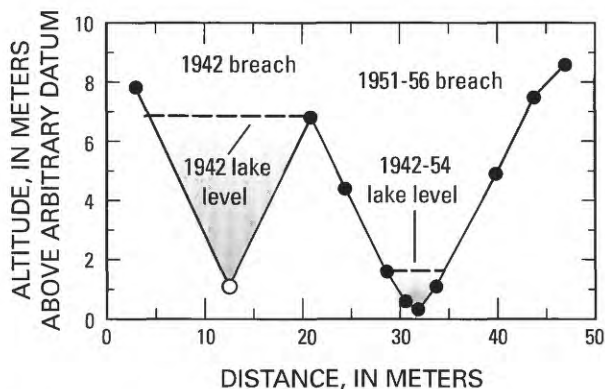


**Figure 28.** Surveyed cross section of outlets to the former lake at the terminus of Collier Glacier. At the time of the survey in 1991, the 1942 breach was partially filled with snow, so the dimensions have been reconstructed (point indicated by open circle) with the aid of figure 27 and August 1987 measurements when the breach was free of snow.

Branch, but entered what Hopson called the “melt hole,” a subsurface outlet through ground moraine and stagnant ice near the northeast margin of the former lake. Glacial meltwater still drained into the “melt hole” from a seasonal pond in the former lake basin when we surveyed the site in August 1991.

The 1942 outbreak transformed into a bouldery debris flow that traveled 7.5 km before ending where White Branch flows onto and drains into the surface of a late Holocene basalt flow from Collier Cone (pl. 2). Inspection of aerial photographs taken in 1949 and 1977 shows that the 1942 debris flow was much larger than any flow that possibly resulted from the 1954-1956 breach. The only apparent effect of the second episode of lake lowering was about 3 m of incision of outwash and till at the breach and within 300 m



**Figure 29.** Oblique aerial view southeast toward remnant lake, breached moraine, and downstream deposits left after the 1942 flow from the lake at Collier Glacier. The 1942 flow resulted from the south breach and caused most of the visible incision in the moraine and the downstream deposition at Sawyer Bar. In this view, the lake drains through a second breach to the north that formed between 1954 and 1956. Photograph by Ackroyd Photography, October 1956.

downstream. Cobbles and boulders along the White Branch channel bottom, shown in unpublished 1942 photographs by Ruth Hobson Keen, were apparently unmoved in 1995, indicating that any post-1942 event has had minimal effect on the channel.

The maximum possible discharge at the lake outlet during the 1942 breach was  $140 \pm 30 \text{ m}^3/\text{s}$ . This discharge was calculated assuming critical flow and a 1942 water surface  $5.4 \pm 0.5 \text{ m}$  above the thalweg of the first breach (fig. 30). Based on our basin survey, the water volume released was  $460,000 \text{ m}^3$ , requiring at least 45 to 70 minutes of flow at peak discharge to lower the lake to the level of the breach thalweg. Our surveys of the outlet area downstream of the breach, and evaluation of photographic and geomorphic evidence of the pre-flow topography, indicate that about  $120,000 \text{ m}^3$  of till and outwash were eroded from the steep outlet area within 300 m of the breach, increasing the flow volume by about 25 percent. As discussed later, most of this material must have entered the flow within a few minutes. Large scallop-shaped reentrants along the channel margins (fig. 29) are interpreted as evidence that a large portion of the material was incorporated by mass movements into the deepening channel during the course of the flow.

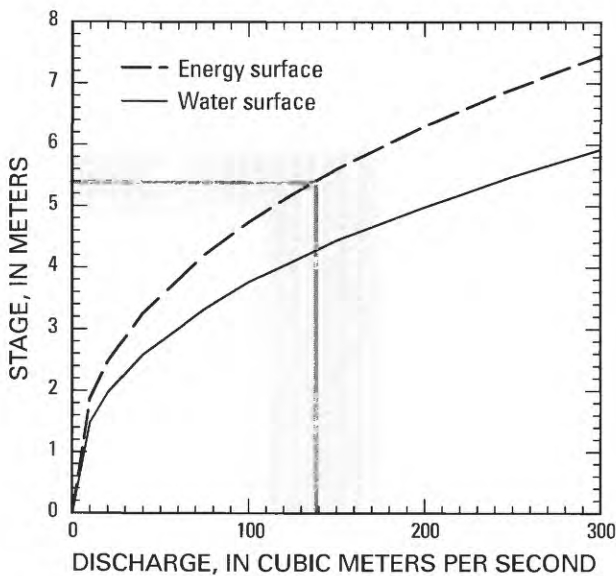


**Figure 30.** Stage-discharge relation for critical flow through the left breach at the outlet to the lake at Collier Glacier.

At the apex of Sawyer Bar (pl. 2), bouldery levees mantled with 1- to 2-meter diameter boulders 6 m above the present channel thalweg indicate that the flow transformed to a debris flow within the intervening 600 m from the breach. The debris flow inundated Sawyer Bar, a Neoglacial outwash surface, and deposited bouldery lobes over its  $50,000\text{-m}^2$  surface (figs. 29 and 31). Downstream, the flow deposited sediment over wider and lower gradient reaches and passed through and eroded sediment from narrower and steeper reaches (pl. 2; fig. 32). In some depositional reaches, bouldery digitate lobes were deposited in mid-valley areas and resemble a single debris flow levee with the largest clasts on the edges (fig. 33). We cannot confidently interpret these features, but they may be the result of deposition on snow-covered surfaces. After the snow melted, the former flow channel that was eroded through the snow cover was preserved as a



**Figure 31.** View east toward Sawyer Bar, which was covered by bouldery deposits from the 1942 breach and debris flow from the lake at the terminus of Collier Glacier.

sinuous ridge of coarse gravel and boulders located in the middle of the valley. In most locations, however, the entire valley was inundated and the flow margins and maximum stage of the debris flow are well defined by a cohesive silty sand that appears to have been the fluid, but viscous, matrix of the flow (fig. 34).

Using this evidence of maximum flow stage, we calculated estimates of instantaneous peak discharge for the largest flow wave at 13 sites along the debris flow path (figs. 32 and 35). Most measurements were made at flow constrictions and at brinks of channel steps where we used the critical-depth procedure. In addition, two velocity-area estimates based on the cross-sectional areas of the flow are included. All reported critical-depth estimates are estimated to be accurate within  $\pm 50$  percent. The velocity-area discharge estimates are generally presented as a range, resulting from an assumed average cross-sectional velocity of 3 and 6 m/s.

The resulting discharge estimates correspond with the overall patterns of erosion and deposition. Two critical-flow estimates between 1.3 and 1.5 km from the breach yield discharge estimates

of 530 and 545  $\text{m}^3/\text{s}$  (fig. 32). These values are similar to a 490  $\text{m}^3/\text{s}$  upper limit of a velocity-area estimate at the upstream end of Sawyer Bar, but slightly larger than a superelevation measurement of 360  $\text{m}^3/\text{s}$  made by Laenen and others (1987) at the downstream end of Sawyer Bar. Recent work in a large experimental flume indicates that when total channel width is used in superelevation calculations, debris-flow wave speed is consistently underestimated (Iverson and others, 1994); thus, discharge is underestimated. The reported value of 360  $\text{m}^3/\text{s}$  (Laenen and others, 1987) is considered a minimum value of discharge at this site.

Taken together, the peak discharge results and the estimates of sediment and flow volumes indicate that the peak flow rate increased from a maximum possible clear-water discharge of  $140 \pm 30 \text{ m}^3/\text{s}$  at the breach to a debris flow of about 500  $\text{m}^3/\text{s}$  at Sawyer Bar. This increase resulted from incorporation of 120,000  $\text{m}^3$  of till and outwash eroded in the 300 m downstream from the breach, producing a peak discharge debris flow that was 65 to 80 percent by volume of entrained till and outwash. Such an entrainment rate could be

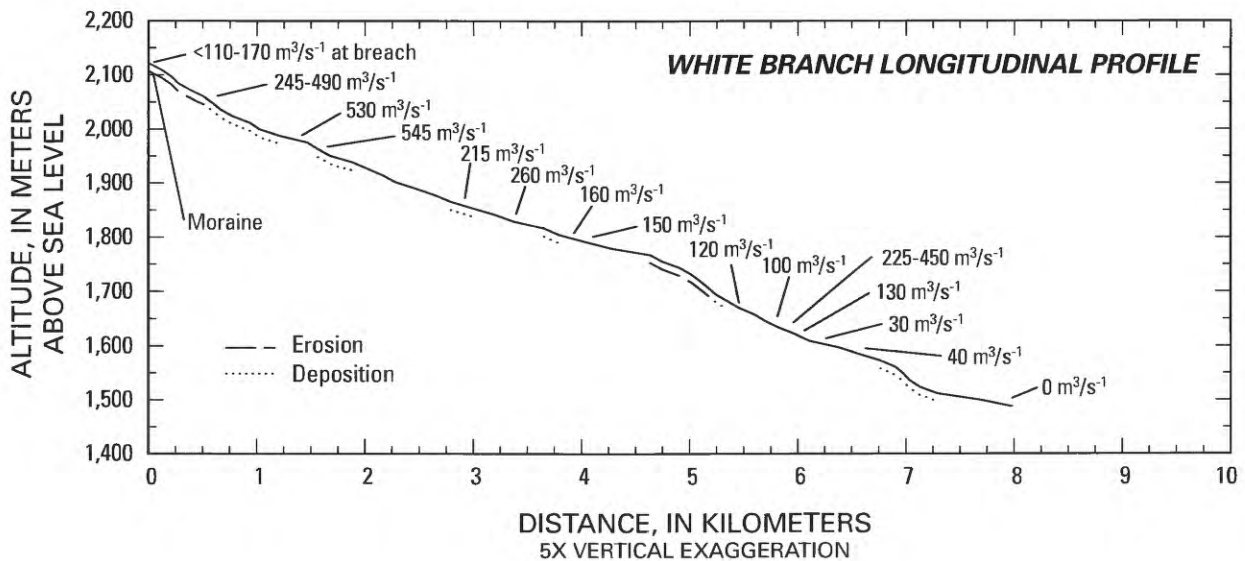


**Figure 32.** Longitudinal profile of White Branch, showing indirect discharge estimates (in cubic meters per second) and reaches of erosion and deposition during the 1942 debris flow from the breach of the lake at the terminus of Collier Glacier. The critical-flow estimates are given as single values and inferred to be accurate to within  $\pm 50$  percent. The velocity-area estimates are given as ranges based on assuming a mean flow velocity of 3 to 6 meters per second.

sustained only for about 6 minutes, considering our estimate of the total volume eroded from below the breach. Because of the large volume of water in the lake, however, most of the released flow must have had a volumetric sediment concentration substantially less than 65 percent.

The discharge estimates for sites farther downstream indicate substantial decrease in the peak discharge—from greater than 500 m<sup>3</sup>/s near Sawyer Bar, 1 km from the outlet, to about 150 m<sup>3</sup>/s, 4 km downstream (fig. 35). This decrease in discharge was over a 4 km reach of declining gradient and substantial deposition (pl. 2; figs. 32 and 35), indicating that the peak flow decreased primarily because of deposition rather than attenuation. Peak discharge may have increased from 225 to 450 m<sup>3</sup>/s within a steep, narrow reach near Obsidian Cliffs, perhaps due to

temporary blockage by wood or large clasts. Farther downstream, three critical-flow estimates indicate a downstream decrease of peak discharge due to continued deposition until the debris flow ended 8 km downstream from the breached moraine in a series of ponded embayments on the surface of a lava flow from Collier Cone (pl. 2).

Most of the material in the debris flow was derived from the moraine and outwash within 600 m from the breach. Some additional sediment, however, apparently was incorporated into the flow from erosion of channel banks in constricted reaches. Cobbles and boulders from talus that flanks constricted valley segments were eroded and entrained. Most of the constrictions are at least partly bounded by lava from Collier Cone or the rhyodacite that forms Obsidian Cliffs (pl. 2). Downstream from the constrictions, these rock



**Figure 33.** Photograph of a single sinuous ridge of bouldery gravel deposited near the center of a wide depositional reach along the 1942 debris flow pathdown White Branch, perhaps the result of deposition onto snow (note person for scale). The maximum stage of the flow is indicated by the prominent light-colored deposits on the talus from the lava flow from Collier Cone, a result of fine sediment filling interstices.

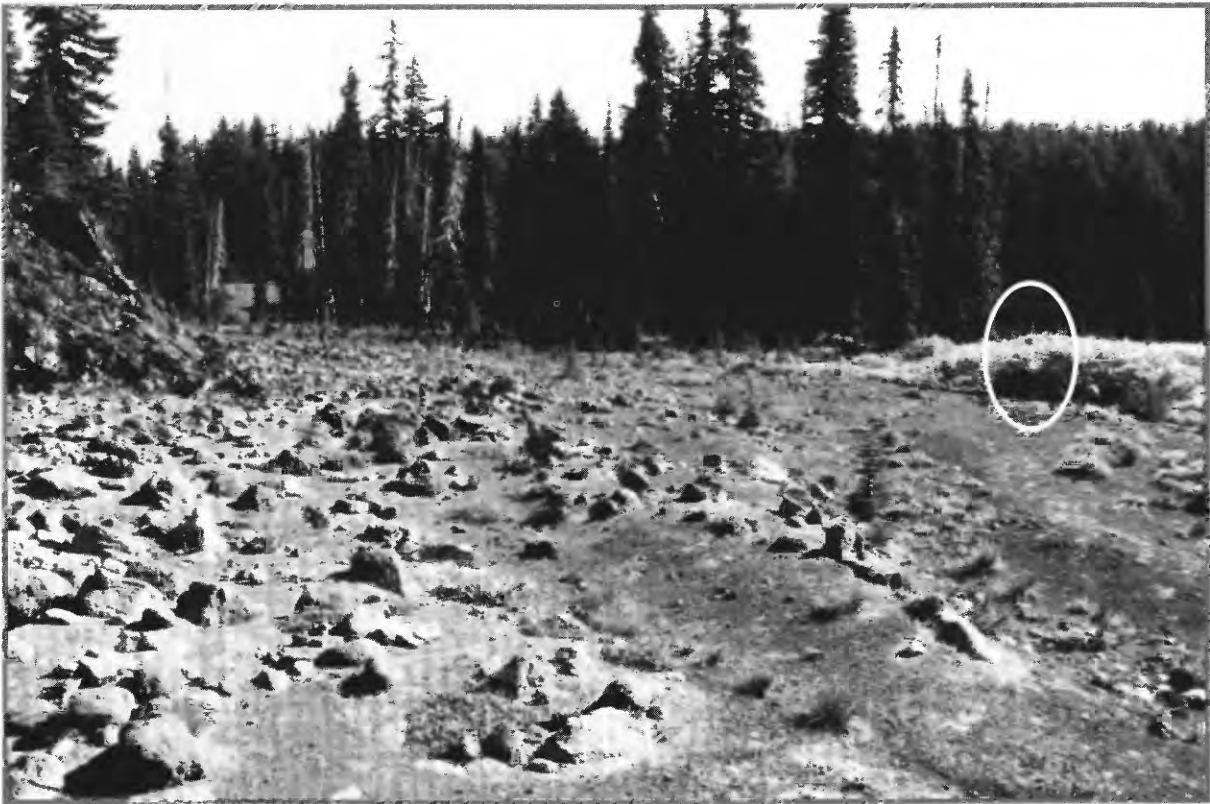


**Figure 34.** View east (upstream) of deposits from the 1942 debris flow down White Branch. The now-inundurated matrix was dense enough to support boulders up to a meter in diameter. Many of the larger clasts in this reach were entrained from talus of the lava flow from Collier Cone (partially visible on the left side of the photograph). Note person for scale.

types constitute most of the larger clasts in depositional areas.

Size distributions of the <32-mm sediment deposited by the flow are consistent with some of the flow aspects described above. The samples were collected by K.M. Scott (written commun., 1991) and analyzed by wet sieve and pipette analysis. Cumulative frequency curves of 13 deposit samples and a sample from the moraine show that most deposits have similar sediment-size distributions and are similar to the moraine material at the outlet. Similarity among deposits is most pronounced for the fine sand, silt, and clay fractions, which is consistent with the field observation that the character of the now-inundurated flow matrix changed little downstream.

Deposits of the White Branch flow had the highest clay content (1 to 6 percent) of all the measured debris flows (figs. 36 and 37). Debris flows with clay content greater than 3 percent have

a degree of cohesion that allows them to travel for relatively long distances without transforming into streamflow (Scott, 1988, p. 70-71; Scott and others, 1992, p. 12-15). The White Branch flow was the only studied debris flow in the Three Sisters and Mount Jefferson Wilderness Areas that did not transform into sediment-laden streamflow.

The content of coarser clasts (greater than 2 mm) in samples of the deposits was more varied than that of the matrix material and ranged from 0 to 54 percent (fig. 37). The actual gravel content of the deposits is greater than the sample analyses indicate because the collected samples systematically excluded clasts larger than 32 mm. Part of this variation probably is due to difficulty in collecting samples from similar depositional environments along the flow course. Nevertheless, there was a general decrease in gravel content and mean particle size within deposits along the first 4.5 km of White Branch, corresponding to the long

reach of declining gradient and diminishing peak discharge (pl. 2; fig. 32). Downstream fining of the deposits is inferred to be at least partly the result of size-selective deposition (Scott, 1967, 1988) by the debris flow. About 5 km from the outlet, White Branch descends through a steep and narrow reach that is constricted by rhyodacite bluffs and talus from the Obsidian Cliffs and by the lava flow from Collier Cone. There, gravel-content variation increased markedly (fig. 37) due to local incorporation and deposition of talus and bank material.

Other sediment-sample statistics, such as mean particle size and sorting, show no clear trend (fig. 37). This lack of trend is probably because of the overall cohesiveness of the flow; consequently, the flow matrix changed little over the length the flow. Also, large site-to-site variation in particle-size characteristics because of variations in local depositional environment probably masks downstream trends.

### Diller Glacier

During maximum Neoglacial advances, Diller Glacier covered 1.03 km<sup>2</sup> on the eastern slope of Middle Sister and formed high lateral and terminal moraines before retreating to a present area less than half its former size. Photographs by

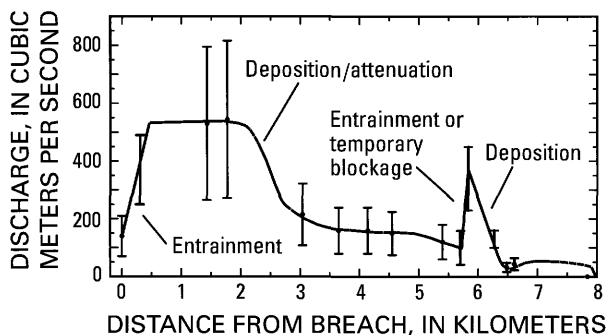


**Figure 35.** Indirect estimates of peak discharge for the 1942 debris flow on White Branch. Data portrayed as points and error bars are critical-flow estimates; data portrayed only as ranges are velocity-area estimates. Solid curve is an interpretation of how peak discharge varied downstream, annotated with inferences of the processes controlling the changes in peak discharge. Compare with figure 32.

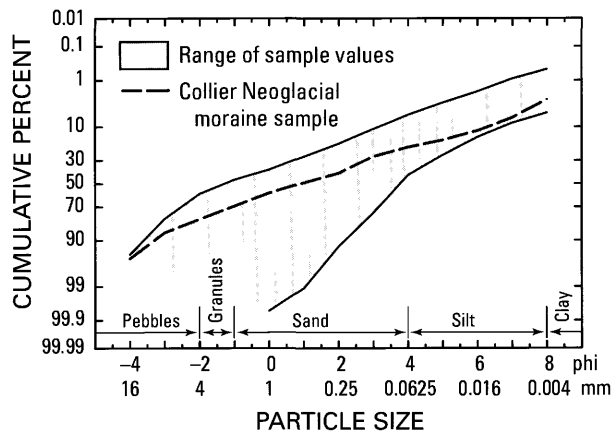


**Figure 36.** Range of cumulative curves for 13 samples of matrix material (less than 32 mm) from the 1942 White Branch debris-flow deposits. Also shown is the cumulative curve for a sample from Collier Glacier Neoglacial moraine. Data provided by K.M. Scott (USGS, written commun., 1991).

I.C. Russell in 1903 (fig. 5) and a 1929 Oregon Historical Society photograph (neg. LOT 311-260) show the glacier in contact with Neoglacial terminal and lateral moraines, but with an ice surface substantially lower than the moraine crests. Between 1929 and 1937, a lake formed at an altitude of 2,300 m between the glacier terminus and the terminal moraine (pl. 2; figs. 15C and 16). On the basis of our survey of the basin (figs. 17 and 18), the lake contained  $3.2 \times 10^5$  m<sup>3</sup> of water and had a maximum depth of 22.4 m.

Aerial photographs taken September 19, 1967, (fig. 15C) and July 17, 1973, (USFS photograph 1672-96) show the moraine dam was breached between these dates, resulting in a debris flow that traveled 9 km down the North Fork of Squaw Creek before transforming into sediment-laden streamflow near the confluence of the North and South Forks (pl. 2; figs. 38 and 39). Sandy deposits from this flow are traceable for another 7 km downstream. Discharge records from a stream gage 24 km from the breach (Squaw Creek near Sisters, Oregon) show a flow pulse of 35 m<sup>3</sup>/s on September 7, 1970, that almost certainly corresponds to this flow. By the time the flood wave reached the town of Sisters, 31 km from the breach, the flow was described as a muddy, 30-cm-high surge (Laenen and others, 1992, p. 153).

The lake completely emptied when the moraine dam failed, releasing 320,000 m<sup>3</sup> of water and entraining about 130,000 m<sup>3</sup> of till and outwash from the impounding moraine and steep outwash surface below the moraine (fig. 38). Three hundred meters from the breach, the flow dropped over a steep reach, eroded the channel to bedrock, and formed a set of falls. On the outwash surface at the base of the falls, the flow deposited a debris fan covering an area of 40,000 m<sup>2</sup>. Near the fan apex, the largest clasts have intermediate diameters as

large as 3 m. Bouldery lobes on the fan surface are cut by lower and less bouldery surfaces (fig. 38), indicating that later phases of the flow were erosive and carried finer sediment. At the distal end of the fan, the debris flow inundated a meadow, covering it with 2 m of 1- to 2-m-diameter boulders within a gravelly sand matrix. Later, the distal fan deposits and the underlying fine-grained fluvial deposits of the meadow were entrenched as much as 4 m, apparently by a final, watery phase of the flow (fig. 40).

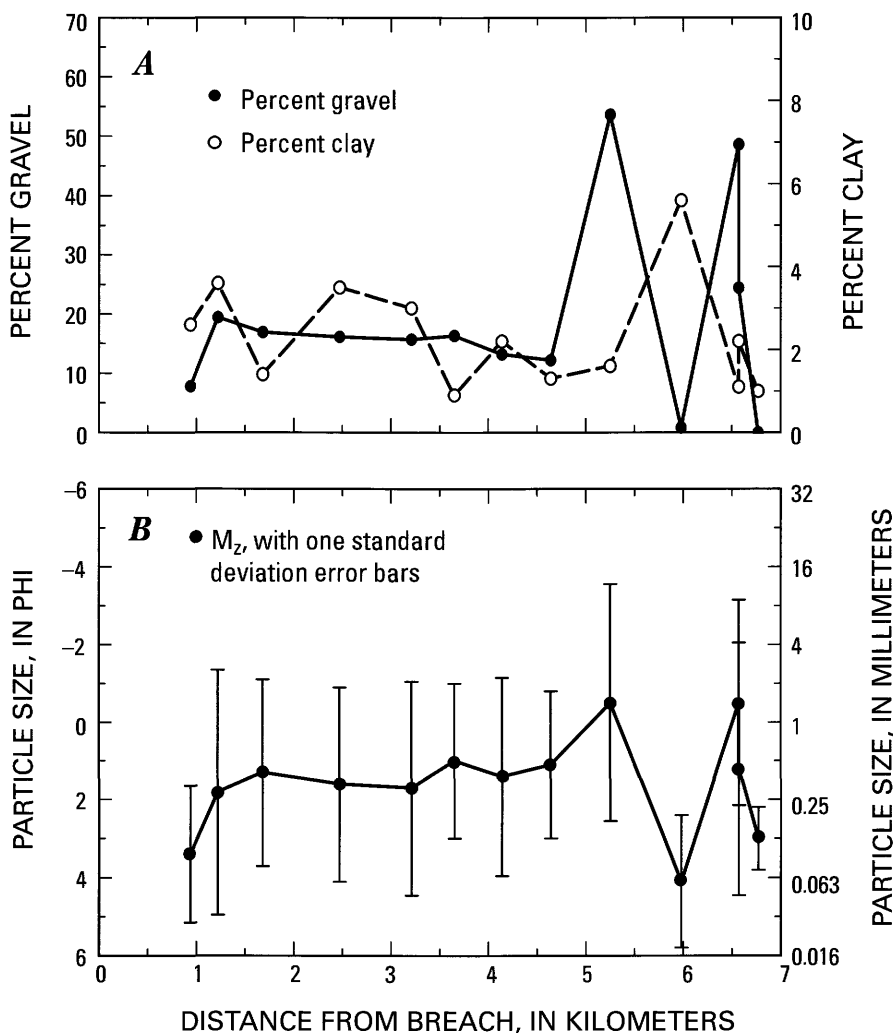
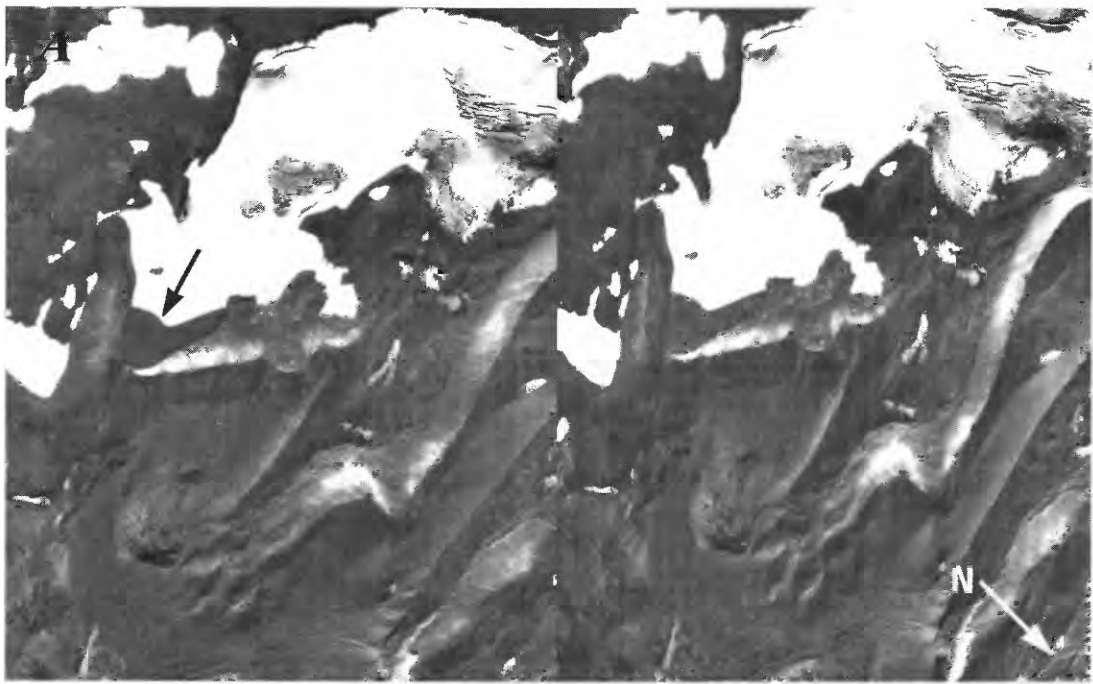


**Figure 37.** Downstream variation in particle-size distribution characteristics of matrix materials (less than 32 mm) for the 1942 White Branch flow. *A*, Clay and gravel content variation. *B*, Graphic mean particle size ( $M_z$ ) and standard deviations as defined by Folk (1980, p. 40-46). Data provided by K.M. Scott (USGS, written commun., 1991).



0 0.5 1 KILOMETERS

**Figure 38.** Stereophotograph pairs of Diller Glacier before and after the September 7, 1970, breach of the moraine-dammed lake at the glacier terminus. Arrows on the left pair show location of the lake. *A*, September 4, 1963; photographs by Austin Post. *B*, September 6, 1974; photographs by U.S. Department of Agriculture, Forest Service.

The debris flow continued down North Fork Squaw Creek, eroding colluvium, till, and outwash from narrow and steep reaches, and deposited levees and boulder berms in wide reaches (fig. 41). At an elevation of 2,000 m, 1.5 km from the breach, the flow bifurcated, with a portion spilling over the left bank and into the drainage from Hayden Glacier before rejoining the main thread of flow 700 m downstream (pl. 2). From this point downstream, interactions between standing timber and logs and wood debris in the flow exerted substantial control on patterns of deposition. Large woody debris incorporated in the flow was lodged in overbank areas and caused large boulder and debris accumulations. Closely spaced standing timber in overbank areas trapped boulders and caused upstream deposition (fig. 42).

At an altitude of 1,840 m, the flow entered a 4-km reach of gradually decreasing gradient (fig. 39, pl. 2). Within this reach, there was substantial deposition, especially in wide, forested, overbank areas. The area covered by debris-flow deposits within this reach was about 130,000 m<sup>2</sup>. Exposures near fan apices indicate deposit thicknesses greater than 4 m (fig. 43). At the

downstream end of this reach, near the confluence with Soap Creek, the flow descended a steep reach of narrow gorges and falls over and within several lava flows that outcrop along the channel. Evidence of the 1970 debris flow within this reach is sparse and includes small levees in locally wide reaches and small deposits of coarse gray sand along channel margins.

At the confluence of the North Fork and South Fork of Squaw Creek, bouldery bars, woody debris, and sand were deposited at the abrupt decrease in gradient (pl. 2; fig. 39). Downstream from the confluence, there are no bouldery levees or other features indicative of continued debris flow. Abundant gravel bars and gray sand deposited on the channel banks over the next 7 km do indicate, however, that a substantial discharge of water and sediment continued down Squaw Creek.

Indirect discharge estimates along the flow route are consistent with mapped patterns of deposition and erosion (pl. 2). We calculated 13 indirect discharge estimates from measured cross sections and highwater marks along the flow path. Highwater evidence consisted of organic flotsam and deposits of gray sand in overbank areas, and

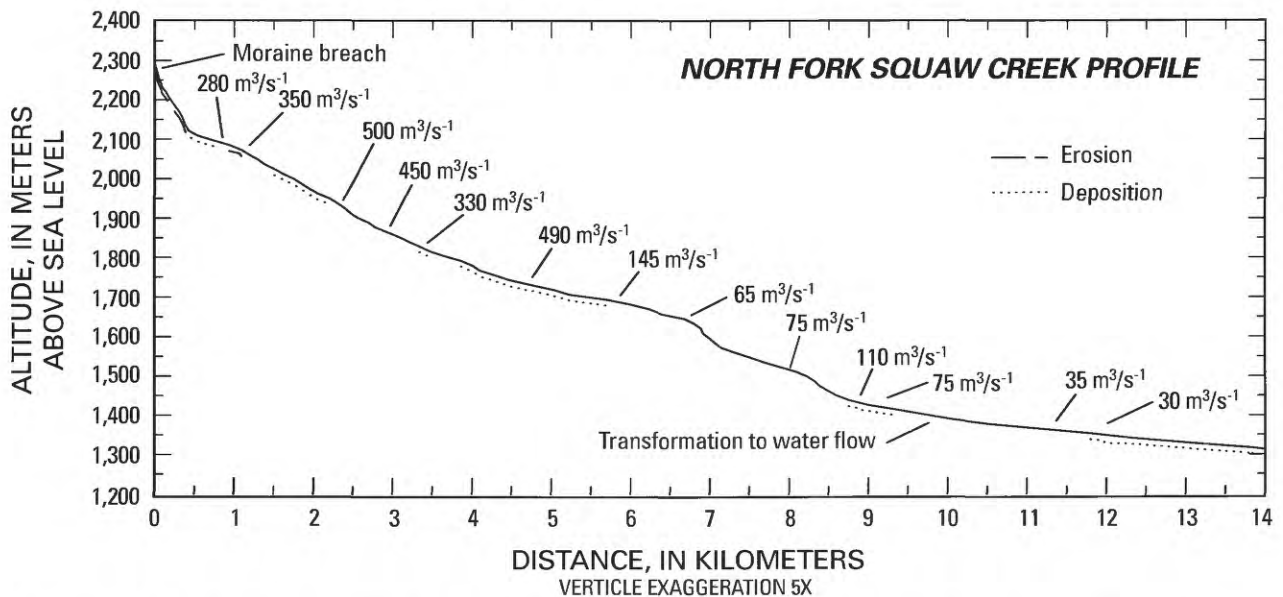


**Figure 39.** Longitudinal profile of North Fork Squaw Creek showing indirect discharge estimates and reaches of erosion and deposition during the September 7, 1970, debris flow and flood from the breach of the lake at the terminus of Diller Glacier.

scars on trees near the channel. Five of these estimates were critical-flow cross sections, seven were velocity-area estimates, and one was a Manning Equation estimate.

Because the lake was deep (22.4 m) and the breach was large, the maximum possible discharge at the outlet, assuming critical flow from maximum lake level through a fully formed breach, is large—about 6,000 m<sup>3</sup>/s. The actual minimum discharge at the breach was probably substantially less because the lake level in this small, but deep, lake would have likely dropped

significantly as the breach developed. The first reliable discharge estimate below the breach is a critical-flow estimate 800 m downstream from the outlet where the maximum discharge was about 280 m<sup>3</sup>/s. Downstream, as the flow eroded outwash and till from the channel banks, peak discharge apparently increased to about 450 m<sup>3</sup>/s, based on a critical-flow estimate at the beginning of the long depositional reach at 1,850 m altitude (pl. 2; fig. 39). Four kilometers downstream, after a large volume of the flow had been deposited, the peak discharge had diminished to about 65 m<sup>3</sup>/s. This



**Diller Glacier  
moraine  
breach**

**Figure 40.** Photograph of distal end of the large bouldery fan deposited below the September 7, 1970, breach in the Diller Glacier moraine. Photograph taken September 11, 1993.



**Figure 41.** View upstream of a debris flow levee or boulder berm (Costa, 1984, p. 292-293) deposited by the 1970 North Fork Squaw Creek debris flow from Diller Glacier. Note people for scale. Photograph taken August 11, 1986.



**Figure 42.** View downstream of boulders trapped by trees in an overbank area during the 1970 North Fork Squaw Creek flow. Photograph taken September 19, 1992.

estimate is consistent with three additional velocity-area estimates over the next 2 km (fig. 39). Downstream from the transformation of the debris flow to water flow, a Manning Equation estimate and a critical-depth estimate yielded discharge estimates of 36 and 32 m<sup>3</sup>/s, respectively. These values are similar to the September 7, 1970, gaged discharge of 35 m<sup>3</sup>/s measured 12 km downstream.

The shape of the recorded hydrograph for September 7, 1970, is typical of floods resulting from dams that fail rapidly (Costa, 1988) (fig. 44). Measured stage rose 0.75 m in less than 10 minutes, corresponding to discharge rising from 5 to 35 m<sup>3</sup>/s. The duration of the flow pulse was less than 1 hour, and the volume of the surge passing the gaging station was 110,000 m<sup>3</sup>, about a third of the volume. The remainder of the water from the lake probably was temporarily stored within the debris-flow deposits and underlying sediment along the floodplain and channel of Squaw Creek.

Overall, deposits from the Squaw Creek debris flow are coarser than deposits left by the flow down White Branch, especially in the finer size fractions (figs. 45 and 46). Whereas samples from the White Branch flow deposits vary between 6.0 and 33.7 percent silt-sized particles (0.0625 mm) and finer, samples from the Squaw Creek debris flow deposits contain only 1.2 to 7.7 percent silt-sized and finer particles. Likewise, clay content of the Squaw Creek flow deposit is less than 0.5 percent compared with clay contents of 1 to 6 percent for deposits left by the White Branch flow. This resulted in a distinct difference in the character of the preserved deposits. The finer matrix of the White Branch flow hardened upon drying, leaving the deposits from the 1942 flow indurated and well-preserved. The matrix of the 1970 Squaw Creek flow was primarily gray sand, resulting in comparatively loose, but distinctive, deposits in overbank areas and along flow margins for the entire flow route.



**Figure 43.** The buried trees in this September 20, 1992, view indicate that there was locally as much as 4 meters of aggradation in depositional areas during the 1970 North Fork Squaw Creek debris flow from Diller Glacier. Note people for scale.

The wide site-to-site variation in sediment texture shown by analyses of deposit samples (fig. 46) is apparent in the field and appears to have resulted from different channel geometries that controlled local patterns of deposition and to facies variations within the deposits. Nevertheless, there is an overall downstream decrease in mean particle size, size variation, and gravel content. Beyond the transformation of the debris flow to sediment-laden streamflow at 9 km from the breach, gravel content of the flow deposits diminished to less than 2 percent. Nevertheless, the gray sand, deposited along the flow margins, is traceable for at least 7 km farther downstream.

Analysis of the boulder and cobble rock types deposited by the flow indicates that there was substantial entrainment and deposition of large clasts along the flow path. Lithology of 50 clasts with diameters larger than 20 cm was noted at each of 3 sites (fig. 47): (1) at the distal end of the large fan 600 m from the breach, (2) in a deposit 2.1 km from the breach, and (3) at the North and South Fork Squaw Creek confluence, 9 km from the breach. Of the boulders deposited at the second site, less than half were of similar rock types to those at the fan immediately downstream of the breach, indicating that most of the larger particles

were entrained in the intervening reach. About 20 percent of the clasts at the second site were of rock types exposed in the channel between the two sites, the others probably came from the till and outwash that composes the channel banks along the remainder of the intervening reach. At the small fan at the North and South Fork confluence, 9 km from the breach, less than 10 percent of the sampled clasts larger than 20 cm are similar to those deposited at either of the upstream sites. Greater than 60 percent of the clasts larger than 20 cm and 21 of the 22 clasts larger than 50 cm appear to have come from basaltic andesite flows exposed in the steep canyon upstream from the fan.

### Eugene Glacier

The first recorded debris flow from a moraine-dammed lake in the Cascade Range was from the failure of a Neoglacial moraine dam near the terminus of Eugene Glacier, a small ice body clinging to the steep, 600-m-high north-northwest facing slope on the north side of South Sister (pl. 2). During maximum Neoglacial advances and until the early 1930's, Eugene Glacier covered 0.21 km<sup>2</sup> and terminated in three separate lobes against large moraines at an altitude of about 2,475 m (figs. 48 and 49). The present ice-covered

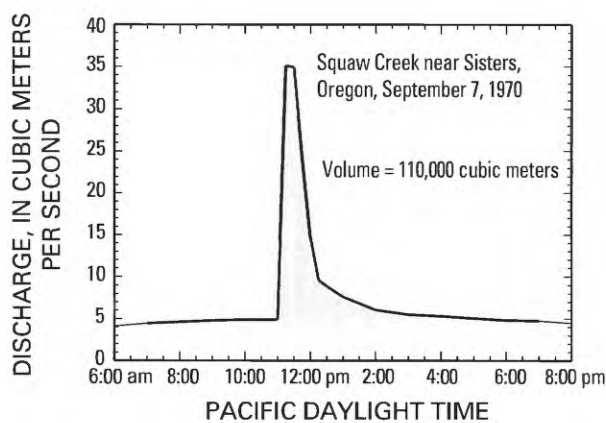


**Figure 44.** Hydrograph for the period 6:00 am to 6:00 pm for September 7, 1970, on Squaw Creek, 24 kilometers from breach (Squaw Creek near Sisters, Oregon: station 14075000). The 11,000 m<sup>3</sup> volume of the flood at the stream gage (indicated by shaded area) was estimated by subtracting an estimate of the baseflow component from the total hydrograph volume.

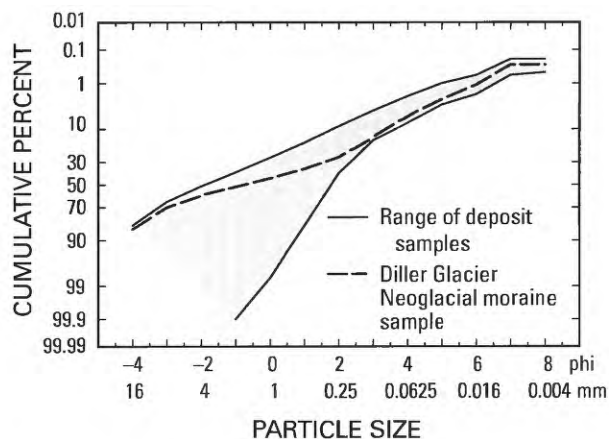


**Figure 45.** Range of cumulative curves for 13 samples of matrix material (less than 32 mm) from the 1970 North Fork Squaw Creek flow debris-flow deposits. Also shown is the cumulative curve for a sample from the Diller Glacier Neoglacial moraine. Data provided by K.M. Scott (USGS, written commun., 1991).

area is about 0.09 km<sup>2</sup>. Two debris flows resulted from moraine-dammed-lake releases at Eugene Glacier. The first, in 1933, was the largest, and involved the central and eastern lobes of ice. The second resulted from a small release between 1933 and 1949 from a lake dammed behind the terminal moraine formed by the western ice lobe.

According to newspaper accounts (The Oregonian, Aug. 14, 17, 20, and 22, 1933), a large volume of water and ice escaped Eugene Glacier on August 12, 1933. The resulting debris flow inundated 250,000 m<sup>2</sup> and traveled 6.3 km (pl. 2) before evolving into sediment-laden water flow. The Oregonian (Aug. 20, 1933) reported that the McKenzie River was “brick red” as far as 100 km downstream at Blue River, and suspended “lava dust” had to be filtered out of Eugene’s water supply.

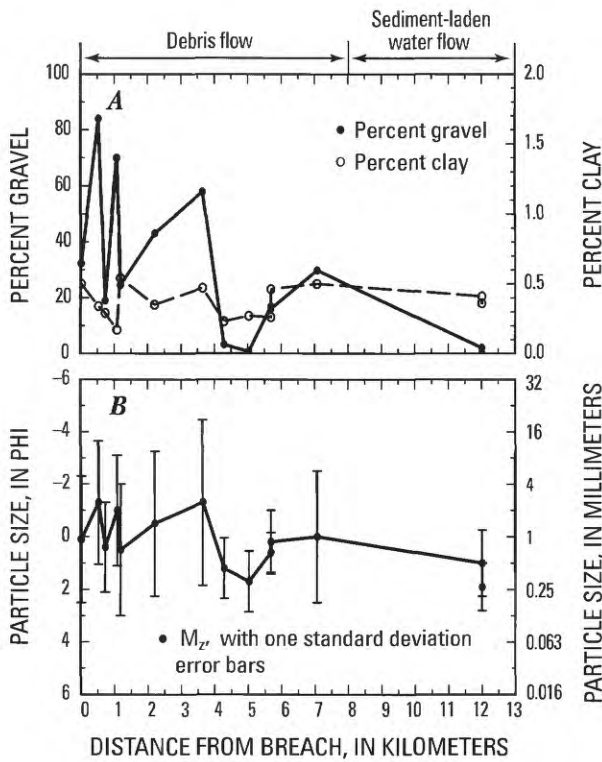


**Figure 46.** Downstream variation in particle-size distribution characteristics of matrix materials (less than 32 mm) for the 1970 North Fork Squaw Creek debris flow. Definitions of graphic mean ( $M_z$ ) and standard deviation are from Folk (1980, p. 40-46). **A**, Clay and gravel content variation. **B**, Graphic mean particle size and standard deviation. Data provided by K.M. Scott (USGS, written commun., 1991).

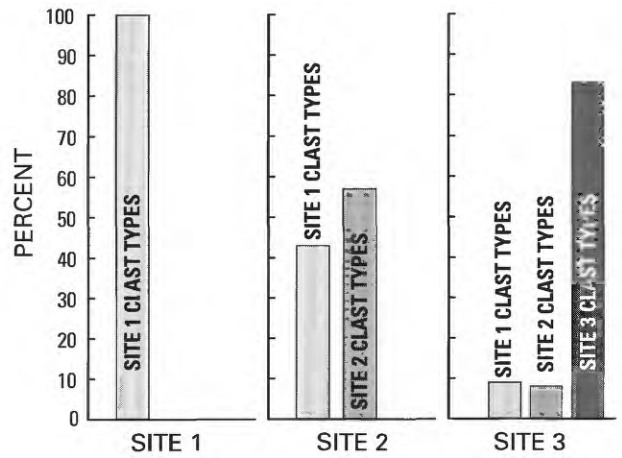


**Figure 47.** Results of rock-type counts of greater than 20-cm diameter clasts ( $n = 50$ ) at sites 1–3 (0.6, 2.1, and 9 km, respectively, downstream from the breach of the moraine at Diller Glacier).

Photographs and reports published by The Oregonian (Aug. 17 and 20, 1933) (fig. 50) provide clues to the sequence of events (note that the glacier is referred to as Skinner Glacier in the newspaper reports). Apparently a body of possibly subglacial water had formed at the central terminal ice lobe. A 1929 photograph (fig. 48) does not show a lake at the location, although this was a period of rapid glacier recession and it is possible that the lake formed in the intervening 3 years. The water body breached a moraine between the central and eastern ice lobes, and escaped eastward, eroding through the eastern ice lobe and the moraine at the end of the lobe. A week after the flow, in the basin formerly occupied by the central ice lobe, there was a subaerial remnant of the lake held by the partially breached moraine, and most of the eastern lobe of ice had been removed (fig. 50).

The outburst apparently transformed into a debris flow within 500 m of the breached moraine and deposited gravelly sand with abundant and distinctive 10- to 20-cm-diameter red cinders over wide and low-gradient parts of the Separation Creek valley (pl. 2). A small portion of the flow spilled into the westernmost Chambers Lakes basins. Most of the material entrained in the flow was derived from Neoglacial and older till and outwash that composes the steep slopes in the proglacial area north of Eugene Glacier. In

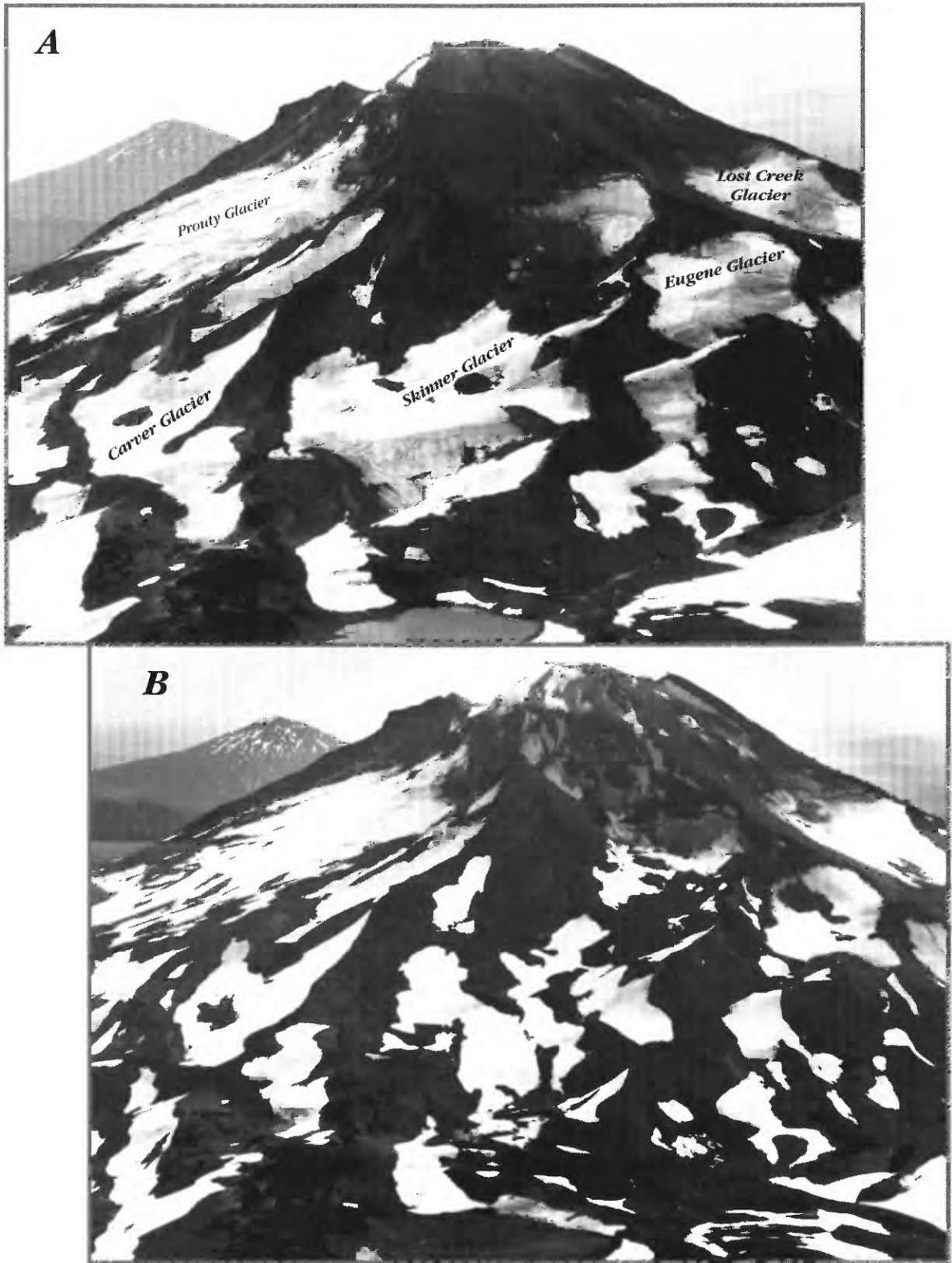


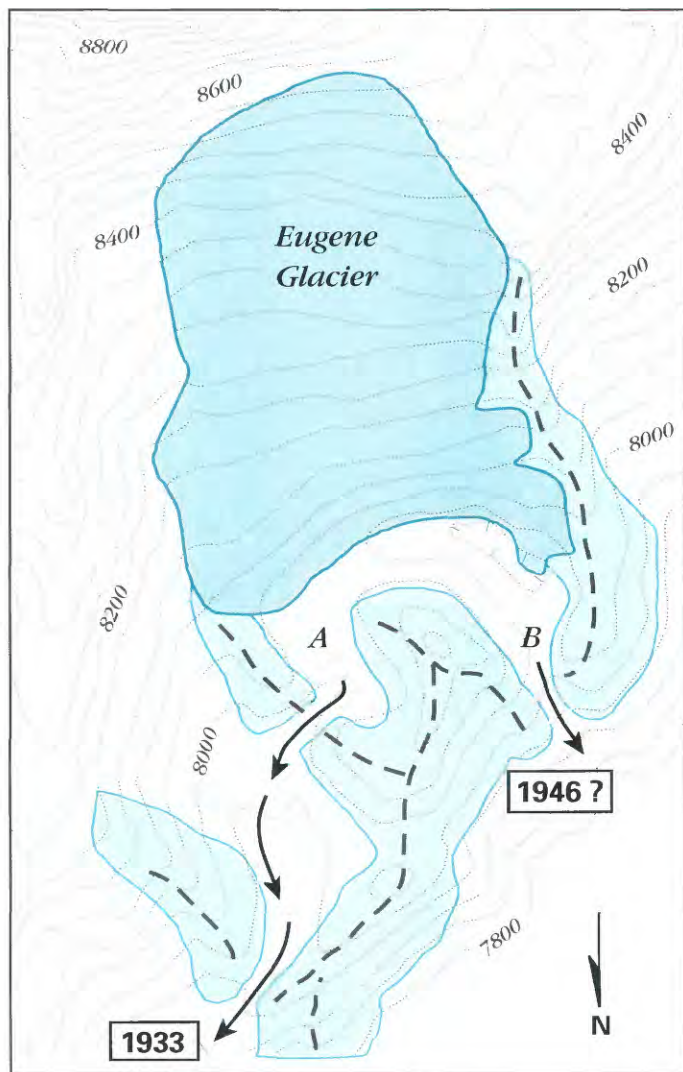
**Figure 48.** Approximately matched views of the north slope of South Sister from the summit of Middle Sister. *A*, 1929 photograph reproduced with permission of the Oregon Historical Society (neg. 311-70). *B*, September 13, 1993, photograph by David E. Wieprecht (USGS).

narrower reaches, bouldery levees define the flow margins.

Deposits from this flow are traceable to Separation Creek Meadow, 6 km from the source (pl. 2; fig. 51), where a thin fan of gravelly sand containing cobbles and boulders was deposited over 20,000 m<sup>2</sup> of the meadow surface. Several channels at the downstream end of the meadow were incised as deeply as 1.5 m, probably by the watery remainder of the flow as it continued across the meadow. According to observations published in *The Oregonian* (Aug. 20, 1933), the flow was 3 to 4 m deep across the meadow, and entrained “tons of the soft red silt from the meadows.” No

evidence of debris flow was observed downstream of Separation Creek Meadow, but a sizeable, sediment-laden flow must have continued far downstream to form the basis of the newspaper accounts of downstream sediment concentrations in the MacKenzie River.

An estimate for the maximum discharge at the breach is 230 m<sup>3</sup>/s, assuming critical flow through the present breach, and assuming flow stage did not reach the level of the uneroded moraine crest. Because the breach was deepening as the flow exited, the actual peak discharge at the outlet was probably much less than 230 m<sup>3</sup>/s. A measured cross section 1 km from the outlet gives a velocity-



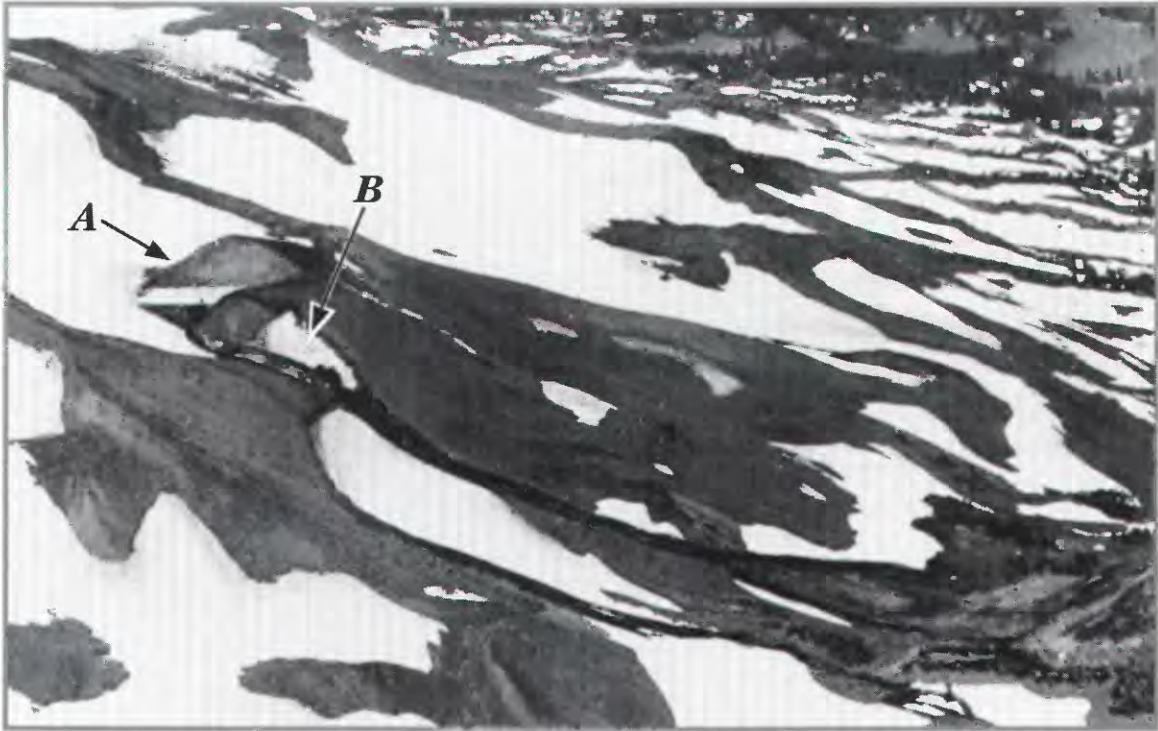
### EXPLANATION

- Neoglacial moraine (Dashed line indicates crest)
- 1981 Glacier

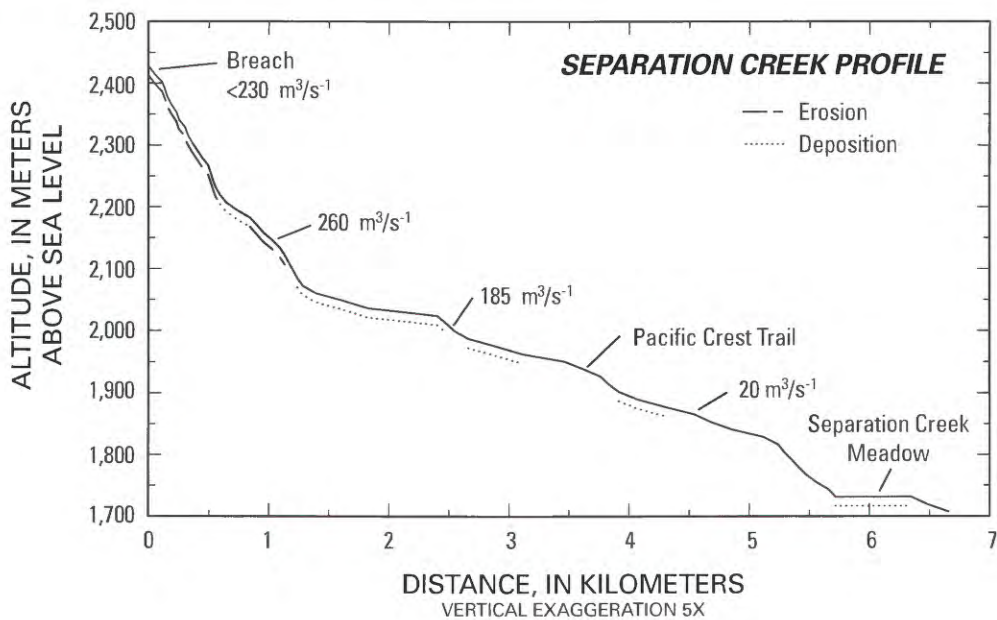
0 150 METERS  
 CONTOUR INTERVAL 40 FEET  
 To convert feet to meters multiply by 0.3049

Figure 49. Topographic setting of August 12, 1933 and 1946(?) moraine-dammed lake releases at Eugene Glacier, South Sister. “A” is the basin, formerly occupied by a central lobe of ice from Eugene Glacier, which was the source of water in the August 12, 1933, flow. A second and much smaller flow, perhaps in 1946, resulted from partial breaching of the moraine impounding the small western basin “B.”

Topography from US Geological Survey  
 North Sister, Oreg., 1988



**Figure 50.** Oblique aerial view west toward the August 12, 1993, lake breach and debris flow from Eugene Glacier. This photograph (reproduced with permission of The Oregonian) was taken about one week after the flow. “A” is the middle basin, from which water escaped by breaching a morainal ridge to the southeast. “B” is the eastern glacial lobe where escaping water eroded through the ice, depositing a track of dark-colored deposits on the ice and downslope on snow and moraines.



**Figure 51.** Longitudinal profile of Separation Creek, showing indirect discharge estimates and reaches of erosion and deposition during the August 12, 1933, debris flow and flood from the breach of the lake at the terminus of Eugene Glacier. The critical depth measurements are given as single values and inferred to be accurate to within  $\pm 50$  percent. The velocity-area measurements are given as ranges.

area estimate of 175 to 350 m<sup>3</sup>/s. This is consistent with a critical-flow estimate of 185 m<sup>3</sup>/s an additional 1.5 km downstream (pl. 2; fig. 51). Farther downstream, the peak discharge apparently attenuated rapidly, decreasing to about 20 m<sup>3</sup>/s at 4.5 km from the breach before transforming to sediment-laden flood flow at Separation Creek Meadow.

A second and much smaller debris flow from Eugene Glacier apparently resulted from rapid release of a small lake impounded by the moraine formed around the western lobe (fig. 49). The date of this flow is not known. On the basis of inspection of oblique and vertical aerial photographs, however, the breach occurred after August 1933, when the lake had not yet formed between the ice margin and the moraine, and before August 25, 1949, when the lake had formed and already partially emptied. A tree in the path of the release was partly knocked over in 1946, providing a tentative date for the release. August 1949 aerial photographs show a small lake with a surface area of about 2,500 m<sup>2</sup> draining from the breached outlet. The flow exiting the lake carved a channel down the 20° moraine slope and deposited a small fan of bouldery gravel and sand on top of deposits from the 1933 debris flow. Deposits from the second flow are traceable only to about 1.2 km from the breach.

### East Bend Glacier

During maximum Neoglacial advances, East Bend Glacier<sup>4</sup> covered about 0.24 km<sup>2</sup> and was contiguous with Bend Glacier before diminishing to a separate ice mass of 0.07 km<sup>2</sup> by 1990 (pl. 1). During retreat, a lake formed between the Neoglacial moraine and the calving glacier (fig. 15) at an altitude of 2,500 m. The date of lake formation is not known precisely. The lake

<sup>4</sup> On early topographic maps, this small glacier in an east-facing cirque on Broken Top was labeled "Crook Glacier" (Hodge, 1925; USGS 1932, Three Sisters, 30-min. Quadrangle). The name Crook Glacier, however, is now assigned on current USGS maps (USGS, 1959, Broken Top, 15-min. and USGS, 1988, Broken Top, 7-1/2-min. Quadrangles) to a small glacier on the south side of Broken Top; the previous Crook Glacier is unnamed. In this report, this unnamed glacier is referred to as "East Bend Glacier."

apparently existed prior to 1928 (Phillips, 1938), and possibly formed after 1924 (no lake is mentioned in Hodge's [1925] report and topographic map of the Three Sisters/Broken Top region). At its largest, the lake contained 340,000 m<sup>3</sup> of water, had a maximum depth of 18 m (figs. 15, 16, and 17), and spilled over an outlet and down the steep distal slope of the moraine.

On October 7, 1966, 140,000 m<sup>3</sup> of water was released and the lake-level lowered 4.4 m in conjunction with partial breaching of the moraine dam. The resulting debris flow flowed down an unnamed tributary, joining Crater Creek 6 km downstream from the breach. The debris flow continued down Crater Creek until it entered Soda Creek 1 km farther downstream. The debris flow followed Soda Creek for another 3 km until it spread out over the broad meadows near Sparks Lake (pl. 2; fig. 52). The flow was described in the Bend Bulletin (Oct. 10 and 11, 1966) and by Nolf (1966), both of whom summarized observations of reconnaissance trips to the source within a week after the event. The writers of these reports each speculated that erosion of the outlet was triggered by a wave caused by calving of a large block of ice into the lake. A photograph (Austin Post, U.S. Geological Survey photograph, 6615-47) taken a week before the release shows a large ice cornice overhanging the west edge of the lake. The lake did not completely empty; 200,000 m<sup>3</sup> of water remains with a maximum depth of 13.7 m (figs. 15 and 17). Downcutting at the outlet possibly was halted by several 0.5- to 2-m-diameter boulders that presently compose the outlet thalweg and margins.

Flow at the outlet evolved into a debris flow by entraining bouldery gravel from the Neoglacial moraine impounding the lake (fig. 53). The debris flow locally eroded bedrock in steeper reaches (fig. 54), whereas small fans and levees were deposited in wide and low-gradient reaches (pl. 2; figs. 52 and 55). Much of the initial debris flow was deposited upstream from the Crater Creek confluence, leaving little evidence of a large discharge along the channel between altitudes of 1,950 and 1,830 m. The flow increased substantially, however, within the steep reach between the Crater Creek and Soda Creek

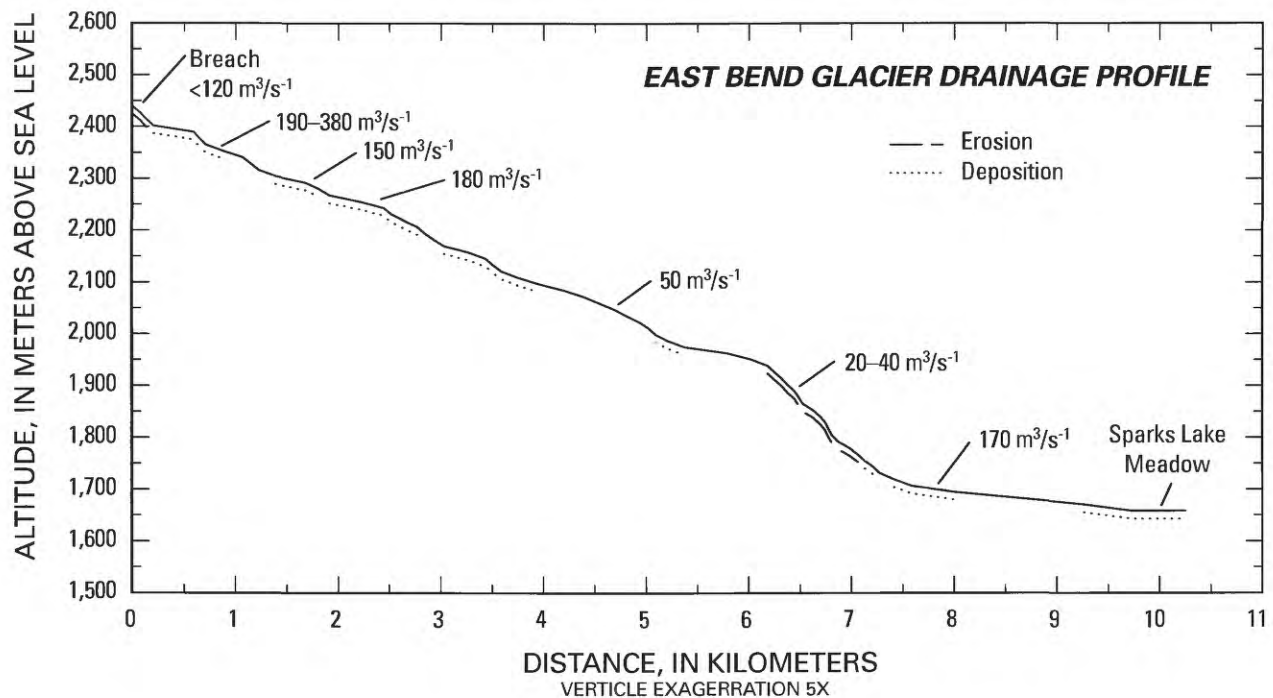


**Figure 52.** Longitudinal profile of the drainage from East Bend Glacier, Broken Top, into Sparks Lake, showing indirect discharge estimates obtained in this study and locations of mapped reaches of erosion and deposition during the October 7, 1966, debris flow and flood from the breach of the lake at the terminus of the glacier. The indirect discharge estimates are by the velocity-area and critical-flow methods. Critical-flow estimates are given as single values and inferred to be accurate to within  $\pm 50$  percent. The velocity-area measurements are given as ranges.

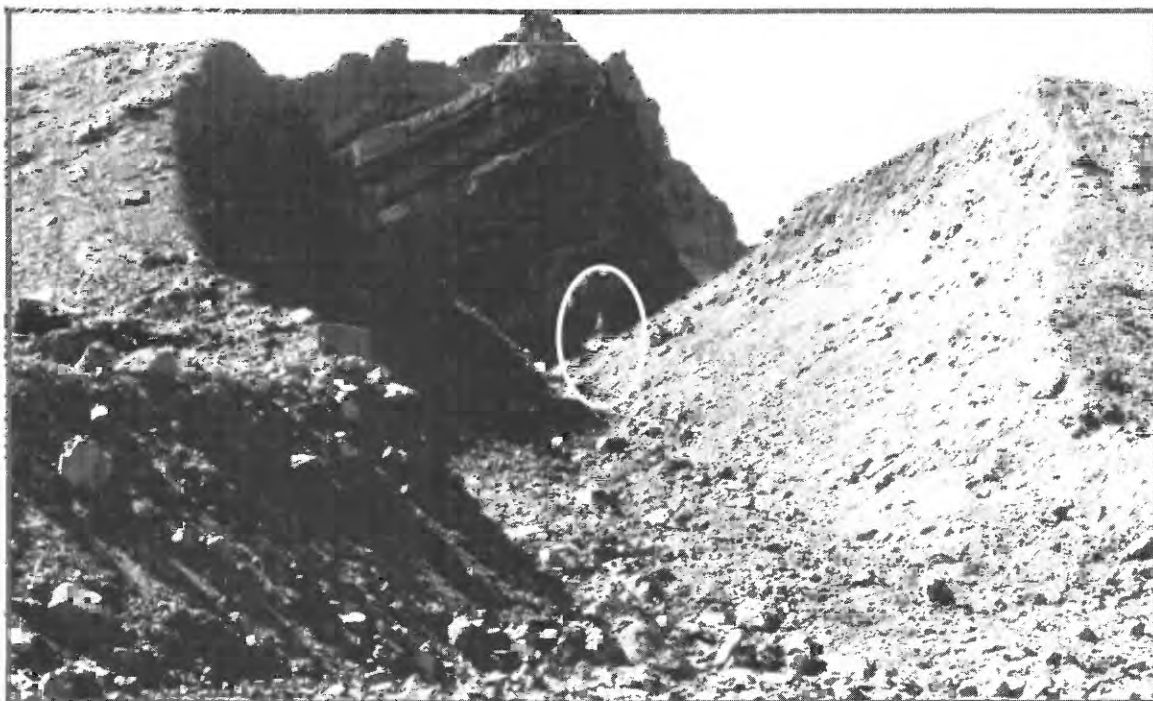


**Figure 53.** View of the October 7, 1966, breach in the Neoglacial moraine impounding the lake at the terminus of East Bend Glacier, Broken Top. The view is from near the base of the moraine, taken October 3, 1991. Note person standing on one of several large boulders at the present lake outlet.



**Figure 54.** View of valley-bottom bedrock erosion about 1.6 kilometers downstream from breach of the East Bend glacial lake. Flow was left to right. Many of the 1- to 2-m clasts eroded from the jointed basaltic andesite flows along the channel bottom were deposited in the next several hundred meters downstream. Photograph taken August 15, 1988.



**Figure 55.** View downstream (southwest) of deposits left by the October 7, 1966, debris flow from the lake at the terminus of East Bend Glacier. The debris fan is about 500 m downstream of the eroded reach shown in figure 54. Part of the flow left the main channel, spilled over the divide to the west (to the right as viewed on this October 3, 1991 photograph), and rejoined the main channel 0.5 km downstream.

confluences by incorporating trees, outwash, and colluvium from the steep valley slopes. Much of this debris was apparently provided by a mass movement of glaciofluvial sediment (about 200,000 m<sup>3</sup>) triggered by undercutting of the valley side at an altitude of about 1,830 m.

At the Soda Creek confluence, the valley widens and the rejuvenated debris flow deposited levees and a large fan of woody debris and bouldery gravel, including boulders with diameters of at least 2 m (fig. 56). Downstream from the fan, flow transformed into sediment and wood-laden streamflow until debouching onto the meadow near the State Highway 46 crossing, burying the road and covering about 250,000 m<sup>2</sup> of the meadow with sand and silt.

Seven indirect estimates of peak discharge along the flow route are consistent with the flow behavior outlined above (fig. 52). A maximum

possible discharge of 80 ±40 m<sup>3</sup>/s at the breach results from calculating the discharge associated with critical flow for conditions of a fully formed breach and maximum lake level. As with other lake releases, the actual maximum discharge at the breach probably was less. A velocity-area estimate of 190 to 380 m<sup>3</sup>/s at a cross-section 700 m from the outlet indicates that peak discharge had increased by a factor of at least 2, owing to entrainment of debris from the distal slope of the moraine. Two critical-flow estimates (150 and 180 m<sup>3</sup>/s) calculated at cross sections measured within 2 km downstream from the 190 to 380 m<sup>3</sup>/s measurement are consistent with the low end of the velocity-area estimate.

Downstream, peak discharge greatly diminished below reaches of substantial deposition (pl. 2). A critical-flow estimate 4 km from the breach indicates a maximum discharge of 50 m<sup>3</sup>/s,



**Figure 56.** View upstream of a boulder and timber fan deposited by the October 7, 1966, debris flow from the lake at the terminus of East Bend Glacier, Broken Top. This site is 150 m downstream from the confluence of Soda and Crater Creeks. Photograph taken August 16, 1988.

and a velocity-area estimate at 6 km from the breach gives a peak-discharge estimate of 20 to 40 m<sup>3</sup>/s. Farther downstream, after entraining substantial debris between the Crater Creek and Soda Creek confluences, peak discharge of the debris flow increased to close to its maximum value of 170 m<sup>3</sup>/s before ending on the Sparks Lake meadows 10 km from the breach (pl. 2; fig. 52).

The discharge values obtained in this study are consistent with two of three indirect estimates made by Laenen and others (1987) by superelevation and slope-area procedures. One superelevation measurement obtained by Laenen and others (1987) of 210 m<sup>3</sup>/s is substantially higher than adjacent estimates of 50 m<sup>3</sup>/s (critical-flow) and 20-40 m<sup>3</sup>/s (velocity-area) obtained by us. We found no field evidence for such changes in flow conditions between measurement sites. Therefore, we think the discharge attained was less than that estimated by Laenen and others (1987), but are uncertain as to the reasons for the discrepancy.

Sediment samples of the moraine, the original source of debris, and of four downstream deposits all have less than 1 percent clay (fig. 57) and have

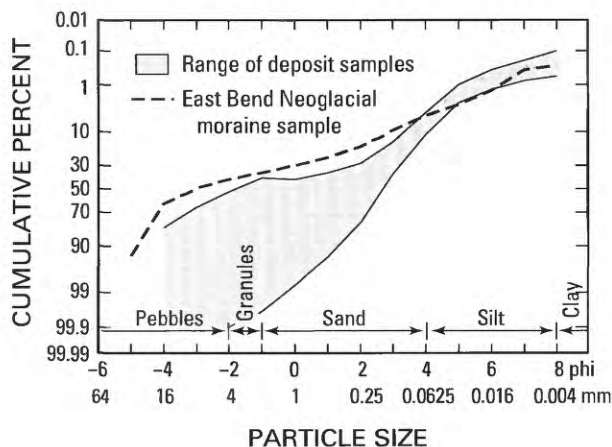


**Figure 57.** Range of cumulative curves for four samples of matrix material and fine gravel (less than 32 mm) from the 1966 debris flow from East Bend Glacier, Broken Top. Also shown is the cumulative curve for a sample from the Neoglacial moraine that impounds the remnant lake. Data provided by K.M. Scott (USGS, written commun., 1991).

distributions similar to samples from the 1970 Squaw Creek debris flow (fig. 36). In part, due to the small amount of silt- and clay-sized particles, the flow from East Bend Glacier behaved similarly to the Squaw Creek flow, transforming from a debris flow to sediment-laden streamflow where most of the coarse fraction was deposited at the pronounced gradient decrease 7.5 km from the breach.

## Processes

Analysis of moraine dam failures and resulting debris flows in the Three Sisters and Mount Jefferson Wilderness Areas provides a basis for interpretation of some natural-dam-failure and debris-flow processes. Only limited conclusions can be gleaned from study of deposits as old as 50 years, and indirect measurements and interpretation of stratigraphy and sedimentology do not fully replace direct observation and measurement. Nevertheless, observations of moraine-dam failures and large debris flows, reconstructed from geologic evidence, provide new information about many aspects of natural-dam failures and resulting flow behavior.

Magnitudes of 20th-century debris flows in the Three Sisters and Mount Jefferson Wilderness Areas varied widely. The largest debris flows traveled as far as 9 km, had peak discharges as great as 500 m<sup>3</sup>/s, and involved up to 1 million m<sup>3</sup> of debris and water. These flows were substantially larger and travelled farther than did the less than 3-km-long debris flows typical of the densely forested Cascade Range and Coast Range watersheds in Washington and Oregon (Benda and Cundy, 1990). The size of the debris flows in the Three Sisters and Mount Jefferson Wilderness Areas is not unusual relative to other alpine debris flows in the Cascade Range (Gallino and Pierson, 1985; Osterkamp and others, 1986; Walder and Driedger, 1994), and other alpine areas (Pierson, 1980; Eisbacher and Clague, 1984; Jackson and others, 1989). The resulting debris flows from breached moraine dams are small, however, compared to Holocene Cascade Range debris flows caused by large volcano sector collapses and volcanic eruptions (Crandell, 1971; Pierson, 1985; Scott, 1988; Scott and others, 1992).

Nonvolcanic debris flows in glacierized alpine environments are generated primarily by three mechanisms: (1) mass movement of debris into stream courses and consequent fluidization and downstream flow, (2) outburst floods of subglacial water accumulations, and (3) rapid release of moraine- and ice-dammed lakes. During the 19th and 20th centuries, incorporation of Neoglacial till and outwash has been a key factor in allowing water flows to evolve into debris flows in proglacial areas (Haeberli, 1983; Evans and Clague, 1993; Zimmerman and Mani, 1993; O'Connor and Costa, 1993; Walder and Driedger, 1994). On steep Cascade Range volcanoes, the abundance of unconsolidated volcanoclastic deposits, locally reworked by glacial processes and then exposed by glacier retreat, further fosters debris-flow activity (Osterkamp and others, 1986). Incorporation of Neoglacial till and outwash appears to have been an important factor for formation of all the alpine debris flows studied in the Three Sisters and Mount Jefferson Wilderness Areas.

## Breaching of Moraine Dams

Moraine dams are especially susceptible to rapid failure because (1) they are composed of loose silt, sand, and gravel, and contain less than 3 percent clay (fig. 58), (2) deep lakes can form behind moraine dams and exert significant hydrostatic forces, (3) width-to-height ratios of moraine dams are usually small, and (4) outlet slopes are generally steep, on the order of  $10^\circ$  to  $30^\circ$  (Costa and Schuster, 1988; Clague and Evans, 1994). Some moraines contain ice cores and melting of these cores possibly contributes to failure (Costa and Schuster, 1988; Reynolds, 1992). Moraine dams, similar to other types of natural and constructed dams, generally fail either by overtopping, piping, or gravitational collapse (Costa and Schuster, 1988; Reynolds, 1992). There are few direct observations of moraine dam failures; consequently, most conclusions regarding initiation mechanisms are inferences from field observations after the event.

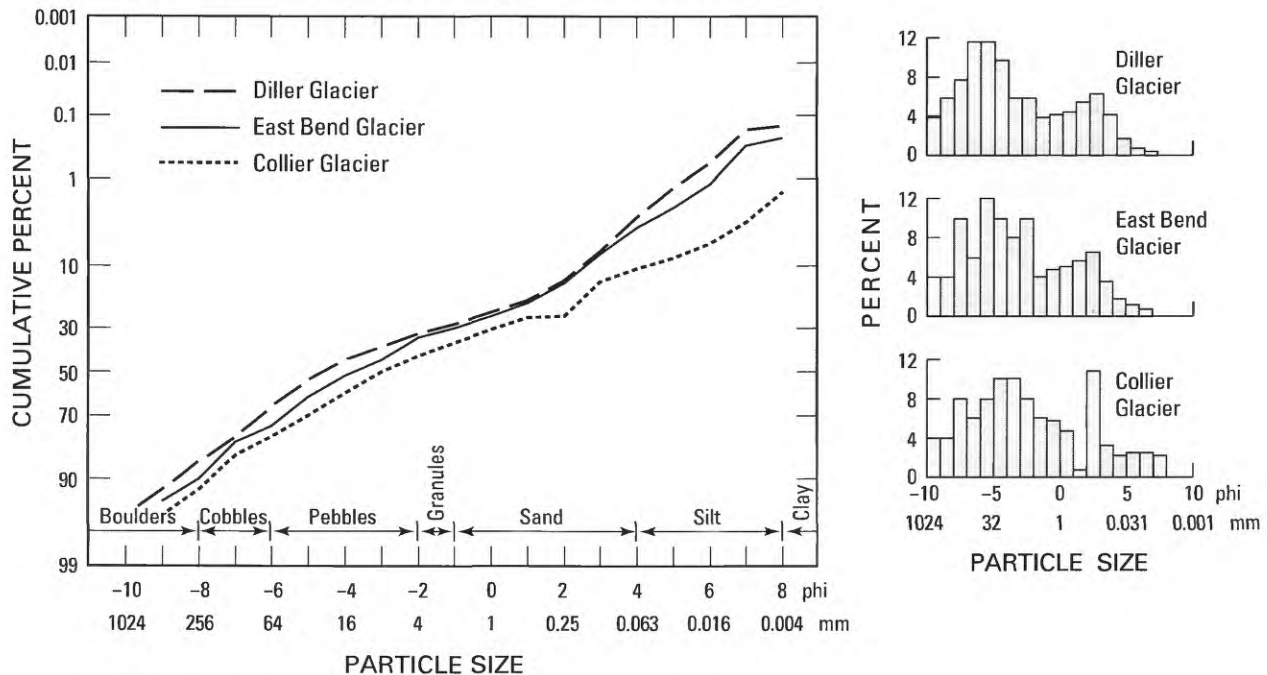


**Figure 58.** Cumulative curves of particle sizes for three Neoglacial moraines in the Three Sisters Wilderness Area. Following the procedure described by Scott (1988, p. 22), particle-size distributions were determined by field measurements of clasts greater than 2 mm combined with laboratory measurements of the sand, silt, and clay fractions.

Overtopping is by far the most common mechanism cited for breaching of moraine dams (Evans, 1987; Costa and Schuster, 1988). Ice falls, rockfalls, and avalanches into the lake frequently are cited as causing large displacement waves that exit the outlet, temporarily increasing the discharge, and eroding the outlet channel (Lliboutry and others, 1977; Blown and Church, 1985; Evans, 1987; Ding and Liu, 1992; Reynolds, 1992). Piping was a factor in only a few failures (Yesenov and Degovets, 1979). In the Cordillera Blanca of Peru, a 1970 breach was triggered by piping following an earthquake (Lliboutry and others, 1977).

Several models exist to help evaluate wave heights as the consequence of avalanches of material into lakes (Noda, 1970; Slingerland and Voight, 1979). Unfortunately, these models require estimates of avalanche volume and velocity in addition to lake geometry. Estimates of avalanche dimensions and velocities prior to a failure are difficult to obtain, and it is uncertain that wave height alone is responsible for initiating failure of Neoglacial moraine dams. Temporary increases in the outlet discharge by other means, such as rapid snowmelt, rainfall (Lliboutry and others, 1977), or sudden releases of subglacial water, also possibly lead to erosion of the outlet and initiation of failure (Blown and Church, 1985; Evans, 1987; Costa and Schuster, 1988; Reynolds, 1992).

It is uncertain what triggered the moraine-dam failures in the central Oregon Cascade Range; no single mechanism is likely to have produced all the failures. The August 12, 1933, and August 21, 1934, debris flows from lakes at the termini of Eugene Glacier on South Sister and Whitewater Glacier on Mount Jefferson resulted from release of short-lived lakes during a several-year period of exceptionally warm temperatures (fig. 13) and rapid glacier retreat (fig. 8). Such dynamic conditions, involving rapidly melting glaciers and associated calving and avalanching, probably lead to increased runoff and/or large wave formation that can cause moraine-dam failures. This sequence may also be true for the July 1942 flow down White Branch Creek from the lake at the terminus of Collier Glacier, Middle Sister. The lake had grown rapidly from its inception in 1934 and reached its maximum size in 1940 (fig. 12).

In contrast, lakes at the termini of Jack, Diller, and East Bend Glaciers drained after several decades of stable termini and lake levels (fig. 16), indicating that these failures may have been unrelated to general changes in lake or glacier conditions. Glaciers terminated at the margins of all three lakes at the time of failure, suggesting the possibility that large blocks of ice calved into the lake, forming waves that triggered erosion of the outlet. Nolf (1966) speculated that glacier calving was the cause of the October 7, 1966, debris flow from the lake at the terminus of East Bend Glacier. Another possible triggering mechanism for the drainage of lakes is rockfall or icefall. Like many Neoglacial-age moraine-dammed lakes, the lakes at the termini of East Bend and Jack Glaciers lie at the base of steep cirque headwalls composed of weathered and hydrothermally altered volcanic breccia and thin lava flows. Mass movements of ice or rock from these slopes could have caused waves that led to partial releases of these lakes.

Dam failures may also be caused by rainfall. Failure of the moraine impounding the lake at the terminus of Diller Glacier on September 7, 1970, was probably triggered by precipitation. According to records at Santiam Pass, 30 km north of Middle Sister, 33 mm of rain fell on September 7, culminating a 5-day total of 80 mm. Similar precipitation over the 1.2 km<sup>2</sup> contributing area for the lake at the terminus of Diller Glacier would equal about 30 percent of the maximum lake volume. Consequently, flow through the lake outlet was undoubtedly greater than normal and perhaps triggered erosion of the steep outlet channel.

Only one observation of a moraine-dam failure and resulting dam-break flood has been reported. At Laguna Jancarurish in the Cordillera Blanca of Peru, engineers were attempting to lower the lake level in 1949 when part of an ice apron flanking the lake calved, creating large waves that overflowed and destroyed the temporary gate at the outlet. According to Lliboutry and others (1977, p. 250), "there was fast regressive erosion of the moraine,... a waterfall formed, which widened while moving towards the lake. Finally the moraine around the gate failed and the big *alluvion* ... took place." Similarly, for all the lake releases in the Three Sisters and Mount Jefferson Wilderness areas, initial erosion during a moraine-dam failure

probably began on the steep outer moraine slopes. Retrograde erosion is probably an important mechanism for breach enlargement. A knickpoint or series of knickpoints proceeds up the channel, ultimately deepening the outlet at the lake, which in turn further increases flow and accelerates erosion. Breaches enlarge, usually forming a parabolic or triangular cross section (fig. 59), until

either the lake drains completely (for example the 1970 Diller Glacier/Squaw Creek release) or erosion of the outlet ceases and the lake stabilizes at a lower level. A photograph (Nolf, 1966), taken days after the partial emptying of the lake at the terminus of East Bend Glacier, Broken Top, helps illustrate the process. The photograph shows that within a few meters of the lake outlet, a 3- to 5-m-

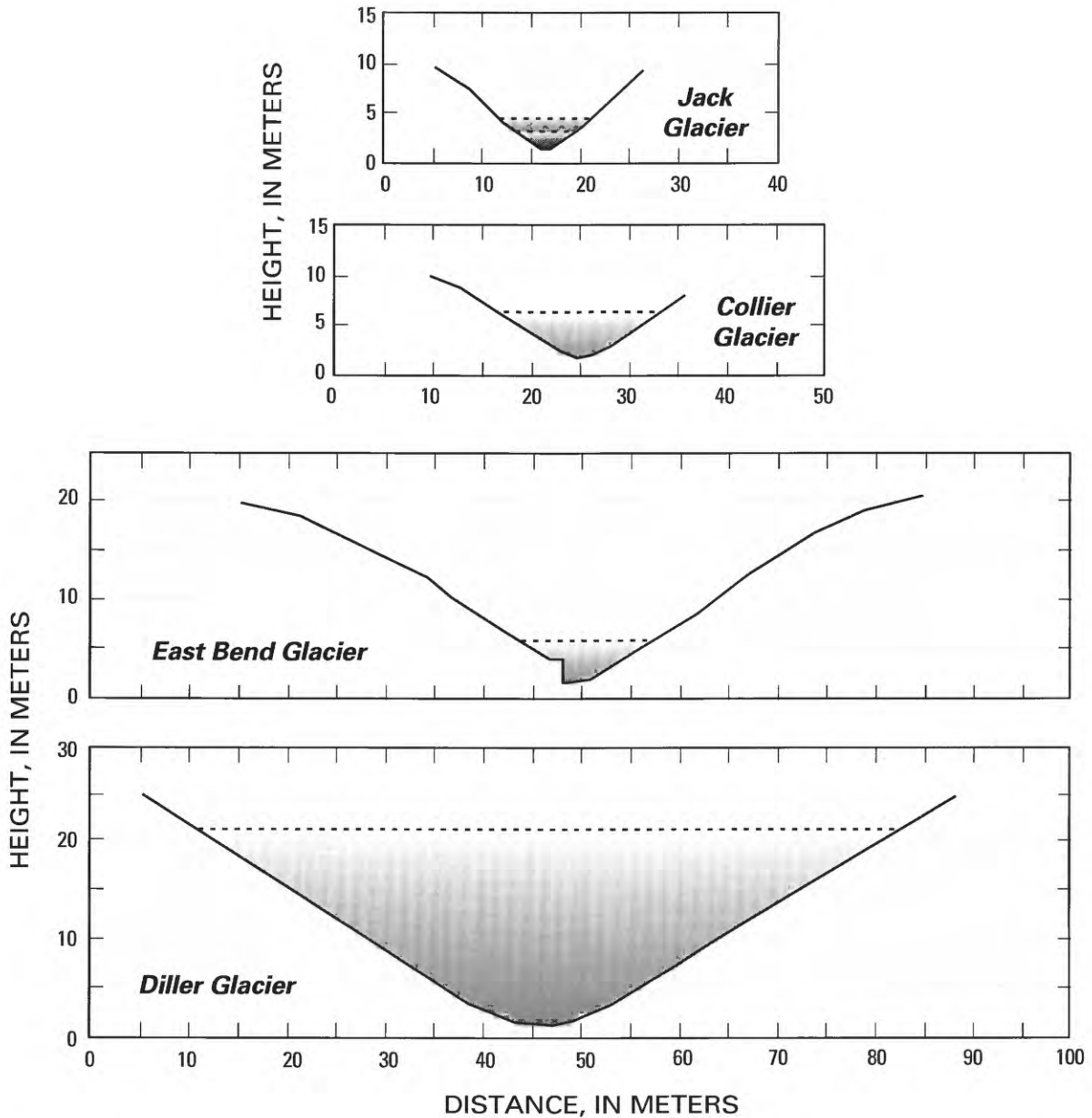


**Figure 59.** Breach cross sections and previous lake levels (indicated by dashed lines) at four sites of moraine-dammed lake releases in the Three Sisters and Mount Jefferson Wilderness Areas. Most breaches have parabolic or triangular shapes, generally with side slopes of 25° to 45°. No vertical exaggeration; datums are arbitrary.

high waterfall tumbles down the outlet channel, apparently the last in a series of knickpoints that migrated up-channel during the lake release. This knickpoint halted just meters from the lake outlet, probably preventing complete emptying of the lake. Subsequently, slumping and hillslope debris from the banks of the outlet filled the channel downstream from the waterfall, increasing the present stability of the outlet. Similar knickpoints were observed in the channel of White Branch Creek after the 1942 breach (Ruth Hobson Keen, oral commun., 1995).

Similar to the 1966 Broken Top release from the lake at East Bend Glacier, other moraine-dam failures in the central Oregon Cascade Range did not result in complete lake drainage, for example the 1942 flow down White Branch Creek, and two releases from the lake at the terminus of Jack Glacier. The thalwegs of the present lake outlets at Broken Top and Three Fingered Jack are paved with cobbles and boulders, many with diameters about 1 m, indicating that armoring of the breach thalweg inhibited erosion of the outlet during previous releases.

As noted in the eyewitness account of the moraine-dam failure in Peru, moraine dams can fail very rapidly. Hydraulic reconstruction of the 1970 Squaw Creek (Diller Glacier) debris flow led Laenen and others (1992) to conclude that the 22.4-m-deep breach was fully formed in about 5 minutes. A similar analysis for a moraine-dam failure in Great Britain resulted in an estimate of 24 minutes for erosion of a 10-m-deep breach (Carling and Glaister, 1987). As described above, the 1942 lake release down White Branch must have entrained a large volume of debris in only a few minutes, implying that the 5.4 m breach eroded quite rapidly. These rates are broadly similar and perhaps greater than the vertical erosion rates of 0.03 to 1.34 m/min documented during earthen-dam failures (Froehlich, 1987; Walder and O'Connor, 1997).

The peak discharge and duration of flow exiting a breaching dam depends on the erosion rate, size and shape of the breach, and the hypsometry of the lake behind the dam. In general, erosion of natural dams, once started, proceeds rapidly and hydrographs of most types of natural dam failures are quite peaked (Costa, 1988). This

was true for the 1970 flow down Squaw Creek, where peak discharge was attained 10 minutes after flow onset (fig. 44). Because critical flow over a weir, analogous to flow exiting a lake through a steep outlet, is a power function of the elevation difference between the lake surface and outlet thalweg (discharge is proportional to the depth at the outlet to the 1.5 power), minor differences in the interplay between the vertical erosion rate at the outlet and lake hypsometry can substantially affect the peak discharge and shape of the outflow hydrograph (Walder and O'Connor, 1997).

## Downstream Flow Characteristics

The presence of channels flanked by bouldery levees and fans of poorly sorted mud and debris is compelling evidence that the lake releases evolved from clear water streamflow at the outlets into rubbly debris flows within a few hundred meters. Flow bulking (Scott, 1988, p. A6) was apparently due to incorporation of till and outwash from the outer moraine slopes and enlargement of outlet channels. Scallop-shaped reentrants into moraines that flank the present outlet channels of lakes that have emptied (fig. 31) are evidence that mass movement of till into the flow was an important mechanism of introducing debris into the flow. David Rasmussen (U.S. Forest Service, oral commun., 1994) visited the site of the 1966 release of the lake at the terminus of East Bend Glacier, Broken Top, and recalls that the moraine slopes above the eroded channel were extremely unstable, and continual mass wasting of debris into the channel near the outlet prevented him from proceeding up the channel. Although difficult to prove, mass movements from the channel margins and channel knickpoint retreat likely were the primary mechanisms of introducing debris into all these flows.

For the larger flows in the Three Sisters Wilderness Area, addition of sediment resulted in debris flows with substantially larger volumes and peak discharges than could be provided solely by the water in the impounded lakes. The 1942 release of the lake at the terminus of Collier Glacier incorporated 120,000 m<sup>3</sup> of till and outwash within the first kilometer from the outlet, increasing the total flow volume by 25 percent and increasing the

peak discharge from 140 m<sup>3</sup>/s to about 500 m<sup>3</sup>/s (figs. 32 and 35). Similar magnitudes of flow bulking probably occurred during partial drainage of the lake at East Bend Glacier, Broken Top, where outflow increased from less than 80 m<sup>3</sup>/s at the outlet to at least 190 m<sup>3</sup>/s 0.5 km downstream, and at Diller Glacier, Middle Sister, where 130,000 m<sup>3</sup> of the impounding moraine was eroded during drainage of the 320,000 m<sup>3</sup> lake.

Direct measurements and observations of debris flows started by controlled releases from a moraine-dammed lake at the Chemolgan Debris-Flow Testing Ground, Kazakhstan, provide support to the indirect observations in the Three Sisters Wilderness Area (Khegai and others, 1992). Release of 400,000 m<sup>3</sup> of clear water at a peak discharge of 22 m<sup>3</sup>/s resulted in a downstream debris flow of substantially larger volume and a peak discharge of 150 to 200 m<sup>3</sup>/s. The measured debris flow hydrograph (fig. 60) portrays an almost instantaneous rise to a peak discharge of 150 to 200 m<sup>3</sup>/s, followed by a series of about seven surges of gradually decreasing peak discharge. The flow front travelled downstream at 4 to 8 m/s. Like flows in the Three Sisters and Mount Jefferson Wilderness Areas, the source of debris is

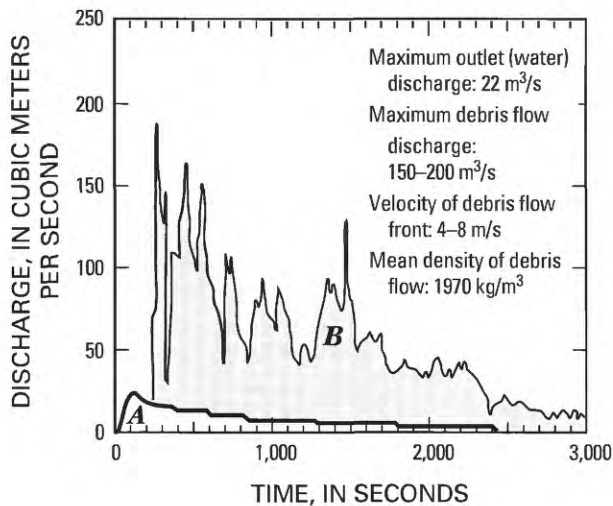


**Figure 60.** Hydrographs and debris flow characteristics at the Chemolgan Debris Flow Testing Ground, Kazakhstan, during a September 12, 1991, experiment. “A” is the hydrograph at the outlet. “B” is the debris flow hydrograph measured approximately 1 km downstream. Modified from Khegai and others (1992).

Quaternary glacial deposits introduced into the flow from the margins of the eroding outlet channel.

Similar conclusions were reached from analysis of debris flows that have been triggered by water flows in other environments. The commonality is an abundance of loose debris on steep slopes. Examples are primarily from mountainous environments and include flows started by natural dam failures (Yesenov and Degovets, 1979; Haeberli, 1983; Blown and Church, 1985; Scott, 1988), high rainfall or cascading streamflow on weak, sheared rock (Fryxell and Horberg, 1943; Pierson, 1980; Webb, 1993), glacial outburst floods (Jackson and others, 1989; Haeberli, 1983; Walder and Driedger, 1994), and debris flows started by meltwater from volcanic eruptions on snow-covered volcanoes (Waitt and others, 1983; Pierson and Scott, 1985).

The largest debris flows in the Three Sisters and Mount Jefferson Wilderness Areas continued several kilometers downstream from outlet areas, eroded channel margins along steep and narrow reaches, and deposited sediment in wider and lower-gradient reaches. Erosion and flow bulking, judging from scoured channel banks and thalwegs, was dominantly in reaches where channel thalweg gradient exceeded 8° (fig. 61). Reaches of net erosion are generally near the release points where gradient is high, the channels are bounded by unconsolidated till and outwash, and hillslopes are sparsely forested. Flows, such as the 1966 Soda Creek debris flow, were locally enlarged by mass movements entering at sites of channel undercutting.

Deposition occurred primarily in reaches of gradients less than 8°, but also occurred locally in channel expansions and on fans with slopes as great as 18° (fig. 61). In lower reaches, where woody debris was abundant in the flow and in overbank areas, extensive overbank deposition was aided by log and boulder jams formed behind standing trees. Similar gradient values for erosional and depositional slopes have been measured for rubbly debris flows in New Zealand (Pierson, 1980), Japan (Ikeya, 1981), Canada (VanDine, 1985; Jackson and others, 1989; Clague and Evans, 1994), the Rocky Mountains in Colorado (Curry, 1966), and in the Cascade and

Coast Ranges of Washington and Oregon (Benda, 1990; Walder and Driedger, 1994).

On sustained gradients of 4° or less, cobbles and boulders were rapidly deposited and all flows ceased behaving like debris flows. Nevertheless, flow records, newspaper reports, and deposit sedimentology of the 1933 Separation Creek and 1970 Squaw Creek flows indicate that substantial sediment-laden streamflow continued downstream from the debris flows, probably as hyperconcentrated streamflow (Pierson and Scott, 1985). As described above, the gaged volume of the Squaw Creek flood wave downstream of the transformation from debris flow to streamflow was about a third of the water released by the lake, indicating that a substantial volume of water was temporarily retained with the deposits left by the debris flow or percolated into fan and channel bottoms.

Deposits of the Squaw Creek and Soda Creek debris flows have clay contents of less than 1 percent (figs. 45 and 57) indicating that these flows were noncohesive; hence, they were susceptible to rapid flow transformations (Scott, 1988, p. 71). Accordingly, both of these flows evolved from debris flow to sediment- and debris-laden streamflow at pronounced gradient decreases about 7 to 9 km from the lake outlets. Qualitative observations of the deposits from the debris flows on the north flank of Mount Jefferson, on Three Fingered Jack, and the 1933 Separation Creek flow indicate that these flows were noncohesive and transformed rapidly to sediment-laden streamflow at locations of substantial gradient decrease. In contrast, the 1942 White Branch flow deposits have clay contents as high as 6 percent (fig. 37), indicating a more cohesive flow.

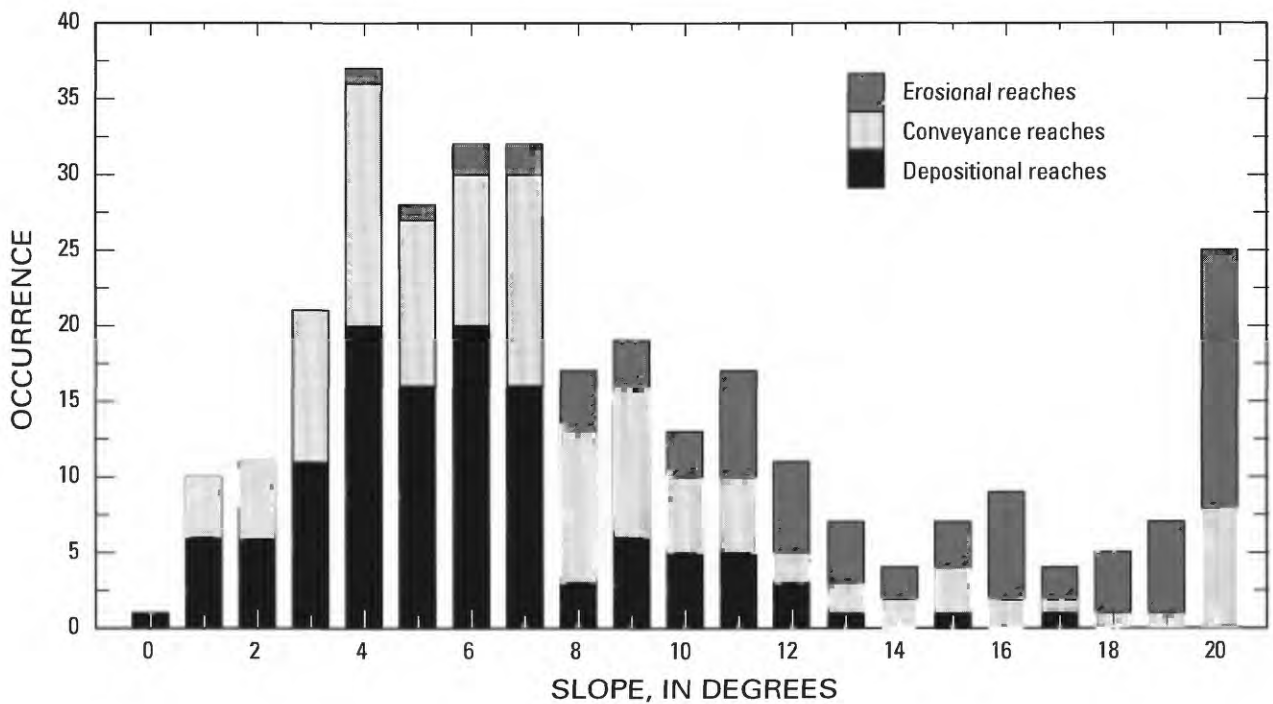


**Figure 61.** Histogram of channel slopes associated with reaches of deposition, erosion, and conveyance (no obvious evidence of erosion or deposition) for the debris flows on White Branch (Collier Glacier), Squaw Creek (Diller Glacier), Separation Creek (Eugene Glacier), and Soda Creek (East Bend Glacier). Channel slopes were measured for the entire length of each debris flow and were compiled on the basis of channel subdivisions defined by 40-foot contour intervals on topographic maps. Reaches of erosion and deposition were mapped in the field. Slopes were determined from 1:24,000-scale topographic maps and field measurements.

Downstream patterns in discharge, sedimentology, and clast lithology indicate that there were substantial interactions between the debris flows and the valley floors and channel substrates, and that these interactions were largely controlled by behavior of the coarse clasts within the debris flows. The noncohesive debris flows transformed into sediment-laden streamflow only after deposition of the coarse fraction of the sediment load. Deposition of large clasts in channel reaches of less than 8° (fig. 61) indicates that continued downstream flow in the form of a debris flow in these channels requires either a channel slope consistently greater than about 8° in order to maintain coarse clast transport or local introduction of large clasts along the flow route. The varied abundance and lithology of coarse clasts along the flow routes indicate that introduction of large clasts was indeed an important process. The coarse phase of the flow also influenced deposition. Boulderly dams fostered deposition, especially in forested overbank areas, and completely plugged smaller channels with lobate deposits. In contrast, the fine-grained component of the debris flows apparently remained constant for the lengths of the flows.

These conclusions regarding flow behavior are consistent with flow processes observed during alpine debris flows. Pierson (1980) witnessed several rubbly debris flows at Mount Thomas, New Zealand, noting that large boulders were suspended in a slurry with a consistency of "wet concrete." According to Pierson (1980), cobbles and boulders were concentrated at the flow fronts during flow pulses, and were forced laterally by internal flow sorting processes to form levees, thereby narrowing the channel. Channel downcutting was accomplished by headward migration of knickpoints, and channel widening resulted from undercutting and slumping of the channel banks into the flow.

## **EVALUATION OF HAZARDS FROM MORaine-DAMMED LAKE BREAKOUTS**

At many locations, floods and debris flows from moraine-dammed lakes pose a serious hazard (Lliboutry and others, 1977; Evans, 1987; Laenen

and others, 1992; Ding and Liu, 1992). Assessing this hazard is difficult because formation of moraine-dammed lakes can depend on interacting and temporally changing factors such as century- to daily-scale changes in climate and weather, glacier behavior, and local topographic setting. Rapid release of lakes, once formed, can be caused by changes in the above factors or triggered by quasi-random events such as weather, rock and ice avalanches, and earthquakes. The downstream flow from a moraine-dam failure is influenced by the volume and rate of water released, downstream channel morphology, and interaction of the flow with the channel and adjacent banks. These varied factors conspire against accurate and precise statements of the likelihood and magnitude of downstream hazards from moraine-dammed lakes.

Nevertheless, qualitative assessments of hazards from moraine-dammed lake releases are possible. Worldwide, there have been several preliminary assessments of hazards from moraine-dammed lakes, mostly in regions such as the Himalayas and the Andes, where there has been interest in developing hydroelectric facilities in glacierized basins and where past floods from moraine-dammed lakes have been lethal. As a first step, most of these assessments are an inventory of moraine-dammed lakes (Lliboutry and others, 1977; Ives, 1986, p. 34-34; Liu and Sharma, 1988; Ding and Liu, 1992). For the Cascade Range of Oregon and Washington, we have compiled a similar inventory, primarily on the basis of aerial-photograph reconnaissance of lakes that are at least partly dammed by Neoglacial moraines (table 1).

## **Assessing Potential Failure of Moraine Dams**

### **Topographic Setting**

An evaluation of topographic setting of a moraine-dammed lake can provide a preliminary assessment of the potential for rapid release (Lliboutry and others, 1977; Ding and Liu, 1992; Clague and Evans, 1994). Dams with lakes that have surficial outlets on steep moraine slopes are more likely than other types to fail because of the high potential for overtopping and retrograde erosion of the outer moraine slope. The amount of

freeboard and the slope of the moraine impoundment also are critical and easily assessed factors. Many overtopping failures are triggered by waves generated by mass movements into the lake (Blown and Church, 1985; Reynolds, 1992). The types of triggering mass movements likely include rockfall, ice avalanches, and ice calving. Consequently, moraine-dammed lakes that are located at the base of steep cirques, or have steep glaciers above or calving into the lake, are susceptible to rapid release (fig. 62).

In the Three Sisters and Mount Jefferson Wilderness Areas, seven lakes presently have surface areas greater than 5,000 m<sup>2</sup> (table 1). The lakes at the termini of Jack, Prouty (Carver Lake), and East Bend Glaciers have steep surface outlets and sit below steep, unstable edifices (figs. 15 and 63). The Chambers Lakes (pl. 1; fig. 15) and the lake at the terminus of Thayer Glacier (fig. 15) have low-gradient or subsurface outlets with up to 25 m of freeboard (fig. 63). Additionally, although the present drainage of Collier Glacier is through the “melthole,” a closed basin still could contain 160,000 m<sup>3</sup> of water if subsurface drainage ceased and the lake filled to the outlet. Considering the present conditions, the moraines impounding Carver Lake and the lakes at the termini of East Bend and Jack Glaciers appear most susceptible to failure owing to steep outlet channels and high potential for rock or icefall into the lakes. If hydrologic/glaciologic conditions change, it is possible that Chambers Lake No. 1 and the basins at the termini of Thayer and Collier Glaciers could fill with water, increasing the potential for rapid release. This assessment considers only the potential for failure by overtopping. Any of these lakes, whether they have freeboard or not, could empty rapidly as a result of piping or mass wasting of the moraine dams.

Quantitatively assessing the likelihood and timing of potential moraine-dam failure is difficult. Accurate geotechnical assessment of moraine dams depends on knowledge of the internal moraine structure and sedimentology—details that are difficult to determine (Reynolds, 1992). Furthermore, triggering mechanisms, such as rockfall, icefall, and rainstorms, are unpredictable and occur in the background of climatologic, glaciologic, and hydrologic changes. Nevertheless,

all 50 northern hemisphere moraine-dam failures with known dates occurred during the July through October melt season, and 39 of 49 were during July and August (table 2). In the central Oregon Cascade Range, the frequency of moraine-dam failures is decreasing. Most moraine-dam failures occurred in the 1930's and 1940's, soon after the period of rapid glacier retreat and lake formation (fig. 64). The presence of lakes dammed by late Pleistocene moraines (for example Camp Lake and Moraine Lake in the Three Sisters Wilderness Area) indicates that lakes can remain stable for thousands of years, especially if they are in settings removed from failure-triggering processes such as rockfall or icefall.

### **Likelihood of Future Breaches in the Central Oregon Cascade Range**

If climatologic, glaciologic, and hydrologic conditions do not change substantially, the rate of moraine-dam failure in the Three Sisters and Mount Jefferson Wilderness Areas likely will continue to decrease. If, however, conditions change rapidly, the potential for failure could increase. More specifically, if glaciers retreat rapidly, ice avalanches or rockfall could become more common (Evans and Clague, 1993; O'Connor and Costa, 1993), increasing the frequency of processes that trigger lake releases. Given these conditions, the moraine dams impounding Carver Lake and the lakes at the termini of Jack and East Bend Glaciers appear to be highly susceptible to failure. If climate conditions change to foster glacier advance, and especially if glaciers reenter lakes, the potential for calving ice to trigger moraine failures will increase. Also, the increased hydrologic flux associated with larger glaciers could lead to (1) erosion of outlets and (2) increasing lake volumes and decreasing freeboard for lake basins not presently draining subaerially. In particular, increased lake volume would substantially increase the hazard posed by the lake at the terminus of Thayer Glacier because of its steep outlet (fig. 63). Considering longer-term possibilities, if glaciers advance to the extent that late-Neoglacial moraines are reoccupied, the present lake bodies will be displaced, and the stage would be set for a new round of moraine-dammed lake formation and failure upon glacier retreat.

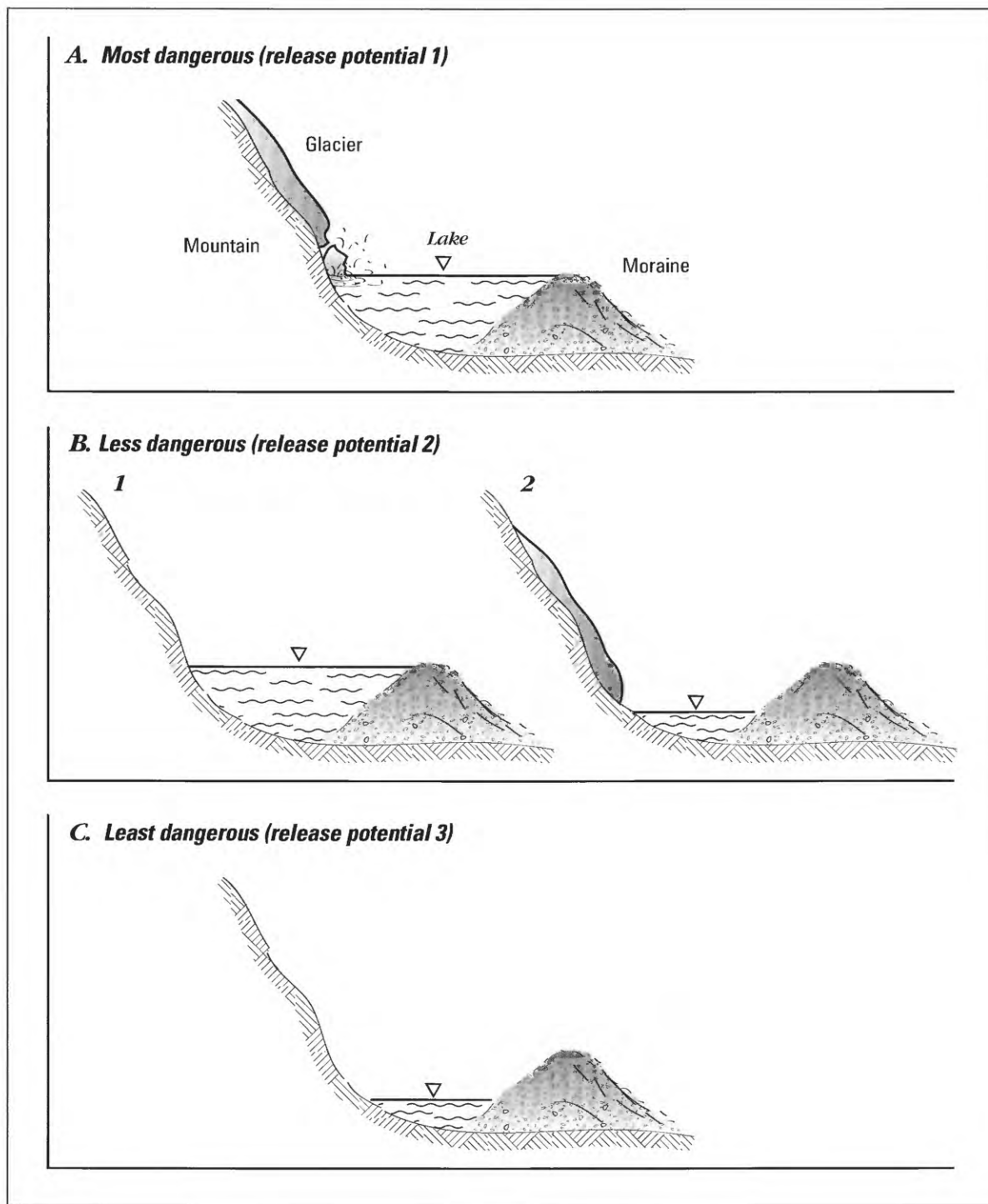


**Figure 62.** Schematic illustration of topographic-setting criteria for qualitative assessment of the potential of a moraine-dam breach. *A*, Most dangerous situation of a steep glacier calving into a brimful moraine-dammed lake (similar to the present setting at Carver Lake and the settings at East Bend Glacier and Diller Glacier before breaching). *B*, Less dangerous settings of (1) a presently unglacierized, but steep, cirque above a brimful moraine-dammed lake (similar to present situation at “Jack” Glacier), or (2) a glacierized cirque above a moraine-dammed lake that does not drain over the moraine crest (similar to present setting at the terminus of Thayer Glacier). *C*, Least dangerous situation of a presently unglacierized valley above a moraine-dammed lake that does not drain over the moraine crest (similar to present setting of Chambers Lake No. 1).

## Assessing Downstream Flow Hazards

Beyond questions of “if” and “when” a particular moraine dam might fail is the issue of determining the downstream hazards from a resulting flow. Assessing downstream hazards from dam failures has been a subject of substantial research and model development, especially for constructed dams (Land, 1980; Ponce and Tsivoglou, 1981; Hunt, 1984; Singh and Quiroga, 1987; Quiroga and Singh, 1987; Fread, 1988; Macchione and Sirangelo, 1990), but also for

natural dams (see Costa, 1988; Costa and Schuster, 1988; Clague and Evans, 1994, for summaries). Most quantitative hazard assessments of dam-break floods consist of two aspects: (1) determining of the outflow hydrograph at the breach and (2) routing floods downstream.

## The Outflow Hydrograph at the Breach

The rate of outflow from a failing dam ultimately depends on the rate and extent of breach growth, breach shape, and basin hypsometry (Walder and O'Connor, 1997). Breach growth and

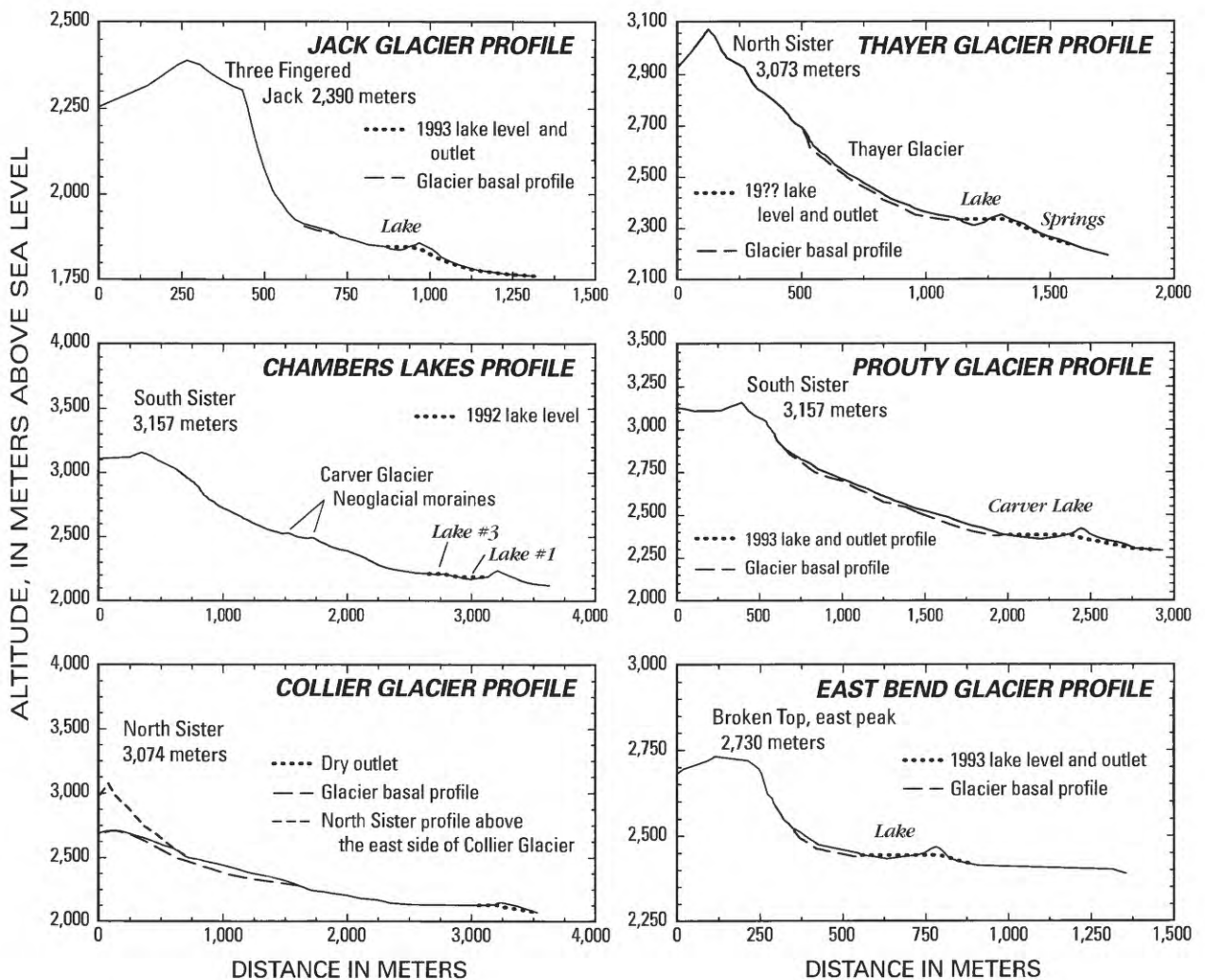


**Figure 63.** Present topographic profiles for the five largest moraine-dammed lakes in the Three Sisters and Mount Jefferson Wilderness Areas, and for Collier Glacier and adjacent basin, where there is potential for a moraine-dammed lake. Datum for horizontal scale is arbitrary.

shape are difficult to predict accurately, but are usually the most important factors in determining the outflow hydrograph for moraine-dam failures. Because most moraine-dammed lakes are on steep slopes, their volumes are relatively small compared to depths; consequently, lake levels lower rapidly as outflow increases. Discharge from the lake, assuming critical flow at the breach and ignoring negative waves propagating from the outlet, depends on the elevation difference between the lowering lake surface and the breach thalweg at the outlet. Depending on breach shape, discharge increases at a rate that exceeds the 1.5 power of the elevation difference between the lake surface and breach bottom (Walder and O'Connor, 1997). Consequently, for outlets that erode slowly, the elevation difference between lake surface and breach thalweg remains small and peak discharge is small. In contrast, if the outlet erodes quickly, a large elevation difference will form between the water surface and breach thalweg, and a much larger peak discharge will result. For large lakes, breaches are likely to form completely prior to significant drawdown. In this situation, the peak

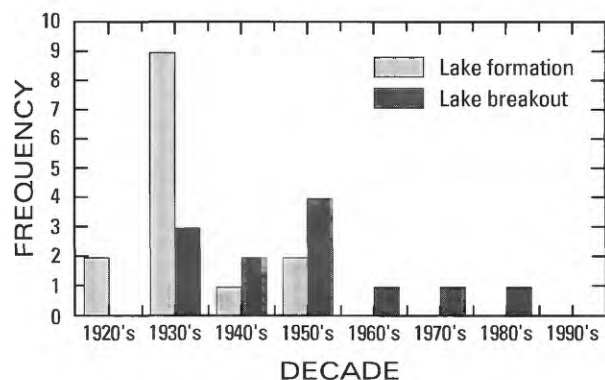


**Figure 64.** Decadal incidence of formation and breaching of Neoglacial moraine-dammed lakes in the Three Sisters and Mount Jefferson Wilderness Areas. For lake formation times and for breaches of that could not be constrained to particular decades (formation of Chambers Lake No. 2 and the lakes at the termini of Thayer and Waldo Glaciers, and the first releases from the lakes at the termini of Waldo and Jack Glaciers), occurrence is plotted by assuming formation or breach to have been within the decade deemed most likely on basis of available information. Plot based on data portrayed in figure 16 and additional information for Waldo Glacier on Mount Jefferson (described in text).

discharge is more a function of breach shape than rate of growth. Using a simplified formulation of this process developed by Walder and O'Connor (1997), we have developed hypothetical hydrographs illustrating the sensitivity of breach hydrographs to breach geometry and breach erosion rate for several lake basins in the Three Sisters and Mount Jefferson Wilderness Areas (figs. 65 and 66).

More-complex physically based mathematical models of breach erosion have been developed recently by Ponce and Tsivoglou (1981) and Fread (1987). The models are similar in that they predict breach size, shape, and rate of growth by coupling lake inflow, outflow, and sediment transport associated with a growing outlet channel. The models use variations of the Meyer-Peter and Muller (1948) sediment-transport relation to calculate the sediment eroded by the breach channel and resulting rate of growth. The BREACH model (Fread, 1987) further considers mass wasting of the outlet sides as a mechanism of breach enlargement. It is not clear, however, if bedload-transport relations of the model simulate conditions in a growing breach more accurately than simple parameterization of an overall erosion rate on the basis of empirical data (Walder and O'Connor, 1997). The Meyer-Peter and Muller bedload-transport relation is based on measurements of sand and gravel (the largest clast size analyzed was 28.6 mm) transport in a flume under conditions of steady or gradually varied flow. Conditions at an eroding outlet, however, are much more complex. Flow is nonuniform and rapidly varying, slopes are steeper, and ranges of particle sizes are larger. Field observations of the overtopping of landslide dams (Costa and Schuster, 1988) suggest that the assumption of the physical process of lowering the outlet thalweg from grain-by-grain entrainment in a vertical fashion may be incorrect. Retrogressive erosion of knickpoints by headcut retreat from the toe of the dam toward the dam crest appears to be an important process, and one that is likely to be more difficult to reliably model.

A further complicating factor for prediction of potential downstream flow conditions and hazard analysis is that breach growth commonly ceases prior to complete evacuation of the impounded

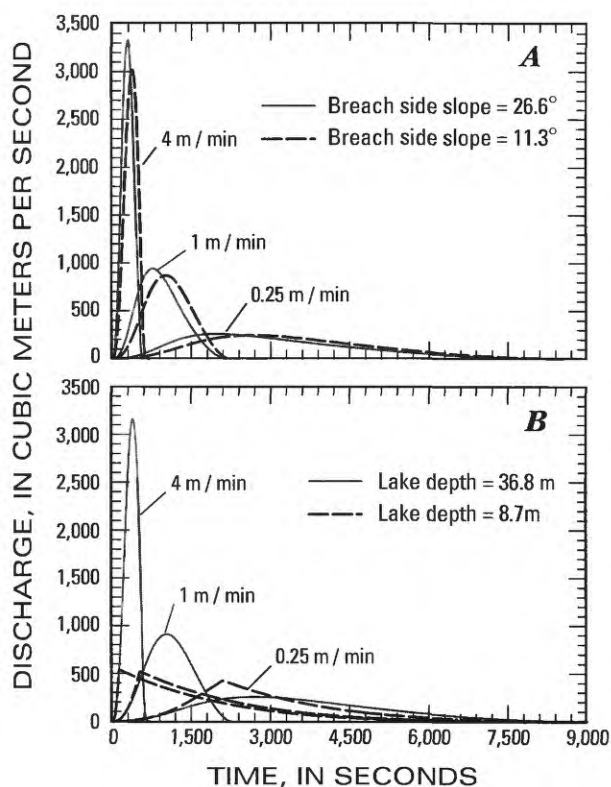


**Figure 65.** Effects of breach shape, erosion rate, and lake hypsometry on calculated hydrographs. Hydrographs are calculated on the basis of formulation in Walder and O'Connor (1997). In all cases, lake volume is assumed to be linearly related to the third power of lake depth, and the entire lake volume is released during the breach. **A**, Effects of breach shape and erosion rate for a lake with a volume and geometry similar to Carver Lake (volume 933,000 m<sup>3</sup>; maximum depth 36 m). Solid lines represent hydrographs for a triangular-shaped breach cross section with side slopes of 26.6° and vertical erosion rates of 4.0, 1.0, and 0.25 m/min. Dashed lines are hydrographs for the same lake volume and erosion rates, but with breach side slopes of 11.3°. **B**, Effects of lake hypsometry and erosion rate for a 1,000,000 m<sup>3</sup> lake with a triangular-shaped breach cross section with side slopes of 26.6° and vertical erosion rates of 4.0, 1.0, and 0.25 m/min. Solid lines are hydrographs for a lake with a maximum depth of 36.8 m (similar to Carver Lake); dashed lines are hydrographs for a lake with a maximum depth of 8.7 m (similar to the lake that breached the moraine dam at the terminus of Collier Glacier).

lake. Breach erosion is commonly arrested by processes that are largely unpredictable in numerical models. Most moraine-dam failures in the Three Sisters and Mount Jefferson Wilderness Areas resulted in only partial emptying of the impounded lakes. For most of these partial releases, large boulders contained in the moraine accumulated in the breach thalwegs, inhibiting downcutting and stabilizing the outlet channels. Likewise, icebergs could accumulate at the outlet, reducing outflow and ending downcutting.

A simpler approach to study downstream hazards from moraine-dammed lakes is to postulate a breach shape, rate of erosion, and ultimate depth on the basis of intuition and data from previous moraine-dam failures. This approach was used by Laenen and others (1987) to evaluate the hazard from Carver Lake, for which it was suggested that a “worst case event is the most appropriate design analysis for planning possible mitigating measures.” Possible outflow hydrographs for lakes in the Three Sisters and Mount Jefferson Wilderness Areas, based on a similar procedure for various failure scenarios, are shown in figure 66 and are summarized in table 3.

### Downstream Flow Behavior

Developed areas near the central Oregon Cascade Range that may be subject to hazards from moraine-dammed lakes are generally many kilometers downstream from the moraine dams. Consequently, evaluating hazards depends on how flow evolves as it moves downstream. This aspect of hazards analysis is also difficult. In addition to the numerical complexity of routing highly unsteady flows down steep channels, lake releases generally evolve into debris flows, which have distinctly different rheologic properties than those of streamflow (Laenen and others, 1987).

All the dam-failure flows in the Three Sisters and Mount Jefferson Wilderness Areas gained and lost volume as they moved downstream. For the debris flows studied, reaches of increasing and decreasing peak discharge largely coincided with channel reaches of erosion and deposition, indicating that exchange of mass with the channel and adjacent banks exerts large control on peak discharge and volume as the flow moves

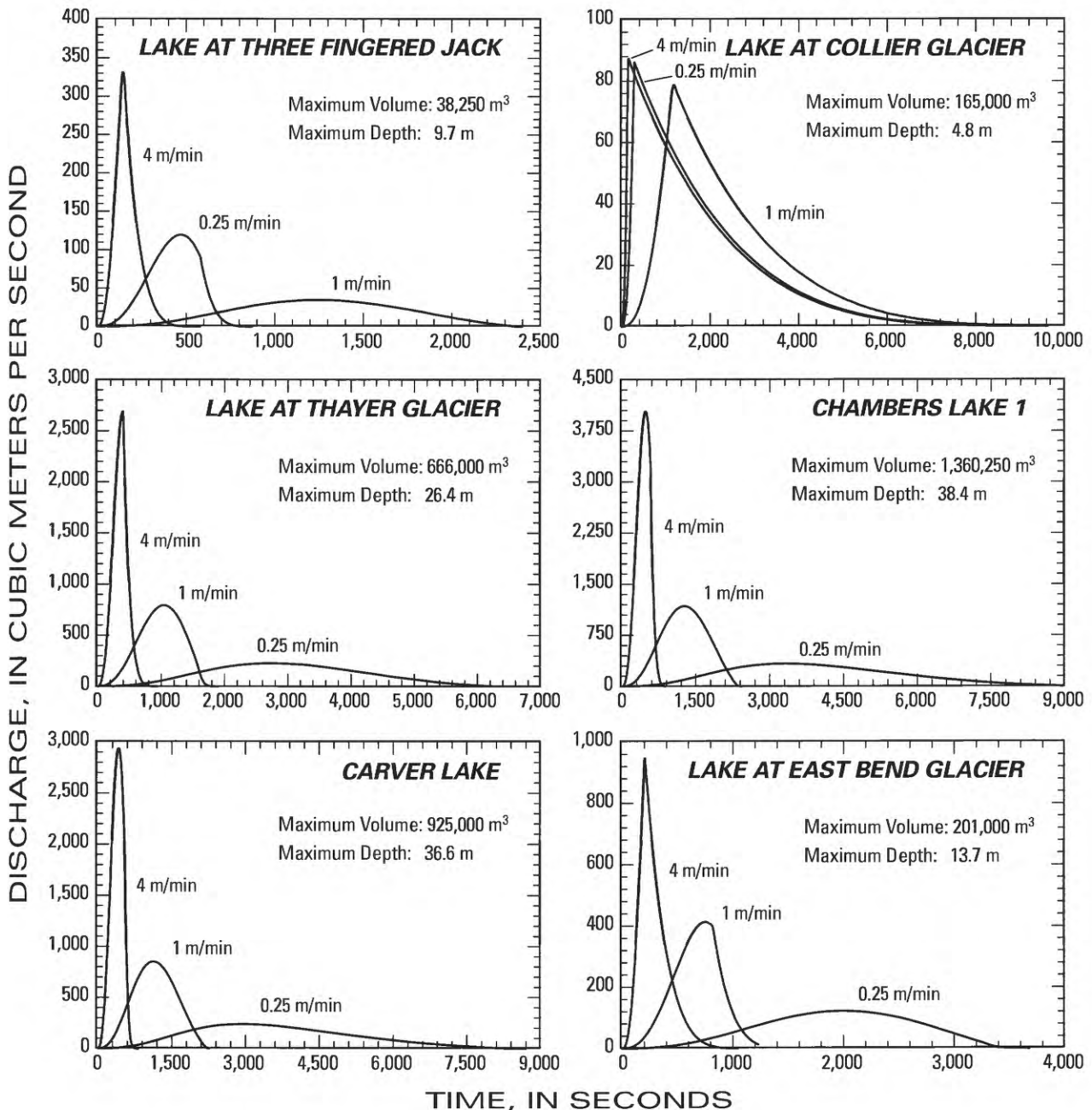


**Figure 66.** Calculated hypothetical hydrographs for six existing and potential moraine-dammed lakes in the Three Sisters and Mount Jefferson Wilderness Areas. Basis and numerical methods of calculating hydrographs are described in Walder and O'Connor (1997). For each lake, the calculated hydrographs are based on the following: (1) complete emptying of the lake, (2) triangular-shaped breach cross sections with side slopes of 26.6°, and (3) uniform erosion rates of 4.0, 1.0, and 0.25 m/min. For Chambers Lake No. 1 and lakes dammed or potentially dammed by moraines at Thayer and Collier Glaciers, the hydrographs are based on assuming that the lake level rises to the low point of the moraine crest before the moraine breaches. For other cases, where lakes now drain over the moraine crests, the calculated hydrographs are for the present lake geometry.

**Table 3.** Hypothetical peak discharges for moraine-dammed lakes in the Three Sisters and Mount Jefferson Wilderness Areas for various breach erosion rates.

[These hypothetical peak discharges are calculated on the basis of the following conditions: (1) Complete emptying of the lake; (2) Triangular-shaped breach cross section with constant side slopes of 26.6°; (3) the breach enlarges at a constant vertical erosion rate until the bottom of the breach reaches the altitude of the lake bottom, at which time vertical erosion ceases and the breach geometry remains constant. Numerical methods for calculating hydrographs are described in Walder and O'Connor (1997).  $m^3$ , cubic meters;  $m$ , meters;  $m/min$ , meters per minute;  $m^3/s$ , cubic meters per second]

Lake name or glacier terminus	Volume ( $m^3$ )	Depth (m)	Vertical erosion rate (m/min)				
			0.25	0.50	1.0	2.0	4.0
			Peak discharge ( $m^3/s$ )				
Carver Lake	925,000	36.6	240	455	850	1,590	2,940
Chambers Lake No.1	1,360,300 <sup>1</sup>	38.4 <sup>1</sup>	335	630	1,175	2,190	4,030
Chambers Lake No.2	76,300	12.8	50	95	175	320	565
Collier Glacier	165,080 <sup>1</sup>	4.8 <sup>1</sup>	80	85	85	90	90
East Bend Glacier	200,930	13.7	120	225	415	710	945
Jack Glacier	38,270	9.7	35	65	120	220	340
Thayer Glacier	666,100 <sup>1</sup>	26.4 <sup>1</sup>	35	65	120	220	340

<sup>1</sup> Volume and depth values (and calculated discharges) are for maximum potential lakes that would be achieved only if lake levels rose so that they were draining over the moraine crest. The present depths and volumes are much smaller.

downstream. Similar observations of peak discharges increasing several-fold have been made for flows resulting from rapid release of moraine-dammed lakes in other parts of the world (fig. 67). This aspect of debris-flow hazard assessment is important because most research in debris-flow modeling has been focused on rheology and the effect of flow rheology on flow behavior (Takahashi, 1978, 1981; Iverson and Denlinger, 1987; O'Brien and others, 1993). Postulated rheologic models of debris flow are usually incorporated into fixed-bed streamflow-routing models to determine downstream propagation of debris-flow hydrographs (Laenen and Hansen, 1986; Fread, 1988; O'Brien and others, 1993; Costa, 1997). For some of the rubbly debris flows from moraine-dammed-lake releases in the central Oregon Cascade Range, material from the bed and banks increased the flow volume by more than 25 percent and increased peak discharge by 100 percent or more (fig. 67). Likewise, deposition resulted in substantial reductions of flow volume and peak discharge over short distances. During the

1970 Squaw Creek flow, about 65 percent of the lake volume was temporarily retained within the flow deposits or elsewhere along the flow route and was not part of the measured flow pulse 24 km downstream. At least for these types of debris flows, depositional and erosional effects on the flow hydrograph potentially overwhelm routing effects that might result from choices of rheologic model and routing scheme.

Crude predictions of flow bulking and debulking are possible on the basis of gradient criteria as described above. The magnitude and locations of erosion and deposition, however, depend on flow size and rheology, channel and overbank substrate, channel geometry, and hillslope stability. All are factors difficult to parameterize accurately in a predictive model. An attempt to construct a model postdictively for the 1970 Squaw Creek flow (Laenen and others, 1987) using only channel friction to attenuate the peak, resulted in peak discharges that failed to match most of the field-based indirect discharge estimates within a factor of two. Combined with the

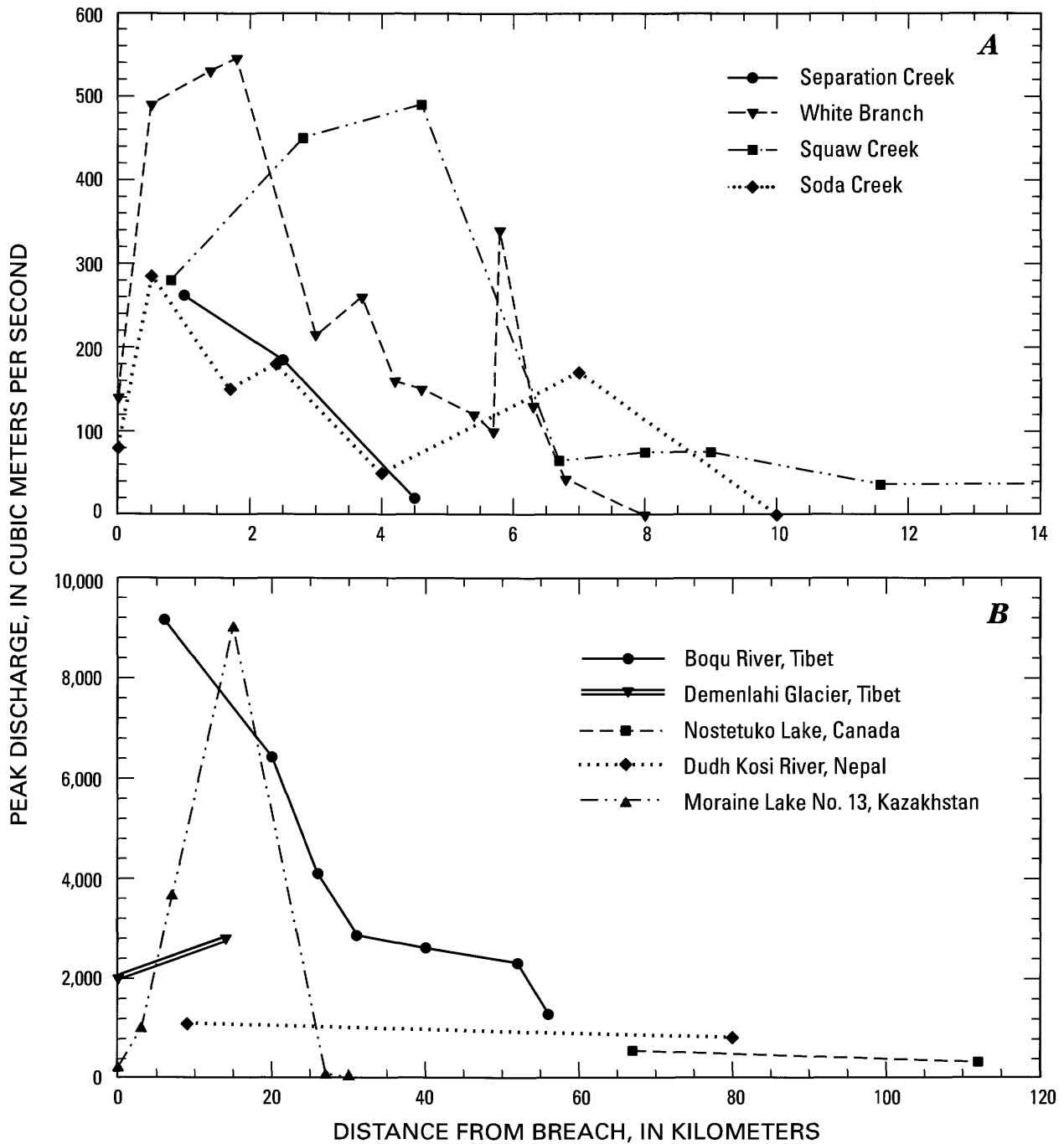


**Figure 67.** Downstream variation in peak discharges for (A) four debris flows from moraine-dammed lake releases in the Three Sisters Wilderness Area and (B) five debris flows and floods from moraine-dammed lake releases in other alpine areas. Sources for data are given in table 2.

considerable uncertainty in the hydrograph at the breach, precisely and accurately assessing the magnitude of downstream debris hazards from rapid release of moraine-dammed lakes is fraught with uncertainty. This uncertainty, however, does not diminish the importance of identifying drainages subject to flows from moraine-dam breakout floods, and increasing our understanding of the processes and conditions that contribute to flow hazards in the Three Sisters and Mount Jefferson Wilderness areas of Oregon.

## CONCLUSIONS

In the wake of regional warming and substantial 20th-century glacier retreat, numerous proglacial lakes have formed in recently deglaciated alpine valleys and cirques in the Cascade Range of Oregon and Washington. In the Three Sisters and Mount Jefferson Wilderness Areas of the central Oregon Cascade Range, at least 14 lakes impounded by late Neoglacial terminal and lateral moraines, have formed since the early 1920's. Six of these lakes had maximum volumes of at least 200,000 m<sup>3</sup>. Many of these moraine dams proved to be unstable, and at least 11 rapid releases of lake water resulted from total or partial breaching of moraine dams. Evaluation of the geologic evidence left by these flows helps to understand aspects of flows caused by natural dam failures in glacierized volcanic terrains.

All of the moraine-dam failures resulted in debris flows, the largest ones attaining peak discharges of about 500 m<sup>3</sup>/s and travelling almost 10 km downstream. Farther downstream, many of the debris flows transformed into sediment-laden streamflow, affecting discharge and water quality for up to 100 km downstream. Water releases at the breaches evolved into debris flows by incorporation of Neoglacial-age morainal and outwash sediment near the outlet channel; in all cases they transformed into debris flows within 500 m. The quantity of debris introduced into the flows was large, in some cases exceeding 25 percent of the volume of water released, and resulted in downstream peak discharges substantially greater than those at the outlet. Morphological evidence indicates that most debris

entered the flows by mass wasting of outlet channel banks and knickpoint migration up the steep outlet channels.

As these debris flows travelled downstream, they eroded material from steeper parts of the channels and deposited sediment in wider, lower-gradient reaches. Most flows ceased continuing as debris flows at channel gradients less than 4°. Erosion and deposition by these debris flows had large effects on the peak discharge as the flow moved downstream. Peak discharges locally doubled in reaches of substantial entrainment.

Several moraine-dammed lakes remain in the Washington and Oregon Cascades, posing downstream hazards to communities and recreationists. Because of the large uncertainties in the present conditions of moraine dams and possible future glaciologic and hydrologic conditions, quantitatively assessing the potential for failure is difficult. Nevertheless, topographic setting provides at least a qualitative indication of the potential of moraine-dam failure, especially by overtopping. If climate and glacier-termini positions remain stable, the likelihood of sudden lake releases will probably continue to diminish. If, however, climate or glaciologic conditions change, causing either substantial glacier retreat or advance, the potential for moraine-dam failures may increase.

The downstream consequences of possible failures of moraine dams are also uncertain and largely unquantifiable. Worst-case scenarios can be defined and could be useful for planning mitigative measures, but the likelihood of such worst-case events may be vanishingly small. Uncertainties in the volume and rate of water release make predicting more likely outflow rates and downstream behavior difficult. Transformation to debris flow, and subsequently to sediment-laden streamflow, plays a large role in the downstream behavior of the flow. Incorporation and deposition of material substantially changes the rheology, volume, and peak discharge of the flow as it travels downstream. These factors, plus the numerical complexity of routing peaked hydrographs down steep channels, conspire against robust quantitative assessment of downstream hazards presented by moraine-dammed lakes.



View west of Broken Top volcano and moraine-dammed lake, Three Sisters Wilderness Area.  
Photograph by Austin Post, USGS, September 22, 1966.

## REFERENCES CITED

- Barnes, H.H., and Davidian, J., 1978, Indirect methods, *in* Hershey, R.W., ed., *Hydrometry*: John Wiley and Sons, p. 49-204.
- Beget, J.E., 1984, Tephrochronology of late Wisconsin deglaciation and Holocene glacier fluctuations near Glacier Peak, North Cascade Range, Washington: *Quaternary Research*, v. 21, p. 304-316.
- Benda, Lee, 1990, The influence of debris flows on channels and valley floors in the Oregon Coast Range, U.S.A.: *Earth Surface Processes and Landforms*, v. 15, p. 457-466.
- Benda, L.E., and Cundy, T.W., 1990, Predicting deposition of debris flows in mountain channels: *Canadian Geotechnical Journal*, v. 27, p. 409-417.
- Blown, Iain, and Church, Michael, 1985, Catastrophic lake drainage within the Homathko River Basin, British Columbia: *Canadian Geotechnical Journal*, v. 22, p. 551-563.
- Bodenlos, A.J., and Ericksen, G.E., 1955, Lead-zinc deposits of the Cordillera Blanca and Northern Cordillera Huayhuash, Peru: *U.S. Geological Survey Bulletin* 1017, 166 p.
- Buchroithner, M.F., Jentsch, G., and Wanivenhaus, B., 1982, Monitoring of recent geological events in the Khumbu area (Himalaya, Nepal) by digital processing of Landsat MSS data: *Rock Mechanics*, v. 15, p. 181-197.
- Burbank, D.W., 1981, A chronology of late Holocene glacier fluctuations on Mt. Rainier, Washington: *Arctic and Alpine Research*, v. 13, p. 369-386.
- , 1982, Correlations of climate, mass balances, and glacial fluctuations at Mount Rainier, Washington, U.S.A., since 1850: *Arctic and Alpine Research*, v. 14, p. 137-148.
- Callaghan, E., and Buddington, A.F., 1938, Metalliferous mineral deposits of the Cascade Range in Oregon: *U.S. Geological Survey Bulletin* 893, 141 p.
- Carling, P.A. and Glaister, M.S., 1987, Reconstruction of a flood resulting from a moraine-dam failure using geomorphological evidence and dam-break modeling, *in* Mayer, L. and Nash, D., *Catastrophic flooding*: Winchester, Mass., Allen and Unwin, p. 181-200.
- Clague, J.J., 1987, Catastrophic outburst floods: *GEOS*, v. 16, no. 2, p. 18-21.
- Clague, J.J., and Evans, S.G., 1992, A self-arresting moraine dam failure, St. Elias Mountains, British Columbia—Current Research, Part A: *Geological Survey of Canada, Paper* 92-1A, p. 185-188.
- , 1993, Historic retreat of Grand Pacific and Melbern Glaciers, Saint Elias Mountains, Canada—An analogue for decay of the Cordilleran ice sheet at the end of the Pleistocene?: *Journal of Glaciology*, v. 39, no. 133, p. 619-624.
- , 1994, Formation and failure of natural dams in the Canadian Cordillera: *Geological Survey of Canada Bulletin* 464, 35 p.
- Clague J.J., Evans, S.G., and Blown, I.G., 1985, A debris flow triggered by the breaching of a moraine-dammed lake, Klattasine Creek, British Columbia: *Canadian Journal of Earth Sciences*, v. 22, p. 1492-1502.
- Conrey, R.M., 1991, Geology and petrology of the Mount Jefferson area, High Cascade Range, Oregon: Pullman, Washington State University, Ph.D. dissertation, 357 p., 2 pls., 94 figs.
- Costa, J.E., 1984, Physical geomorphology of debris flows, *in* Costa, J.E., and Fleisher, P.J., eds., *Developments and applications of geomorphology*: Berlin, Springer-Verlag, p. 268--317.
- , 1988, Floods from dam failures, *in* Baker, V.R., Kochel, R.C., and Patton, P.C., eds., *Flood geomorphology*: John Wiley and Sons, p. 439-463.
- , 1997, Hydraulic modeling for lahar hazards at Cascade volcanoes: *Environmental and Engineering Geoscience*, v. III, p. 21-30.
- Costa, J.E., and Schuster, R.L., 1988, The formation and failure of natural dams: *Geological Society of America Bulletin*, v. 100, p. 1054-1068.
- Crandell, D.R., 1965, The glacial history of western Washington and Oregon, *in* Wright, H.E., Jr., and Frey, D.G., eds., *The Quaternary of the United States*: Princeton, N.J., Princeton University Press, p. 341-353.
- Crandell, D.R., 1971, Postglacial lahars from Mount Rainier Volcano, Washington: *U.S. Geological Survey Professional Paper* 677, 73 p.
- Crandell, D.R., and Miller, R.D., 1974, Quaternary stratigraphy and extent of glaciation in the Mount Rainier region, Washington: *U.S. Geological Survey Professional Paper* 847, 59 p.

- Curry, R.R., 1966, Observation of alpine mudflows in the Tenmile Range, central Colorado: Geological Society of America Bulletin, v. 77, p. 771–776.
- Davis, P.T., 1988, Holocene glacier fluctuations in the American Cordillera: Quaternary Science Reviews, v. 7, p. 127–157.
- Dethier, D.P., 1980, Reconnaissance study of Holocene glacier fluctuations in the Broken Top area, Oregon [abs.]: Geological Society of America Abstracts with Programs, v. 11, p. 104.
- Ding Yongjian, and Liu Jingshi, 1992, Glacier lake outburst flood disasters in China: Annals of Glaciology, v. 16, p. 180–184.
- Driedger, C.L., 1986, A visitor's guide to Mount Rainier glaciers: Longmire, Washington, Pacific Northwest National Parks and Forests Association, 80 p.
- , 1993, Glaciers on Mount Rainier: Water Fact Sheet, U.S. Geological Survey Open-File Report 92-474, 2 p.
- Driedger, C.L., and Kennard, P.M., 1986, Ice volumes on Cascade volcanoes—Mount Rainier, Mount Hood, Three Sisters, and Mount Shasta: U.S. Geological Survey Professional Paper 1365, 28 p.
- Dutto, Furio, and Mortar, Giovanni, 1992, Rischi connessi con la dinamica glaciale nelle Alpi italiane [Glacial hazards in the Italian Alps]: Geografica Fisica Dinamica Quat., v. 15, p. 85–99. [In Italian, English summary and figure captions.]
- Eisbacher, G.H., 1982, Mountain torrents and debris flows: Episodes, v. 1982, no. 4, p. 12–17.
- Eisbacher, G.H., and Clague, J.J., 1984, Destructive mass movements in high mountains—Hazard and management: Geological Survey of Canada Paper 84-16, 230 p.
- Ericksen, G.E., Plafker, George, and Conch, J.F., 1970, Preliminary report on the geologic events associated with the May 31, 1970, Peru earthquake: U.S. Geological Survey Circular 639, 25 p.
- Evans, S.G., 1987, The breaching of moraine-dammed lakes in the southern Canadian Cordillera, *in* International Symposium on Engineering Geological Environment in Mountainous Areas, Beijing, 1987, Proceedings: v. 2, p. 141–150.
- Evans, S.G., and Clague, J.J., 1993, Glacier-related hazards and climatic change, *in* Bras, Rafael, ed., Conference on The World at Risk—Natural Hazards and Climate Change, Cambridge, Mass., 1992: New York, American Institute of Physics, p. 48–60.
- Folk, R.L., 1980, Petrology of sedimentary rocks: Austin, Texas, Hemphill Publishing, 184 p.
- Folland, C.K., Karl, T.R., and Vinnikov, K.Y.A., 1990, Observed climate variations and change, *in* Houghton, J.T., Jenkins, G.J., and Ephraums, J.J., eds., Climate Change—The IPCC Scientific Assessment: Cambridge, Mass., Cambridge University Press, p. 195–238.
- Fread, D.L., 1987, BREACH—An erosion model for earthen dam failures: Silver Spring, Maryland, Hydrologic Research Laboratory, National Weather Service, 34 p.
- Fread, D.L., 1988, The NWS DAMBRK model—Theoretical background/user documentation: Silver Spring, Maryland, Hydrologic Research Laboratory, National Weather Service, 120 p.
- Froehlich, D.C., 1987, Embankment-dam breach parameters, *in* Ragan, R.M., ed, Hydraulic Engineering, Proceedings of the 1987 National Conference on Hydraulic Engineering: New York, American Society of Civil Engineers, p. 570–575.
- Fryxell, F.M., and Horberg, L, 1943, Alpine mudflows in Grand Teton National Park, Wyoming: Geological Society of America Bulletin, v. 54, p. 457–472.
- Fushimi, H., Ikegami, K., Higuchi, K., and Shankar, K., 1985, Nepal case study: catastrophic floods, *in* Young, G.J., ed., Techniques for prediction of runoff from glacierized areas: International Association of Hydrological Sciences (IAHS-AISH) Publication No. 149, p. 125–130.
- Galay, V.J., 1985, Hindu Kush-Himalayan erosion and sedimentation in relation to dams, *in* International Workshop on Water Management in the Hindu Kush-Himalaya region, Chengu China, 1985: Kathmandu, Nepal, International Centre for Integrated Mountain Development (ICIMOD), 24 p.
- Gallino, G.L., and Pierson, T.C., 1985, Polallie Creek debris flow and subsequent dam-break flood of 1980, East Fork Hood River basin, Oregon: U.S. Geological Survey Water Supply Paper 2273, 22 p.
- Gerasimov, V.A., 1965, Issykskaia katastrofa 1963 g. i otrazhenie ee in geomorfoogii doliny r. Issyk [The Issyk catastrophe in 1963 and its effect on

- geomorphology of the Issyk River valley]: *Akademiia Nauk SSSR, Izvestiia Vsesoiuznogo, Geograficheskogo Obshchestva*, v. 97, p. 6, p. 541–547. [In Russian.]
- Grove, J.M., 1988, *The Little Ice Age*: London, Methuen, 498 p. [Reprinted 1990, New York, Routledge.]
- Haeblerli, Wilfried, 1983, Frequency and characteristics of glacier floods in the Swiss Alps: *Annals of Glaciology*, v. 4, p. 95–90.
- Haeblerli, W., Alean, J.-C., Müller, P., and Funk, M., 1989, Assessing risks from glacier hazards in high mountain regions: some experiences in the Swiss Alps: *Annals of Glaciology*, v. 13, p. 96–102.
- Hansen, J., and Lebedeff, S., 1988, Global surface temperatures—Update through 1987: *Geophysical Research Letters*, v. 15, p. 323–326.
- Hatch, Laura, 1917, The glaciers of Mount Jefferson: *Mazama*, v. 5, no. 2 (December, 1917), p. 136–139.
- Heikkinen, O.O., 1984, Dendrochronological evidence of variations of Coleman Glacier, Mount Baker, Washington, U.S.A.: *Arctic and Alpine Reserach*, v. 16, p. 53–64.
- Henderson, F.M., 1966, *Open-channel flow*: MacMillan, N.Y., 522 p.
- Hodge, E.T., 1925, *Mount Multnomah—Ancient ancestor of the Three Sisters*: Eugene, Oregon, University of Oregon, 158 p., 1 pl.
- Hopkins, D.M., 1975, *Geology of the south and east slope of Mount Adams volcano, Cascade Range, Washington*: Seattle, Washington, University of Washington, Ph.D. dissertation, 79 p.
- Hopson, R.E., 1960, *Collier Glacier—A photographic record*: *Mazama*, v. 42, no. 13, p. 15–26.
- , *Collier Glacier, 1961*: *Mazama*, v. 43, no. 13, p. 37–39.
- , *Collier Glacier, 1962*: *Mazama*, v. 44, no. 13, p. 44–47.
- , *Collier Glacier, 1963*: *Mazama*, v. 45, no. 13, p. 48–49.
- , *Collier Glacier, 1963*: *Mazama*, v. 47, no. 13, p. 54–56.
- Hubley, R.C., 1956, *Glaciers of the Washington Cascade and Olympic Mountains; their present activity and its relation to local climatic trends*: *Journal of Glaciology*, v. 2, p. 669–674.
- Hunt, Bruce, 1984, *Dam-break solution*: *Journal of Hydraulic Engineering*, v. 110, no. 6, p. 675–686.
- Hupp, C.R., Osterkamp, W.R., and Thornton, J.L., 1987, *Dendrogeomorphic evidence and dating of recent debris flows on Mount Shasta, Northern California*: U.S. Geological Survey Professional Paper 1396-B, 39 p.
- Ikeya, H., 1981, A method for designation for area in danger of debris flow, *in* Davies, T.R.H., and Pearce, A.J., eds., *Proceedings of the Christchurch Symposium, January 1981, Erosion and Sediment Transport in Pacific Rim Steeplands*: International Association of Hydrological Sciences (IAHS-AISH) Publication No. 132, p. 576–588.
- Indacochea, A.J., and Iberico Mariano, 1947, *Aluvionamiento de Chavin de Huantar el 17 de enero de 1945*: *Boletin de la Sociedad Geológica del Peru*, v. 20, p. 21–28. [In Spanish.]
- Iverson, R.M., and Denlinger, R.P., 1987, The physics of debris flows—A conceptual approach, *in* Beschta, R.L., Blinn, T., Grant, G.E., Ice, G.G., and Swanson, F.J., eds., *Erosion and Sedimentation in the Pacific Rim*: International Association of Hydrological Sciences (IAHS-AISH) Publication No. 165, p. 155–165.
- Iverson, R.M., LaHusen, R.G., Major, J.J., and Zimmerman, C.L., 1994, *Debris flow against obstacles and bends—Dynamics and deposits*: *EOS, American Geophysical Union*, v. 75, no. 44, p. 274.
- Ives, J.D., *Glacial lake outburst floods and risk engineering in the Himalaya: Kathmandu, Nepal*, International Centre for Integrated Mountain Development (ICIMOD) Occasional Paper No. 5, 42 p.
- Jackson, L.E., Jr., 1979, *A catastrophic glacial outburst flood (jökulhlaup) mechanism for debris flow generation at the Spiral Tunnels, Kicking Horse River basin, British Columbia*: *Canadian Geotechnical Journal*, v. 16, p. 806–813.
- Jackson, L.E., Jr., Hungr, O., Gardber, J.S., and Mackay, C., 1989, *Cathedral Mountain debris flows, Canada*: *International Association of Engineering Geology Bulletin*, no. 40, p. 35–54.
- Johnson, A.M., 1970, *Physical processes in geology*: San Francisco, Freeman and Cooper, 577 p.
- Jones, P.D., 1988, *Hemispheric surface air temperature variations—Recent trends and an update to 1987*: *Journal of Climatology*, v. 1, p. 654–660.
- Jones, P.D., and Bradley, R.S., 1992, *Climatic variations in the longest instrumental records*, *in*

- Bradley, R.S., and Jones, P.D., eds., *Climate since A.D. 1500*: London, Routledge, p. 246–268.
- Keen, R.H., 1969, *Collier Glacier report: 1966-1969*: *Mazama*, v. 51, p. 42–46.
- , 1978, *Collier Glacier: 1970-1978*: *Mazama*, v. 60, p. 22–35.
- , 1981, *Collier Glacier: 1979, 1980, 1981*: *Mazama*, v. 63, p. 59–62.
- Khegai, A.Y., Popov, N.V., Plekhanov, P.A., and Keremkulov, V.A., 1992, Experiments at the Chemolgan debris-flow testing ground, Kazakhstan: *Landslide News*, no. 6 (August 1992), p. 27–28.
- Kinzl, H., 1940, La ruptura del lago glacial en la quebrada de Ulta an el año 1938: *Boletín del Meseo de Historia Natural “Javier Prado”* [Lima, Peru], v. 4, no. 13, p. 152–167. [In Spanish.]
- Laenen, Antonius, and Hansen, R.P., 1986, Simulation of three lahars in the Mount St. Helens, Washington area, using a one-dimensional, unsteady-state streamflow model: *U.S. Geological Survey Water-Resources Investigations Report 88-4004*, 20 p.
- Laenen, Antonius, Scott, K.M., Costa, J.E., and Orzol, L.L., 1987, Hydrologic hazards along Squaw Creek from a hypothetical failure of the glacial moraine impounding Carver Lake near Sisters, Oregon: *U.S. Geological Survey Open-File Report 87-41*, 48 p.
- Laenen, Antonius, Scott, K.M., Costa, J.E., and Orzol, L.L., 1992, Modeling flood flows from a hypothetical failure of the glacial moraine impounding Carver Lake near Sisters, Oregon, *in* Subitzky, Seymour, ed., *Selected papers in the hydrologic sciences, 1988-92*: *U.S. Geological Survey Water Supply Paper 2340*, p. 151–164.
- Land, L.F., 1980, Evaluation of selected dam-break floodway models by using field data: *U.S. Geological Survey Water-Resources Investigations Report 80-44*, 54 p.
- Lawrence, D.B., 1948, Mount Hood’s latest eruption and glacier advances: *Mazama*, v. 30, p. 22–29.
- Leonard, E.M., 1985, Glaciological and climatic controls on lake sedimentation, Canadian Rocky Mountains: *Zeitschrift für gletscherkunde und Glacialgeologie*, v. 21, p. 35–42.
- Liu Chaohai, and Sharmal, C.K. (eds.), 1988, Report on first expedition to glaciers and glacier lakes in the Pumqu (Arun) and Poiqu (Bhote-Sun Kosi) River basins, Xizang (Tibet), China: Beijing, China, Science Press, 192 p.
- Lliboutry, Louis, Arnao, B.M., Pautre, Andre, and Schneider, Bernard, 1977, Glaciological problems set by the control of dangerous lakes in Cordillera Blanca, Peru. I. Historical failures of morainic dams, their causes and prevention: *Journal of Glaciology*, v. 18, p. 239–254.
- Li Deji, and You Yong, 1992, Bursting of the Midui Moraine Lake in Bomi, Xizang: *Mountain Research [China]*, v. 10, no 4. p. 219–224. [In Chinese, English summary.]
- Lu Ruren, and Li Dehi, 1986, Debris flow induced by ice lake burst in the Tangbulang gully, Gongbujiangda, Xizang (Tibet): *Journal of Glaciology and Geocryology*, v. 8, p. 61–71. [In Chinese, English summary.]
- Luckman, B.H., Holdsworth, Gerald, and Osborn, G.D., 1993, Neoglacial glacier fluctuations in the Canadian Rockies: *Quaternary Research*, v. 39, p. 144–153.
- Lundstrom, S.C., 1992, The budget and effect of superglacial debris on Eliot Glacier, Mount Hood, Oregon: Boulder, Colo., University of Colorado, Ph.D. dissertation, 193 p., 61 figs.
- Lü Ruren, and Li Deji, 1986, Debris flow induced by ice lake burst in the Tangbulang Gully, Gonbujiangda, Xizang (Tibet): *Journal of Glaciology and Geocryology [China]*, v. 8, no. 1, p. 61–70. [In Chinese, English summary.]
- Lynch, Margaret, 1929, An ascent of Three Finger Jack: *Mazama*, v. 11, no. 12, p. 110–114.
- Macchinio, F., and Sirangelo, B., Floods resulting from progressively breached dams, *in* *Proceedings of Lausanne Symposia, August 1990, Hydrology in Mountainous Regions*: International Association of Hydrological Sciences (IAHS-AISH) Publication No. 194, p. 325–332.
- McDonald, Gregory, D., Changes in mass of Collier Glacier, Oregon, 1910-1994: Corvallis, Oregon, Oregon State University, M.S. thesis, 183 p.
- Meier, M.F., and Post, Austin, 1962, Recent variations in mass budgets of glaciers in Western North America, *in* *Symposium of Obergurgl*: International Association of Hydrologic Sciences (IAHS-AISH) Publication No. 58, p. 63–77.
- Noda, Edward, 1970, Water waves generated by landslides: *Journal of the Waterways, Harbors,*

- and Coastal Engineering Division, American Society of Civil Engineers, v. WW4, p. 835–855.
- Nolf, Bruce, 1966, Broken Top breaks—Flood released by erosion of glacial moraine: *Ore Bin*, v. 28, no. 10, p. 182–188.
- O'Brien, J.S., Julien, P.Y., and Fullerton, W.T., 1993, Two-dimensional water flood and mudflow simulation: *Journal of Hydraulic Engineering*, v. 119, no. 2, p. 244–261.
- O'Connor, J.E., and Costa, J.E., 1993, Geologic and hydrologic hazards in glacierized basins in North America resulting from 19th and 20th century global warming: *Natural Hazards* v. 8, p. 121–140.
- Oppenheim, Victor, 1946, Sobre las lagunas de Huaraz: *Boletín de la Sociedad Geológica del Perú*, v. 19, p. 68–80. [In Spanish.]
- Osborn, G.D., and Luckman, B.H., 1988, Holocene glacier fluctuations in the Canadian Cordillera (Alberta and British Columbia): *Quaternary Science Reviews*, v. 7, p. 115–128.
- Osterkamp, W.R., Hupp, C.R., and Blodgett, J.C., 1986, Magnitude and frequency of debris flows, and areas of hazard on Mount Shasta, Northern California: U.S. Geological Survey Professional Paper 1396-C, 21 p.
- Pelto, M.S., 1993, Current behavior of glaciers in the North Cascades and effect on regional water supplies: *Washington Geology*, v. 21, no. 2, p. 3–10.
- Phillips, K.N., 1938, Our vanishing glaciers: *Mazama*, v. 20, no. 12, p. 24–41.
- Pierson, T.C., 1980, Erosion and deposition by debris flows at Mount Thomas, North Canterbury, New Zealand: *Earth Surface Processes*, v. 5, p. 227–247.
- , 1985, Initiation and flow behavior of the 1980 Pine Creek and Muddy River lahars, Mount St. Helens, Washington: *Geological Society of America Bulletin*, v. 96, p. 1,056–1,069.
- Pierson, T.C. and Costa, J.E., 1987, A rheological classification of subaerial sediment-water flows: *in* Costa, J.E. and Wieczorek, G.F., eds., *Debris flows/avalanches: process, recognition, and mitigation*: Geological Society of America *Reviews in Engineering Geology*, v. 7, p. 1–12.
- Pierson, T.C., and Scott, K.M., 1985, Downstream dilution of a lahar—Transition from debris flow to hyperconcentrated streamflow: *Water Resources Research*, v. 21, p. 1511–1524.
- Porter, S.C., and Denton, G.H., 1967, Chronology of Neoglaciation in the North American Cordillera: *American Journal of Science*, v. 265, p. 177–210.
- Ponce, V.M., and Tsivoglou, A.M., 1981, Modeling gradual dam breaches: *Journal of the Hydraulics Division, Proceedings of the American Society of Civil Engineers*, v. 107, no. HY7, p. 829–838.
- Popov, N., 1990, Debris flows and their control in Alma-Ata, Kazakh SSR, USSR: *Landslide News*, no. 4 (July 1990), p. 25–27.
- Quiroga, C.A., and Singh, V.P., 1987, A dam-breach erosion model—II. Application: *Water Resources Management*, v. 1, p. 199–221.
- Rabassa, Gorge; Rubulis, Sigfrido; and Suárezm Jorge, 1979, Rate of formation and sedimentology of (1976-1978) push-moraines, Frias Glacier, Mount Tronador (41°10'S; 71°53'W), Argentina, *in* Schlüchter, C., ed., *Moraines and varves*: Rotterdam, A.A. Balkema, p. 65–79.
- Rector, M.L., 1988, An analysis of suspected Neoglacial ice-cored moraines impounding Carver Lake, South Sister region, High Cascades, Oregon: Corvallis, Oregon State University, Research paper in partial fulfillment of the requirement for the degree of Master of Science, 29 p.
- Research Committee of The Mazamas, 1938, An aerial photographic survey of the glaciers of Mount Hood, Mount Jefferson and The Three Sisters, Oregon: 47 p. [Copy available for inspection at Mazama Clubhouse, Portland, Ore.]
- Reynolds, J.J., 1990, Geological hazards in the Cordillera Blanca, Peru: *AGID News*, no. 61/62, p. 31–33.
- , 1992, The identification and mitigation of glacier-related hazards—Examples from the Cordillera Blanca, Peru, *in* McCall, G.J.H., Laming, D.J.C., and Scott, S.C., eds., *Geohazards—Natural and man-made*: London, Chapman and Hall, p. 143–157.
- Russell, I.C., 1885, Existing glaciers of the United States: U.S. Geological Survey Fifth Annual Report (1883-1884), p. 303–355.
- , 1905, Preliminary report on the geology and water resources of central Oregon: U.S. Geological Survey Bulletin 252, 138 p.

- Ryder, J.M., 1989, Holocene glacier fluctuations, *in* Fulton, R.J., ed., Chapter 1 of Quaternary Geology of Canada and Greenland: Geological Survey of Canada, Geology of Canada, no. 1, p. 74–75. [also Geological Society of America, The Geology of North America, v. K-1.]
- , 1991, Geomorphological processes associated with an ice-marginal lake at Bridge Glacier, British Columbia: *Géographie physique et Quaternaire*, v. 45, p. 34–44.
- Scott, K.M., 1967, Downstream changes in sedimentological parameters illustrated by particle distribution from a breached rockfill dam, *in* Symposium on river morphology, General Assembly of Bern, 1967: International Association of Scientific Hydrology, International Union Geodesy and Geophysics, Publication No. 75, p. 309–318.
- , 1988, Lahars and lahar-runout flows in the Toutle-Cowlitz River system, Mount St. Helens, Washington—Origins, behavior, and sedimentology: U.S. Geological Survey Professional Paper 1447-A, 74 p.
- Scott, K.M., Pringle, P.T., and Vallance, J.W., 1992, Sedimentology, behavior, and hazards of debris flows at Mount Rainier, Washington: U.S. Geological Survey Open-File Report 90-385, 105 p.
- Scott, W.E., 1974, Quaternary glacial and volcanic environments, Metolius River area, Oregon: Seattle, Washington, University of Washington, Ph.D. dissertation, 95 p., 23 figs., 1 plate (1:62,500).
- , 1977, Quaternary glaciation and volcanism, Metolius River area, Oregon: Geological Society of America Bulletin, v. 88, p. 113–124.
- , 1987, Holocene rhyodacite eruptions on the flanks of South Sister volcano, Oregon, *in* Fink, J.H., ed., The emplacement of silicic domes and lava flows: Geological Society of America Special Paper 212, p. 35–53.
- , 1989, Temporal relations between eruptions of the Mount Bachelor volcanic chain and fluctuations of late Quaternary glaciers, *in* Scott, W.E., Gardner, C.A., and Sarna-Wojcicki, A.M., Guidebook for field trip to the Mount Bachelor-South Sister-Bend area, Central Oregon High Cascades: U.S. Geological Survey Open-File Report 89-645, p. 10–18.
- Scott, W.E., and Gardner, C.A., 1992, Geologic map of the Mount Bachelor volcanic chain and surrounding area, Cascade Range, Oregon: U.S. Geological Survey Miscellaneous Investigations Map I-1967, scale 1:50,000.
- Sharp, R.P., and Nobles, L.H., 1953, Mudflow of 1941 at Wrightwood, Southern California: Geological Society of America Bulletin, v. 64, p. 547–560.
- Sherrod, D.R., 1986, Geology, petrology, and volcanic history of a portion of the Cascade Range between latitudes 43°–46° N, central Oregon, U.S.A.: Santa Barbara, University of California, Ph.D. dissertation, 320 p., 4 pls., 33 figs.
- Sherrod, D.R., and Smith, J.G., 1989, Preliminary map of upper Eocene to Holocene volcanic and related rocks of the Cascade Range, Oregon: U.S. Geological Survey Open-File Report 81-14, scale 1:500,000.
- Sigafoos, R.S., and Hendricks, E.L., 1972, Recent activity of glaciers of Mount Rainier, Washington: U.S. Geological Survey Professional Paper 387-B, 24 p.
- Singh, V.P., and Quiroga, C.A., 1987, A dam-breach erosion model—I. formulation: *Water Resources Management*, v. 1, p. 177–197.
- Slingerland, R.L. and Voight, B., 1979, Occurrences, properties, and predictive models of landslide-generated water waves, *in* Voight, B., ed., *Rockslides and avalanches*, Vol. 2: Amsterdam, Elsevier, p. 317–397.
- Small, R.J., 1983, Lateral moraines of glacier de Tsidojore Nouve—Form, development, and implications: *Journal of Glaciology*, v. 29, p. 250–259.
- Takahashi, Tamotsu, 1978, Mechanical characteristics of debris flow: *Journal of the Hydraulics Division, American Society of Civil Engineers*, v. 104, p. 1153–1169.
- Takahashi, Tamotsu, 1981, Debris flow: *Annual Reviews of Fluid Mechanics*, v. 13, p. 57–77.
- Tangborn, W.V., 1980, Two models for estimating climate-glacier relationships in the North Cascades, Washington, U.S.A.: *Journal of Glaciology*, v. 25, p. 3–21.
- Taylor, E.M., 1978, Field geology of the S.W. Broken Top Quadrangle, Oregon: Oregon Department of Geology and Mineral Industries Special Paper 2, 50 p., 1 plate.

- 1981, Central High Cascade roadside geology, Bend, Sisters, McKenzie Pass, and Santiam Pass, Oregon, in Johnston, D.A., and Donnelly-Nolan, J., eds., *Guides to some volcanic terranes in Washington, Idaho, Oregon, and Northern California*: U.S. Geological Survey Circular 838, p. 55–83.
- , 1987, Field geology of the northwest quarter of the Broken Top 15' quadrangle, Deschutes County, Oregon: Oregon Department of Geology and Mineral Industries Special Paper 21, 20 p., 1 plate.
- Taylor, E.M., MacLeod, N.S., Sherrod, D.R., and Walker, G.W., 1987, Geologic map of the Three Sisters Wilderness, Deschutes, Lane, and Linn Counties, Oregon: U.S. Geological Survey Miscellaneous Field Studies Map MF-1952, scale 1:62,500.
- Taylor, G.H., 1993, Normal annual precipitation, State of Oregon: Corvallis, Oregon, Oregon Climate Service. [Isohyetal map and explanatory text, scale approximately 1:1,000,000.]
- VanDine, D.F., 1985, Debris flows and debris torrents in the southern Canadian Cordillera: *Canadian Geotechnical Journal*, v. 22, p. 44–68.
- Vuichard, Daniel, and Zimmermann, Markus, 1987, The 1985 catastrophic drainage of a moraine-dammed lake, Khumbu Himal—Cause and consequences: *Mountain Research and Development*, v. 7, p. 91–110.
- Waite, R.B., Pierson, T.C., McLeod, N.S., Janda, R.J., Voight, B., and Holcomb, R.T., 1983, Eruption-triggered avalanche, flood, and lahar at Mount St. Helens—Effects of winter snowpack: *Science*, v. 221, p. 1394–1397.
- Walder, J.S., and Driedger, C.L., 1994, Geomorphic change caused by outburst floods and debris flows at Mount Rainier, Washington, with emphasis on Tahoma Creek valley: U.S. Geological Survey Water-Resources Investigations Report 93-4093, 93 p.
- Walder, J.S., and O'Connor, J.E., 1997, Methods for predicting peak discharge of floods caused by failure of natural and constructed earthen dams: *Water Resources Research*, v. 33, no. 10, p. 2337–2348.
- Webb, R.H., 1993, Initiation and frequency of debris flows in Grand Canyon [abs.]: *Geological Society of America Abstracts with Programs*, v. 25, no. 7, p. A-395.
- Williams, I.A., 1916, *Glaciers of the Three Sisters: Mazama*, v. 5, no. 1 (December, 1916), p. 14–23.
- Xu Daoming, 1988, Characteristics of debris flow caused by outburst of glacial lakes on the Boqu River in Xizang, China: *Geojournal*, v. 17, p. 569–580.
- Yesenov, U.Y., and Degovets, A.S., 1979, Catastrophic mudflow on the Bol'shaya Almatinka River in 1977: *Soviet Hydrology, Selected Papers*, v. 18, p. 158–160.
- Zimmermann, Markus, and Mani, Peter, 1993, The effect of global warming on debris flow activity in the Swiss Alps: A challenge for the 21st century [abs.]: *Programme with Abstracts, Third International Geomorphology Conference*, Hamilton, Ontario, p. 282.

---

# Availability of Publications of the U.S. Geological Survey

---

Order U.S. Geological Survey (USGS) publications by calling the toll-free telephone number 1-888-ASK-USGS or contacting the offices listed below. Detailed ordering instructions, along with prices of the last offerings, are given in the current-year issues of the catalog *New Publications* of the U.S. Geological Survey.

## Books, Maps, and Other Publications

### *By Mail*

Books, maps, and other publications are available by mail from USGS Information Services, Box 25286, Federal Center, Denver, CO 80225. Publications include Professional Papers, Bulletins, Water-Supply Papers, Techniques of Water-Resources Investigations, Circulars, Fact Sheets, publications of general interest, single copies of permanent USGS catalogs, and topographic and thematic maps.

### *Over the Counter*

Books, maps, and other publications of the U.S. Geological Survey are available over the counter at the following USGS Earth Science Information Centers (ESIC's), all of which are authorized agents of the Superintendent of Documents:

- Anchorage, Alaska—Rm. 101, 4230 University Dr.
- Denver, Colorado—Bldg. 810, Federal Center
- Menlo Park, California—Rm. 3128, Bldg. 3, 345 Middlefield Rd.
- Reston, Virginia—Rm. 1C402, USGS National Center, 12201 Sunrise Valley Dr.
- Salt Lake City, Utah—2222 West, 2300 South
- Spokane, Washington—Rm. 135, U.S. Post Office Building, 904 West Riverside Ave.
- Washington, D.C.—Rm. 2650, Main Interior Bldg., 18th and C Sts., NW.

Maps only may be purchased over the counter at the following USGS office:

- Rolla, Missouri—1400 Independence Rd.

### *Electronically*

Some USGS publications, including the catalog *New Publications* of the U.S. Geological Survey are also available electronically on the USGS's World Wide Web home page at <http://www.usgs.gov>

### **Preliminary Determination of Epicenters**

Subscriptions to the periodical *Preliminary Determination of Epicenters* can be obtained only from the Superintendent of Documents. Check or money order must be payable to the Superintendent of Documents. Order by mail from

Superintendent of Documents  
Government Printing Office  
Washington, DC 20402

### **Information Periodicals**

Many Information Periodicals products are available through the systems or formats listed below:

#### *Printed Products*

Printed copies of the *Minerals Yearbook* and the *Mineral Commodity Summaries* can be ordered from the Superintendent of Documents, Government Printing Office (address above). Printed copies of *Metal Industry Indicators* and *Mineral Industry Surveys* can be ordered from the Center for Disease Control and Prevention, National Institute for Occupational Safety and Health, Pittsburgh Research Center, P.O. Box 18070, Pittsburgh, PA 15236—0070.

#### *Mines FaxBack: Return fax service*

1. Use the touch-tone handset attached to your fax machine's telephone jack. (ISDN [digital] telephones cannot be used with fax machines.)
2. Dial (703) 648-4999.
3. Listen to the menu options and punch in the number of your selection, using the touch-tone telephone.
4. After completing your selection, press the start button on your fax machine.

#### **CD-ROM**

A disc containing chapters of the *Minerals Yearbook* (1993–95), the *Mineral Commodity Summaries* (1995–97), statistical compendium (1970–90), and other publications is updated three times a year and sold by the Superintendent of Documents, Government Printing Office (address above).

#### **World Wide Web**

Minerals information is available electronically at <http://minerals.er.usgs.gov/minerals/>

#### **Subscription to the catalog *New Publications* of the U.S. Geological Survey**

Those wishing to be placed on a free subscription list for the catalog *New Publications* of the U.S. Geological Survey should write to

U.S. Geological Survey  
903 National Center  
Reston, VA 20192

---

# Selected Series of U.S. Geological Survey Publications

---

## Books and Other Publications

**Professional Papers** report scientific data and interpretations of lasting scientific interest that cover all facets of USGS investigations and research.

**Bulletins** contain significant data and interpretations that are of lasting scientific interest but are generally more limited in scope or geographic coverage than Professional Papers.

**Water-Supply Papers** are comprehensive reports that present significant interpretive results of hydrologic investigations of wide interest to professional geologists, hydrologists, and engineers. The series covers investigations in all phases of hydrology, including hydrogeology, availability of water, quality of water, and use of water.

**Circulars** are reports of programmatic or scientific information of an ephemeral nature; many present important scientific information of wide popular interest. Circulars are distributed at no cost to the public.

**Fact Sheets** communicate a wide variety of timely information on USGS programs, projects, and research. They commonly address issues of public interest. Fact Sheets generally are two or four pages long and are distributed at no cost to the public.

**Digital Data Series (DDS)** distribute large amounts of data through digital media, including compact disc-read-only memory (CD-ROM). They are high-quality, interpretive publications designed as self-contained packages for viewing and interpreting data and typically contain data sets, software to view the data, and explanatory text.

**Water-Resources Investigations Reports** are papers of an interpretive nature made available to the public outside the formal USGS publications series. Copies are produced on request (unlike formal USGS publications) and are also available for public inspection at depositories indicated in USGS catalogs.

**Open-File Reports** can consist of basic data, preliminary reports, and a wide range of scientific documents on USGS investigations. Open-File Reports are designed for fast release and are available for public consultation at depositories.

## Maps

**Geologic Quadrangle Maps (GQ's)** are multicolor geologic maps on topographic bases in 7.5- or 15-minute quadrangle formats (scales mainly 1:24,000 or 1:62,500) showing bedrock, surficial, or engineering geology. Maps generally include brief texts; some maps include structure and columnar sections only.

**Geophysical Investigations Maps (GP's)** are on topographic or planimetric bases at various scales. They show results of geophysical investigations using gravity, magnetic, seismic, or radioactivity surveys, which provide data on subsurface structures that are of economic or geologic significance.

**Miscellaneous Investigations Series Maps or Geologic Investigations Series (I's)** are on planimetric or topographic bases at various scales; they present a wide variety of format and subject matter. The series also includes 7.5-minute quadrangle photogeologic maps on planimetric bases and planetary maps.

**Information Periodicals Metal Industry Indicators (MII's)** is a free monthly newsletter that analyzes and forecasts the economic health of five metal industries with composite leading and coincident indexes: primary metals, steel, copper, primary and secondary aluminum, and aluminum mill products.

**Mineral Industry Surveys (MIS's)** are free periodic statistical and economic reports designed to provide timely statistical data on production, distribution, stocks, and consumption of significant mineral commodities. The surveys are issued monthly, quarterly, annually, or at other regular intervals, depending on the need for current data. The MIS's are published by commodity as well as by State. A series of international MIS's is also available.

Published annually, **Mineral Commodity Summaries** is the earliest Government publication to furnish estimates covering nonfuel mineral industry data. Data sheets contain information on the domestic industry structure, Government programs, tariffs, and 5-year salient statistics for more than 90 individual minerals and materials.

**The Minerals Yearbook** discusses the performance of the worldwide minerals and materials industry during a calendar year, and it provides background information to assist in interpreting that performance. The Minerals Yearbook consists of three volumes. Volume I, Metals and Minerals, contains chapters about virtually all metallic and industrial mineral commodities important to the U.S. economy. Volume II, Area Reports: Domestic, contains a chapter on the minerals industry of each of the 50 States and Puerto Rico and the Administered Islands. Volume III, Area Reports: International, is published as four separate reports. These reports collectively contain the latest available mineral data on more than 190 foreign countries and discuss the importance of minerals to the economies of these nations and the United States.

## Permanent Catalogs

**"Publications of the U.S. Geological Survey, 1879–1961"** and **"Publications of the U.S. Geological Survey, 1962–1970"** are available in paperback book form and as a set of microfiche.

**"Publications of the U.S. Geological Survey, 1971–1981"** is available in paperback book form (two volumes, publications listing and index) and as a set of microfiche.

**Annual supplements** for 1982, 1983, 1984, 1985, 1986, and subsequent years are available in paperback book form.